Technical Report Series on Global Modeling and Data Assimilation

Max J. Suarez, Editor
Goddard Space Flight Center
Greenbelt, Maryland

Volume 1

Documentation of the Goddard Earth Observing System (GEOS) General Circulation Model - Version 1

Lawrence L. Takacs
Andrea Molod
Tina Wang
*General Sciences Corporation*
Laurel, Maryland

Abstract

This report is a documentation of Version 1 of the Goddard Earth Observing System (GEOS) General Circulation Model (GCM) developed by NASA's Data Assimilation Office and the Climate and Radiation Branch. The report is separated into three parts. Part I describes the overall features of the GCM, including numerical schemes for the hydrodynamics, sub-grid scale physical parameterizations, and boundary conditions. Part II provides a comprehensive description of the diagnostics available within the model, including the methodology for their selection and retrieval. Part III concludes the report with a User's Guide, which includes the location of frozen versions of the GEOS system, instructions on how to create user-defined applications for running the GEOS system, and an overview of established production applications and output utilities available to the communitiy.
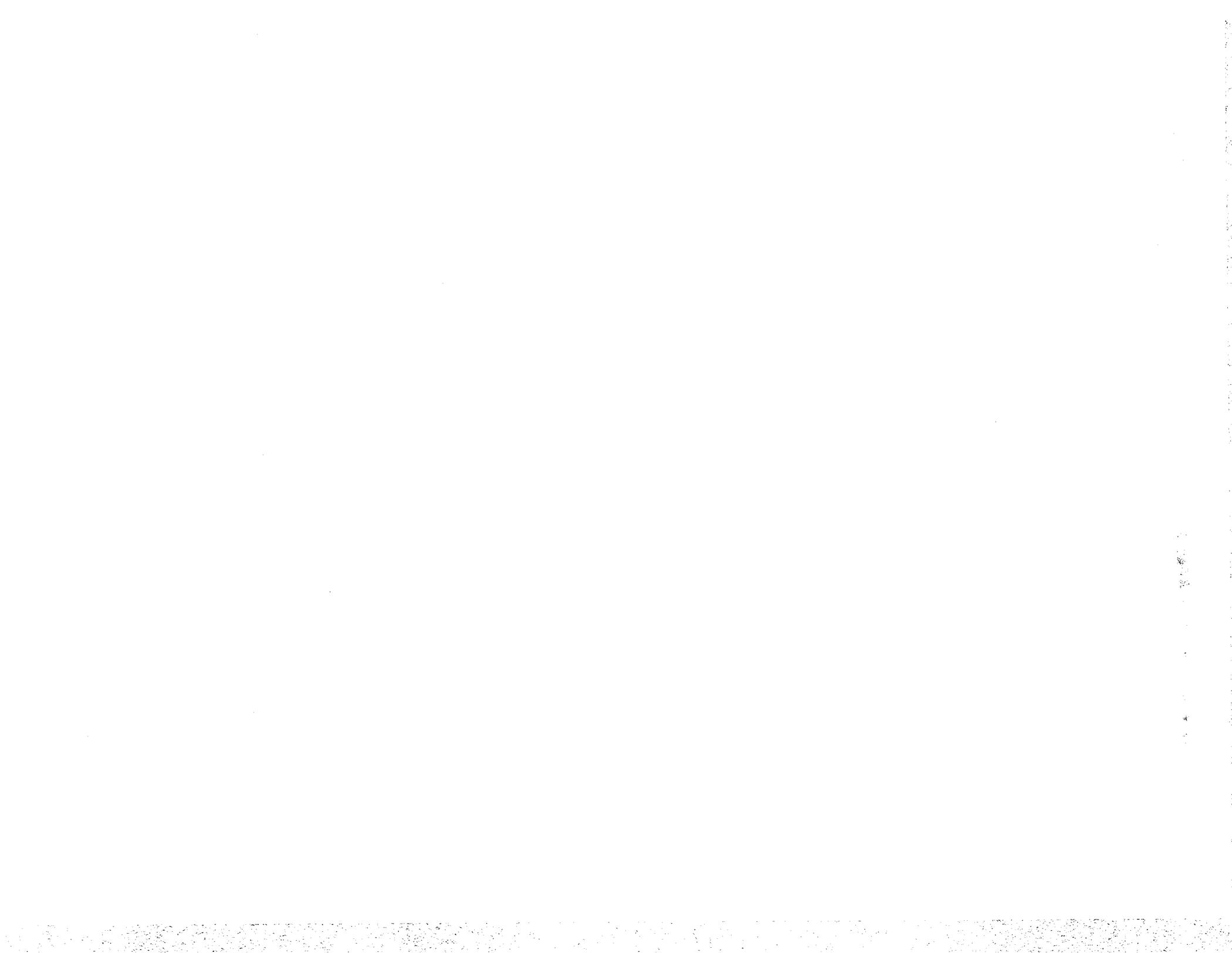
Contents

List of Figures

Part I

GEOS-1 GCM: A Descriptive Documention

1 Introduction and Model Lineage

The Goddard Earth Observing System-1 (GEOS-1) General Circulation Model (GCM) was developed by the Data Assimilation Office (DAO) at the Goddard Laboratory for Atmospheres (GLA), in collaboration with the Climate and Radiation Branch, for use in the system being developed to analyze EOS data. The GEOS Data Assimilation System (DAS), currently using the GEOS-1 GCM in conjuction with an Optimal Interpolation (OI) analysis scheme, has been used to produce a multi-year global atmospheric data set for climate research (Schubert et al., 1993). The GEOS-1 GCM has also been used to produce multiple 10-year climate simulations as part of the DAO's participation in the Atmospheric Model Intercomparison Project (AMIP) sponsored by the Program for Climate Model Diagnostics and Intercomparison (PCMDI) (see Gates, 1992). The GEOS-1 DAS has been used operationally to provide scientific flight guidance during NASA's participation in the Measurements for Assessing the Effects of Stratospheric Aircraft (MAESA) experiment.

The earliest predecessor of the GEOS-1 GCM was developed in 1989 based on the "plug-compatible" concepts outlined in Kalnay et al. (1989), and subsequently improved in 1991 (Fox- Rabinovitz, et al., 1991, Helfand et al., 1991). The plug-compatibility of the physical parameterizations together with the plug-compatible "Dynamical Core" introduced by Suarez and Takacs (1994) facilitate the development and testing of new algorithms. Together the DAO and the Climate and Radiation Branch at GLA have produced a library of physical parameterizations and dynamical algorithms which can be utilized for various GCM applications.

1.1 Relevant Model Documentation

A description of the overall features of the GEOS Data Assimilation System (DAS) used by the DAO may be found in Schubert et al. (1993). A comprehensive documentation of the Aries/GEOS Dynamical Core incorporating the horizontal and vertical discretization and finite-difference schemes used is given in Suarez and Takacs (1994). The Relaxed Arakawa-Schubert cumulus convective parameterization and the re-evaporation of falling rain are based upon the works of Moorthi and Suarez (1992) and Sud and Molod (1988), while the radiative processes are described by Harshvardhan et al. (1987). The planetary boundary

layer (PBL) and the upper level turbulence parameterization are based on the level 2.5 closure model of Helfand and Labraga (1988) and Helfand et al. (1991). Additional postscript copies of *this* document may be obtained through anonymous ftp from *hera.gsfc.nasa.gov*. The path and filename of the document is:

$$\text{pub/gcm/geos1.0\_gcm.doc.ps}$$

2   Atmospheric Dynamics

The momentum equations used in the GEOS-1 GCM are written in the "vector invariant" form, as in Sadourney (1975) and Arakawa and Lamb (1981), to facilitate the derivation of the energy and potential enstrophy conserving differencing scheme. The thermodynamic (potential temperature) and moisture (specific humidity) equations are written in flux form to facilitate potential temperature and moisture conservation. A complete description of the finite-difference scheme used can be found in Suarez and Takacs (1994).

The GEOS GCM uses a σ coordinate defined by

$$\sigma = \frac{p - p_T}{\pi}, \tag{1}$$

where p is the pressure, $\pi \equiv p_s - p_T$, p_s is the surface pressure, and p_T is a constant prescribed pressure at the top of the model atmosphere. With $p_T = 0$ this coordinate reduces to the conventional σ coordinate proposed by Phillips (1957).

With this vertical coordinate, the continuity equation becomes

$$\frac{\partial \pi}{\partial t} = -\nabla_\sigma \cdot (\pi \mathbf{v}) - \frac{\partial (\pi \dot{\sigma})}{\partial \sigma}, \tag{2}$$

where $\mathbf{v}$ is the horizontal velocity vector. Integrating (2) and assuming $\dot{\sigma} = 0$ at $p = p_s$ and $p = p_T$, we obtain the forms used in the model:

$$\frac{\partial \pi}{\partial t} = -\int_0^1 \nabla_\sigma \cdot (\pi \mathbf{v}) \, d\sigma \tag{3}$$

and

$$(\pi \dot{\sigma}) = -\sigma \frac{\partial \pi}{\partial t} - \int_0^\sigma \nabla_\sigma \cdot (\pi \mathbf{v}) \, d\sigma. \tag{4}$$

The equation of state for an ideal gas is $\alpha = RT/p$, where α is the specific density, T is the temperature, and R is the gas constant. The following alternative forms will be used below

$$\alpha = R\theta \frac{P}{p} = c_p \theta \frac{\partial P}{\partial p} = \frac{c_p \theta}{\pi} \left(\frac{\partial P}{\partial \sigma} \right)_\pi = \frac{c_p \theta}{\sigma} \left(\frac{\partial P}{\partial \pi} \right)_\sigma, \tag{5}$$

2

where $\theta \equiv T/P$ is the potential temperature, $P \equiv (p/p_0)^\kappa$, $\kappa = R/c_p$, c_p is the specific heat at constant pressure, and p_0 is a reference pressure. In obtaining the forms in (5) we have used $\frac{\partial P}{\partial p} = \kappa \frac{P}{p}$ and the relation

$$\left(\frac{dP}{d\sigma}\right)_\pi = \frac{\pi}{\sigma}\left(\frac{dP}{d\pi}\right)_\sigma. \tag{6}$$

For the time being virtual effects are neglected.

The hydrostatic equation is

$$\frac{\partial \Phi}{\partial p} = -\alpha,$$

where Φ is the geopotential. Using (5) and (6), this can be written:

$$\frac{\partial \Phi}{\partial \sigma} = -\pi\alpha = -c_p\theta\frac{\pi}{\sigma}\left(\frac{dP}{d\pi}\right)_\sigma = -c_p\theta\left(\frac{dP}{d\sigma}\right)_\pi. \tag{7}$$

From (7) we obtain

$$\frac{\partial \Phi}{\partial P} = -c_p\theta, \tag{8}$$

which, following Arakawa and Suarez (1983), is the form used in the model.

The thermodynamic equation is written in flux form to facilitate the derivation of a θ-conserving differencing scheme:

$$\frac{\partial(\pi\theta)}{\partial t} = -\nabla_\sigma \cdot (\pi\mathbf{v}\theta) - \frac{\partial(\pi\dot\sigma\theta)}{\partial\sigma} + \frac{\pi Q}{c_p P}, \tag{9}$$

where Q is the diabatic heating per unit mass.

In addition to the equations of motion, the Aries/GEOS Dynamical Core computes tendencies for an arbitrary number of atmospheric contituents, such as water vapor and ozone. These are also written in flux form:

$$\frac{\partial(\pi q^{(k)})}{\partial t} = -\nabla_\sigma \cdot (\pi\mathbf{v}q^{(k)}) - \frac{\partial(\pi\dot\sigma q^{(k)})}{\partial\sigma} + \pi\mathcal{S}^{(k)}, \tag{10}$$

where $q^{(k)}$ is the specific mass of the kth constituent, and $\mathcal{S}^{(k)}$ is its source per unit mass of air.

The momentum equation is written in "vector-invariant" form, as in Sadourney (1975) and Arakawa and Lamb (1981), to facilitate the derivation of an energy- and enstrophy-conserving differencing scheme:

$$\begin{aligned}\frac{\partial \mathbf{v}}{\partial t} &= -(f + \zeta)\mathbf{k}\times\mathbf{v} - \dot\sigma\frac{\partial\mathbf{v}}{\partial\sigma} - \nabla_\sigma(\Phi + K) - c_p\theta\nabla_\sigma P - \frac{g}{\pi}\frac{\partial T}{\partial\sigma}, \tag{11}\\ &= -\eta\,\mathbf{k}\times(\pi\mathbf{v}) - \dot\sigma\frac{\partial\mathbf{v}}{\partial\sigma} - \nabla_\sigma(\Phi + K) - c_p\theta\left(\frac{dP}{d\pi}\right)_\sigma\nabla\pi - \frac{g}{\pi}\frac{\partial T}{\partial\sigma}, \tag{12}\end{aligned}$$

3

where

$$\eta = \frac{(f + \zeta)}{\pi}$$

is an "external" potential vorticity, f is the Coriolis parameter, $\mathbf{k}$ is the unit vector in the vertical,

$$\zeta \equiv \nabla_\sigma \times \mathbf{v}$$

is the vertical component of the vorticity along σ surfaces,

$$K \equiv \frac{1}{2}(\mathbf{v} \cdot \mathbf{v})$$

is the kinetic energy per unit mass, g is the acceleration of gravity, and $\mathcal{T}$ is the horizontal frictional stress.

2.1   Horizontal and Vertical Discretization

The GEOS-1 GCM is constructed in the horizontal using the staggered Arakawa C-grid and employs Version 1 of the Aries/GEOS Dynamical Core for the finite-differencing algorithm. The Aries/GEOS Dynamical Core is a plug-compatible dynamics module which is used at both the DAO in the GEOS GCM as well as at the Climate and Radiation Branch in the Aries GCM. The Aries GCM has been extensively used in many climate and coupled ocean/atmosphere simulations (eg. Schubert et al. 1993, Higgins and Schubert, 1993). Version 1 of the Aries/GEOS Dynamical Core is the second-order energy and potential enstrophy conserving scheme of Sadourny described by Burridge and Haseler (1977), while Version 2, to be used in subsequent versions of the GEOS GCM, is the fourth-order formulation described in Suarez and Takacs, 1994. This scheme conserves total energy and potential enstrophy for the non-divergent component of the flow in the shallow water equations.

The Aries/GEOS Dynamical Core uses a Lorenz or unstaggered vertical grid in generalized sigma coordinates. The vertical differencing scheme is that of Arakawa and Suarez (1983) which ensures that:

- The pressure gradient force generates no circulation of vertically integrated momentum along a contour of surface topography
- The finite-difference analogues of the energy-conversion term have the same form in the kinetic energy and thermodynamic equations
- The global mass integral of the potential temperature is conserved under adiabatic processes
- The hydrostatic equation for the lowest thickness has a local form
- The hydrostatic equation is exact for vertically isentropic atmospheres

4

- The pressure-gradient force is exact for three-dimensionally isentropic atmospheres

The GEOS-1 AMIP simulation was run using a global 4° x 5° latitude/longitude grid in the horizontal, together with 20 sigma levels in the vertical. The GEOS-1 DAS 5-year re-analysis was run using 2° x 2.5° horizontal resolution. The vertical distribution of the sigma levels is such as to provide enhanced resolution in the planetary boundary layer and at the jet level. The model top pressure was prescribed to be 10 mb with a rigid lid. For a surface pressure of 1000 mb, the lowest sigma level is at 994 mb while the highest sigma level is at 19 mb. There are 5 sigma levels below 800 mb, and 7 sigma levels above 200 mb. The sigma-level pressure used in the 20-level GEOS-1 GCM are shown in Figure 1.

2.2 Time Integration Scheme

The GEOS GCM has the ability to use the Matsuno time integration scheme or the Leapfrog time integration scheme together with an Asselin (1972) time filter. The GEOS GCM multi-year simulations have all been run using the Leapfrog time scheme together with the Asselin averaging parameter equal to 0.05. The GEOS-DAS 5-year Re-analysis used the Matsuno time scheme. The GEOS GCM employs a somewhat unique method for incorporating adjustments due to diabatic processes (ie, moist convection, radiation and turbulence) and the analysis increments during an assimilation. At every model time step, all prognostic fields are updated due to both dynamical and sub-grid scale diabatic processes, shown schematically using the Leapfrog time scheme for an arbitrary prognostic field q as:

$$q^{n+1} = q^{n-1} + 2\Delta t \left(\frac{\partial q^n}{\partial t} \right)_{total} \tag{13}$$

where

$$
\begin{aligned}
\left(\frac{\partial q^n}{\partial t} \right)_{total} =\ & \left(\frac{\partial q^n}{\partial t} \right)_{Dynamics} + \left(\frac{\partial q^{n-1}}{\partial t} \right)_{Shapiro\ Filter} \\
& + \left(\frac{\partial q}{\partial t} \right)_{Moist\ Processes} + \left(\frac{\partial q}{\partial t} \right)_{Turbulence} \\
& + \left(\frac{\partial q}{\partial t} \right)_{Longwave\ Radiation} + \frac{S_0}{R_a^2} \cdot cos\phi_z \left(\frac{\partial q}{\partial t} \right)_{Shortwave\ Radiation} \\
& + \left(\frac{\partial q}{\partial t} \right)_{Analysis\ Increment}
\end{aligned}
\tag{14}
$$

with S_0 defined as the solar contant, R_a as the earth-sun distance in Astronomical Units, and $cos\phi_z$ as the cosine of the zenith angle. The Dynamics and Shapiro Filter time tendencies are updated every model time step. The diabatic time tendencies are computed
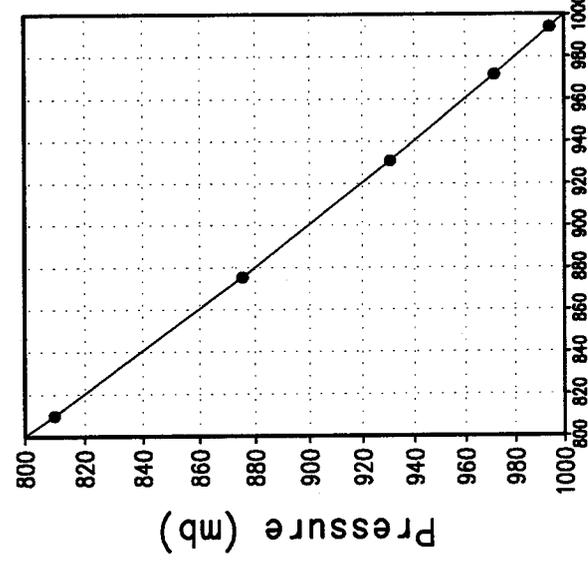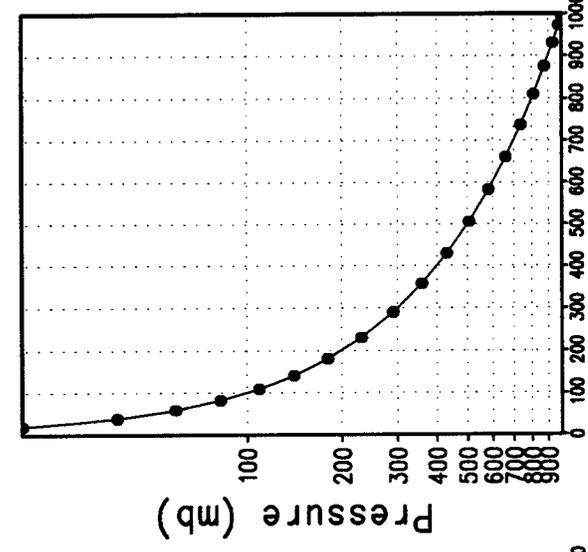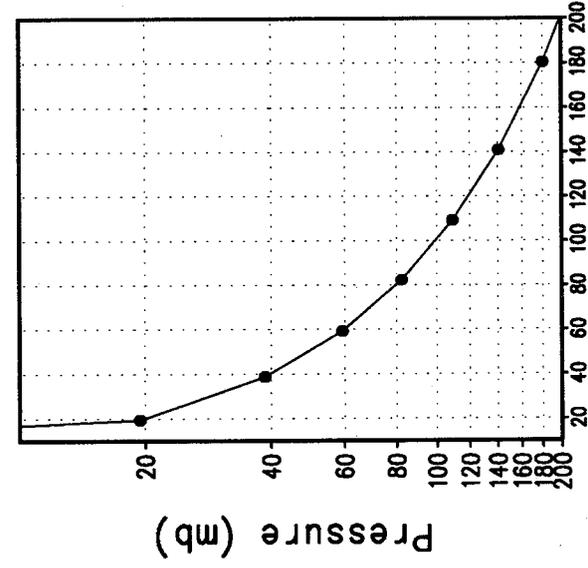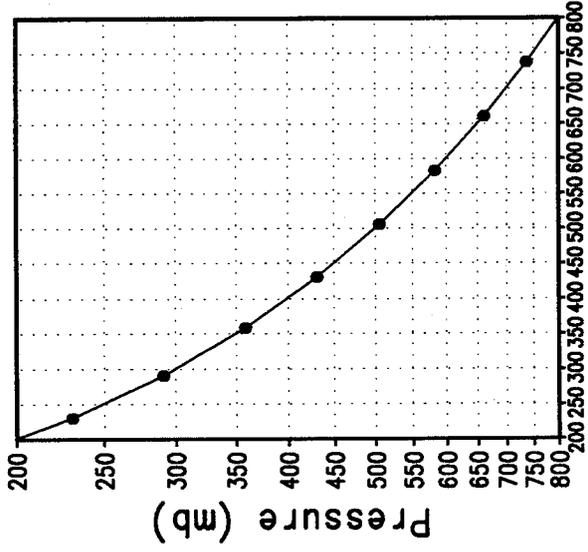
Figure 1: Sigma-level pressures used in the 20-level GEOS-1 GCM.

(updated) at a time step appropriate to the physical parameterizations, and are held constant between Physics calls. The time tendency for Moist Convection is updated every 10 minutes, and for Turbulence every 30 minutes. The time tendency for Longwave Radiation is updated every 3 hours. Shortwave Radiation is updated once every three hours assuming a normalized incident solar radiation, and adjusted at every model time step by the true incident radiation. During GEOS-1 DAS assimilations, the Analysis Increment is updated every synoptic time period, or 6 hours. By gradually incorporating the diabatic adjustments during the model integration, shocks and dynamical imbalances are greatly reduced (cf. Bloom, et al. 1991).

2.3   Smoothing / Filling

An eighth- (sixteenth-) order Shapiro (1970) filter adjustment is computed for the winds, potential temperature, and specific humidity in conjunction with the 2° x 2.5° (4° x 5°) GEOS GCM in order to globally damp small-scale dispersive waves. In order to reduce the dynamical imbalances generated by intermittent use of the full filter, a Shapiro filter tendency for any quantity q is defined as:

$$\left(\frac{\partial q}{\partial t}\right)_{Shapiro\ Filter} = \frac{q^F - q}{\tau} \tag{15}$$

where q^F is the quantity after application of the full Shapiro filter, q is the unfiltered quantity, and τ is an adjustable time scale. Thus, a fraction $\frac{\Delta t}{\tau}$ of the full Shapiro filter is incorporated at each model timestep. In the GEOS-1 GCM, the time scale τ is equal to 1.5 hours, and has been chosen so as to remove the two-grid interval wave in about six hours. The Shapiro filter response function used in the 2° x 2.5° GEOS-1 GCM is shown in Figure 2. The GEOS-1 GCM also uses a high-latitude Fourier filter to avoid linear instability due to violation of the CFL condition for the Lamb wave and internal gravity waves near the poles. This polar filter is only applied to the time-tendencies of the prognostic fields, ie. winds, potential temperature, specific humidity, and surface pressure.

For the moisture equation, negative values computationally generated through advection are filled by "borrowing" from below while conserving the vertically integrated moisture, ie.,

$$\left(\int_{le+1}^{le-1} \rho q\,dz\right)_{final} = \left(\int_{le+1}^{le-1} \rho q\,dz\right)_{initial} \tag{16}$$

Using the hydrostatic relation $\rho\delta z = -\frac{\delta p}{g} = -\frac{\pi}{g}\delta\sigma$, we may write
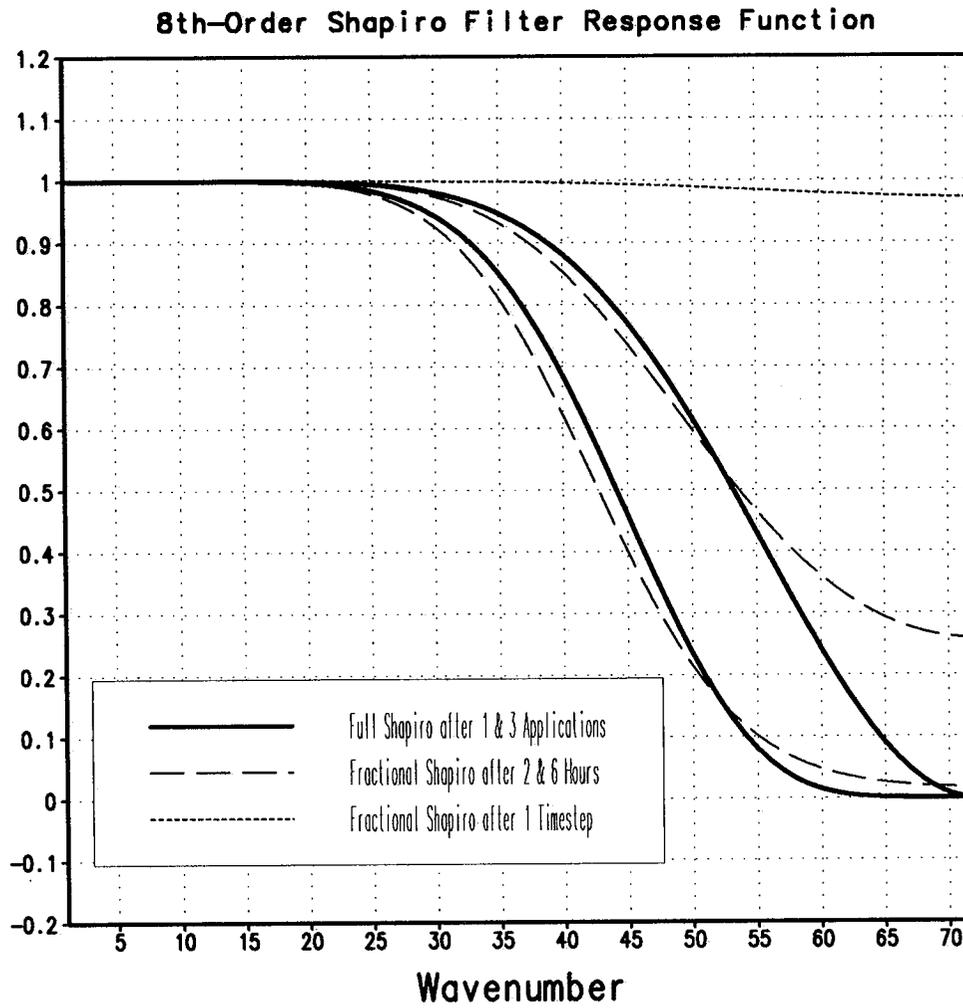
Figure 2: Shapiro filter response function used in the 2° x 2.5° GEOS-1 GCM.

$$\left(\int_{le+1}^{le-1} \pi q d\sigma \right)_{final} = \left(\int_{le+1}^{le-1} \pi q d\sigma \right)_{initial} \tag{17}$$

Approximating equaton (17) by

$$\left(\pi q_l \Delta\sigma_l + \pi q_{l-1} \Delta\sigma_{l-1} \right)_{final} = \left(\pi q_l \Delta\sigma_l + \pi q_{l-1} \Delta\sigma_{l-1} \right)_{initial} \tag{18}$$

an expression for the updated moisture at level l is given by

$$\pi q_{l_{final}} = \left(\pi q_l + \pi q_{l-1} \frac{\Delta\sigma_{l-1}}{\Delta\sigma_l} \right)_{initial} - \left(\pi q_{l-1} \frac{\Delta\sigma_{l-1}}{\Delta\sigma_l} \right)_{final} \tag{19}$$

Assuming that πq_{l-1} is initially negative, we require that its final value is set to zero. Thus

$$
\begin{aligned}
\pi q_{l-1_{final}} &= 0, \\
\pi q_{l_{final}} &= \left(\pi q_l + \pi q_{l-1} \frac{\Delta\sigma_{l-1}}{\Delta\sigma_l} \right)_{initial}
\end{aligned}
\tag{20}
$$

This process is repeated until the lowest level is reached. If the resulting πq_{nlay} is negative, the mass-weighted specific humidity in the lowest model level is simply set to zero.

3 Atmospheric Physics

3.1 Moist Convective Processes

3.1.1 Sub-grid and Large-scale Convection

Sub-grid scale penetrative and shallow cumulus convection are parameterized using the Relaxed Arakawa Schubert (RAS) scheme of Moorthi and Suarez (1992), which is a simplified Arakawa Schubert type scheme. The RAS scheme predicts mass fluxes from cloud types which have different entrainment rates and levels of neutral bouyancy, depending on the properties of the large scale environment.

The thermodynamic variables that are used in RAS to describe the grid scale vertical profile are the dry static energy, $s = c_p T + gz$, the moist static energy, $h = c_p T + gz + Lq$, and the saturation moist static energy, $h^* = c_p T + gz + Lq^*$, where the superscript $*$ refers to the saturation value.

9

The conceptual model behind RAS depicts the cloud as a rising plume, entraining mass from the environment during ascent, and detraining mass at the level of neutral buoyancy. RAS assumes that the cloud mass flux, η, normalized by the cloud base mass flux, is a linear function of height, expressed as:

$$\frac{\partial \eta(z)}{\partial z} = \lambda \quad or \quad \frac{\partial \eta(P^\kappa)}{\partial P^\kappa} = -\frac{c_p}{g}\theta\lambda$$

where we have used the hydrostatic equation written in the form:

$$\frac{\partial z}{\partial P^\kappa} = -\frac{c_p}{g}\theta$$

The entrainment parameter, λ, characterizes a particular cloud type based on its detrainment level, and is obtained by assuming that the level of detrainment is the level of neutral buoyancy, ie., the level at which the moist static energy of the cloud, h_c, is equal to the saturation moist static energy of the environment, h^*. Following Moorthi and Suarez (1992), λ may be written as

$$\lambda = \frac{h_B - h_D^*}{\frac{c_p}{g}\int_{P_D}^{P_B} \theta(h_D^* - h)dP^\kappa},$$

where the subscript B refers to cloud base, and the subscript D refers to the detrainment level.

The convective instability is measured in terms of the cloud work function A, defined as the rate of change of cumulus kinetic energy. The cloud work function is related to the buoyancy, or the difference between the moist static energy in the cloud and in the environment:

$$A = \int_{P_D}^{P_B} \frac{\eta}{1+\gamma}\left[\frac{h_c - h^*}{P^\kappa}\right] dP^\kappa$$

where γ is $\frac{L}{c_p}\frac{\partial q^*}{\partial T}$ obtained from the Claussius Clapeyron equation, and the subscript c refers to the value inside the cloud.

To determine the cloud base mass flux, the rate of change of A in time *due to dissipation by the clouds* is assumed to approximately balance the rate of change of A *due to the generation by the large scale*. This is the quasi-equilibrium assumption, and results in an expression for m_B:

$$m_B = \frac{-\left.\frac{dA}{dt}\right|_{ls}}{K}$$

where K is the cloud kernel, defined as the rate of change of the cloud work function per unit cloud base mass flux, and is obtained by differentiating the expression for A in time. The rate of change of A due to the generation by the large scale is written as the difference between the current $A(t + \Delta t)$ and its value after the previous convective time step $A(t)$, divided by the time step. Since the convective parameterization is designed to nearly neutralize the instability, $A(t)$ is approximated as some (near zero) critical A_{crit}.

10

The predicted convective mass fluxes are used to solve grid-scale temperature and moisture budget equations to determine the impact of convection on the large scale fields of temperature (through latent heating and compensating subsidence) and moisture (through precipitation and detrainment):

$$\left.\frac{\partial \theta}{\partial t}\right|_c = \alpha R \frac{m_B}{c_p P^\kappa} g\eta \frac{\partial s}{\partial p}$$

and

$$\left.\frac{\partial q}{\partial t}\right|_c = \alpha R \frac{m_B}{L} g\eta \left(\frac{\partial h}{\partial p} - \frac{\partial s}{\partial p}\right)$$

where $\theta = \frac{T}{P^\kappa}$, and $P = (p/p_0)$.

As an approximation to a full interaction between the different allowable cloud types, many clouds are simulated frequently, each modifying the large scale environment some fraction α of the total adjustment. The parameterization thereby "relaxes" the large scale environment towards neutrality.

In addition to the RAS cumulus convection scheme, the GEOS-1 GCM employs a Kessler-type scheme for the re-evaporation of falling rain (Sud and Molod, 1988), which correspondingly adjusts the impact on the large scale environment by the factor R. The scheme accounts for the rainfall intensity, the drop size distribution, and the temperature, pressure and relative humidity of the surrounding air. The moisture deficit in any model layer into which the rain may re-evaporate is a free parameter.

Due to the increased vertical resolution in the Planetary Boundary Layer (PBL), the lowest two model layers are averaged to provide the sub-cloud layer for RAS (nominally 50 mb thick). Each time RAS is invoked (every ten simulated minutes), the possiblity for shallow convection is checked for the two layers just above cloud base. RAS also randomly chooses 10 other cloud-top levels for the possibility of convection, from just above cloud base to the model top layer.

Supersaturation or large-scale convection is defined in the GEOS GCM whenever the specific humidity in any grid-box exceeds its supersaturation value. The large-scale precipitation scheme rains at supersaturation, and re-evaporates during descent to partially saturate lower layers in a process that accounts for some simple microphysics.

3.1.2 Cloud Formation

Convective and large-scale cloudiness which is used for cloud-radiative interactions are determined diagnostically as part of the cumulus and large-scale parameterizations. The convective and large-scale cloud fractions are combined into two separate arrays for use in

the shortwave and longwave radiation packages, one array for random overlap (CLRO) and one array for maximum overlap (CLMO) cloudiness.

If convection occurs with a cloud-top pressure less than 400 mb, a cloud fraction equal to 1.0 is assigned into CLMO at the detrainment level. These tall convective towers are said to be maximumly overlapped, ie. they are radiatively correlated in the vertical. If shallow convection occurs with a detrainment level within 1 or 2 levels above the cloud base, a cloud fraction equal to 0.5 is assigned into CLRO, again at the detrainment level. These shallow clouds are not correlated in the vertical and are said to be randomly overlapped. No cloud fractions are prescribed to convection whose cloud-top is between 400 mb and 2 levels above cloud-base.

Supersaturation or large scale cloudiness is defined whenever the large scale precipitation scheme determines that the grid box at any level becomes supersaturated. In order to ensure that at any instant the total cloud fraction be less than or equal to 1.0, supersaturation clouds are only prescribed when there are no deep convective clouds. Under such conditions, the grid box is assumed to be instantaneously fully covered with randomly overlapped clouds, with a cloud fraction of 1.0 being assigned into CLRO.

3.2 Radiation

The parameterization of radiation includes both shortwave radiation and longwave radiation in the GEOS-1 GCM. A single model "sponge" layer is inserted into the GEOS-1 GCM above P_{Top} with a temperature equal to the GCM's first level temperature. This is done in order to avoid exposing the first GCM level to a zero downward thermal flux condition at P_{Top}. Radiative fluxes are calculated at each model edge-level in both up and down directions. The heating rates/cooling rates are then obtained from the vertical divergence of the net radiative fluxes.

The net flux is

$$F = F^\uparrow - F^\downarrow$$

where F is the net flux, $F^\uparrow$ is the upward flux and $F^\downarrow$ is the downward flux.

The heating rate due to the divergence of the radiative flux is given by

$$\frac{\partial \rho c_p T}{\partial t} = -\frac{\partial F}{\partial z}$$

or

$$\frac{\partial T}{\partial t} = \frac{g}{c_p \pi} \frac{\partial F}{\partial \sigma}$$

where g is the accelation due to gravity and c_p is the heat capacity of air at constant pressure.

The infrared and solar radiation parameterizations employed in the GEOS-1 GCM follow closely those described by Harshvardhan et al. (1987). The time tendency for Longwave Radiation is updated every 3 hours. The time tendency for Shortwave Radiation is updated once every three hours assuming a normalized incident solar radiation, and subsequently modified at every model time step by the true incident radiation. For the AMIP simulations, the GEOS-1 GCM used the AMIP-prescribed solar constant value of 1365 W/m^2 and a CO_2 mixing ratio of 345 ppm. For the 5-year GEOS-DAS re-analysis, a solar constant value of 1380 W/m^2 was used together with a CO_2 mixing ratio value of 330 ppm. For the ozone mixing ratio, monthly mean zonally averaged climatological values specified as a function of latitude and height (Rosenfield, et al., 1987) are linearly interpolated to the current time.

3.2.1 Shortwave Radiation

The parameterization of heating due to shortwave radiation is an extension of that developed by Lacis and Hansen (1974). The documentation of the computational aspects of the scheme are given in Davis (1982). Harshvardhan improved the treatment of the cloud scattering by allowing it to depend on the solar zenith angle. Two major absorbers, H_2O and O_3, are considered in the scheme. Radiative heating by water vapor absorption is modeled in the 0.7-0.4 μm region. The total absoption of the ozone includes the absoption of visible radiation by the Chappuis bands (450-750 nm) and the absorption of ultraviolet radiation by the Hartly (240-280 nm) and Huggins bands (280-360 nm). For a cloudy atmosphere, the Meadow-Weaver (1980) modified Eddington approximation is adopted to solve the radiative transfer equation in a scattering medium. The multiple-scattering computation with the k-distribution functions is used to calculate the cloudy-sky water absorption.

3.2.2 Longwave Radiation

The parameterization of longwave radiation employs a wide band model. Four broadband transmissions have been used in the model. The parameterization of the H_2O, containing the two water bands at 15 μm and 9.6 μm, is calculated using the method of Chou (1984) based on the water vapor line and water vapor e-type absorption approximations. The CO_2 band employs the scheme of Chou and Peng (1983) which seperates the band wing and band center scaled paths. The O_3 parameterization approach applies the formulation of Rosenfield et al. (1987), which modifies the line width used by Rodgers (1968) to include the affects of Doppler broadening.

3.2.3 Cloud-Radiation Interaction

The cloud fraction values produced by the Moist Convective Processes are used for cloud-radiation interactions as a means for evaluating clear line-of-site probabilities and effective optical thicknesses.

If we define the time-averaged random and maximum overlapped cloudiness as CLRO and CLMO respectively, then the probability of clear sky associated with random overlapped clouds at any level is (1-CLRO) while the probability of clear sky associated with maximum overlapped clouds at any level is (1-CLMO). The total clear sky probability is given by (1-CLRO)*(1-CLMO), thus the total cloud fraction at each level may be obtained by 1-(1-CLRO)*(1-CLMO).

At any given level, we may define the clear line-of-site probability by appropriately accounting for the maximum and random overlap cloudiness. The clear line-of-site probability is defined to be equal to the product of the clear line-of-site probabilities associated with random and maximum overlap cloudiness. The clear line-of-site probability $C(p, p')$ associated with maximum overlap clouds, from the current pressure p to the model top pressure, $p' = p_{top}$, or the model surface pressure, $p' = p_{surf}$, is simply 1.0 minus the largest maximum overlap cloud value along the line-of-site, ie.

$$1 - MAX_p^{p'} (CLMO_p)$$

Thus, even in the time-averaged sense it is assumed that the maximum overlap clouds are correlated in the vertical. The clear line-of-site probability associated with random overlap clouds is defined to be the product of the clear sky probabilities at each level along the line-of-site, ie.

$$\prod_{p}^{p'} (1 - CLRO_p)$$

The total cloud fraction at a given level associated with a line- of-site calculation is given by

$$1 - \left(1 - MAX_p^{p'} [CLMO_p]\right) \prod_{p}^{p'} (1 - CLRO_p)$$

The GEOS-1 GCM cloud optical thicknesses are specified based on cloud type and temperature. The "maximum overlap" clouds are assigned an optical thickness of 0.16 km^{-1}

14

for the shortwave radiative feedback. The "random overlap" clouds are assigned an optical thickness based on an empirical relation between local temperature and optical thickness. The relation gives a thicker cloud when the temperature is higher and is expressed:

$$\tau = \begin{cases} 0 & \text{for} \quad T < 190.66 \\ (T - 190.66)^2 * 2x10^{-6} & \text{for} \quad 190.66 < T \leq 263.16 \\ 6.95x10^{-3} * T - 1.82 & \text{for} \quad 263.16 < T \leq 273.38 \\ 0.08 & \text{for} \quad 273.38 < T \end{cases}$$

The relation for the range $190.66 < T \leq 263.16$ is from Platt and Harshvardahn, 1988. The optical thickness for the longwave radiative feedback is assumed to be 75% of these values.

The entire Moist Convective Processes Module is called with a frequency of 10 minutes. The cloud fraction values are time-averaged over the period between Radiation calls (every 3 hours). Therefore, in a time-averaged sense, both random overlap and maximum overlap cloudiness can exist in a given grid-box.

3.3 Turbulence

The GEOS GCM turbulence parameterization consists of elements which handle vertical diffusion (Helfand and Labraga, 1988) and surface fluxes of heat, moisture and momentum (Helfand, et al, 1991, and Helfand and Schubert, 1994). The parameterization is invoked every 30 minutes, and employs a backward-implicit iterative time scheme with an internal time step of 5 minutes. The vertical regime is divided into a free atmosphere, a surface layer, and a viscous sub-layer above the surface roughness elements. The turbulent eddy fluxes are calculated using a variety of methods depending on the vertical location in the atmosphere.

Turbulent eddy fluxes of momentum, heat and moisture in the surface layer are calculated using stability-dependant bulk formulae based on Monin-Obukhov similarity functions. For an unstable surface layer, the chosen stability functions are the KEYPS function (Panofsky, 1973) for momentum, and its generalization for heat and moisture. The function for heat and moisture assures non-vanishing heat and moisture fluxes as the wind speed approaches zero. For a stable surface layer, the stability functions are those of Clarke (1970), slightly modified for the momemtum flux. The moisture flux also depends on a specified evapotranspiration coefficient, set to unity over oceans and dependant on the climatological ground wetness over land. The gradients in the viscous sublayer are based on Yaglom and Kader (1974). The surface roughness length over oceans is computed as an interpolation between the functions of Large and Pond (1981) for high winds and of Kondo (1975) for weak winds, and over land is specified from the climatology of Dorman and Sellers (1989).

Above the surface layer, turbulent fluxes of momentum, heat and moisture are calculated by the Level 2.5 Mellor-Yamada type closure scheme of Helfand and Labraga (1988), which predicts turbulent kinetic energy and determines the eddy transfer coefficients used for vertical diffusion.

3.3.1 Planetary Boundary Layer

The Planetary Boundary Layer (PBL) height is diagnosed by the parameterization as the level at which the turbulent kinetic energy is reduced to a tenth of its surface value, and generally occurs within the first two to four sigma levels above the surface (sigma equal 0.994 to about sigma equal 0.875).

4 Boundary Conditions

The conditions at the lower boundary which are not explicitly predicted during execution must be specified from observed fields. Boundary condition data sets are available at present in monthly mean increments, at the model's 4° x 5° and 2° x 2.5° resolutions, for either climatological or yearly varying conditions (beginning from 1979). Monthly mean values are interpolated during each model timestep to the current time. Future model versions will incorporate boundary conditions at higher spatial (1° x 1°) and temporal resolutions.

4.1 Orography

Surface geopotential heights are provided from an averaging of the Navy 10 minute by 10 minute dataset supplied by the National Center for Atmospheric Research (NCAR) to the model's grid resolution. For the 2° x 2.5° GEOS-1 GCM, the averaged topography was then passed through a Lanczos (1966) filter in both dimensions which removes the smallest scales while inhibiting Gibbs phenomena. Negative values in the topography resulting from the filtering procedure were *not* filled.

In one dimension, we may define a cyclic function in x as:

$$f(x) = \frac{a_0}{2} + \sum_{k=1}^{N} \left(a_k \cos(kx) + b_k \sin(kx) \right) \tag{21}$$

where $N = \frac{IM}{2}$ and IM is the total number of points in the x direction. Defining $\Delta x = \frac{2\pi}{IM}$, we may define the average of $f(x)$ over a $2\Delta x$ region as:

$$\overline{f(x)} = \frac{1}{2\Delta x} \int_{x-\Delta x}^{x+\Delta x} f(x')dx' \tag{22}$$

Using equation (21) in equation (22) and integrating, we may write:

$$\overline{f(x)} = \frac{a_0}{2} + \frac{1}{2\Delta x} \sum_{k=1}^{N} \left[a_k \frac{\sin(kx')}{k} \bigg/ \bigg|_{x-\Delta x}^{x+\Delta x} - b_k \frac{\cos(kx')}{k} \bigg/ \bigg|_{x-\Delta x}^{x+\Delta x} \right] \tag{23}$$

or

$$\overline{f(x)} = \frac{a_0}{2} + \sum_{k=1}^{N} \frac{\sin(k\Delta x)}{k\Delta x} \left(a_k \cos(kx) + b_k \sin(kx) \right) \tag{24}$$

Thus, the Fourier wave amplitudes are simply modified by the Lanczos filter response function $\frac{\sin(k\Delta x)}{k\Delta x}$. This may be compared with an mth-order Shapiro (1970) filter response function, defined as $1 - \sin^m(\frac{k\Delta x}{2})$, shown in Figure 3.

4.2   Land-Sea-Ice Surface Type

The determination of the land or sea category of surface type was made from NCAR's 10 minute by 10 minute Navy topography dataset, which includes information about the percentage of water-cover at any point. The data were averaged to the model's 4° x 5° and 2° x 2.5° grid resolutions. Any grid-box whose averaged water percentage was ≥ 60% was defined as a water point. Permanent ice or glacier points for the 2° x 2.5° grid were identified from the climatology of Parkinson's satellite-derived fields (NASA SP 459: Arctic Sea Ice, 1973-1976, and NASA SP 489: Antartic Sea Ice, 1973-1976). The Land/Water masks and topography used for the 4° x 5° and 2° x 2.5° GEOS-1 GCM grids are shown in Figure 4 and Figure 5, respectively.

4.3   Sea Surface Temperature

Climatological sea surface temperatures for the 4° x 5° and 2° x 2.5° grid resolutions are interpolated from the data of Reynolds, 1988. Yearly varying monthly mean data for the 4° x 5° grid are from the AMIP specified monthly mean fields (Gates, 1992), and for the 2° x 2.5° grid are interpolated from Reynolds' (1988) data. Monthly mean data are interpolated linearly to the current time at every GCM timestep.

17
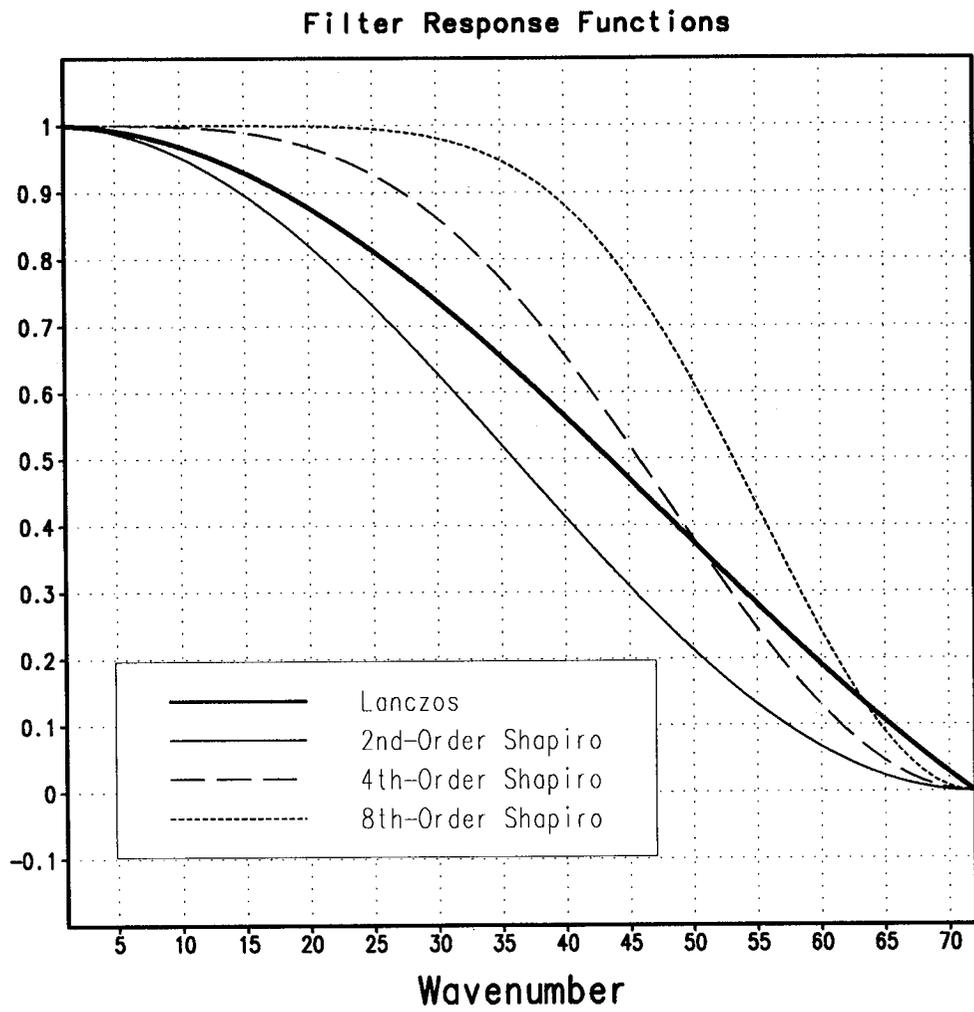
Figure 3: Comparison between the Lanczos and mth-order Shapiro filter response functions for $m = 2$, 4, and 8.
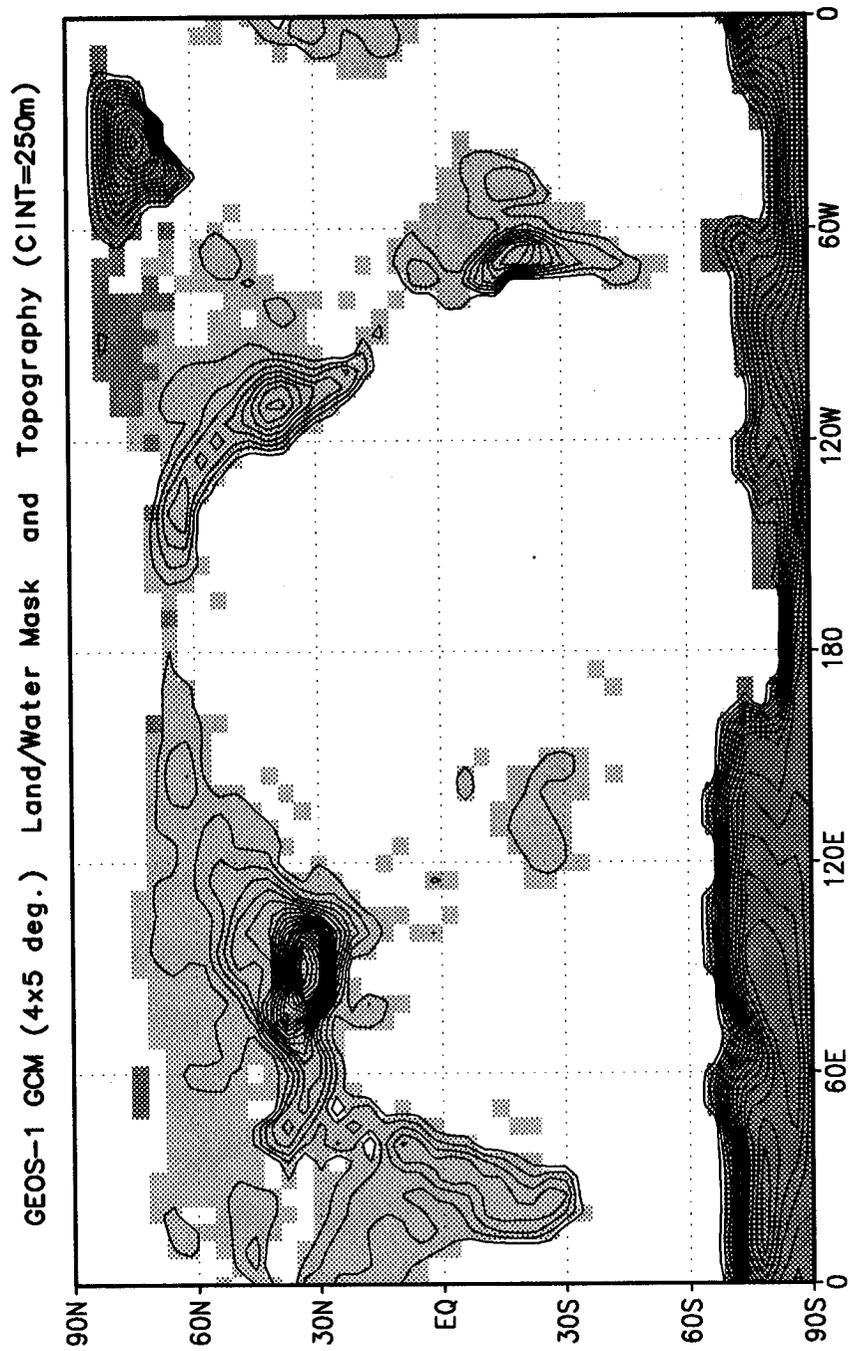
Figure 4: GEOS-1 GCM Land/Water Mask and Topography used at 4° x 5° resolution. Light grey shading denotes land surfaces, while dark grey denotes permanent glacier.
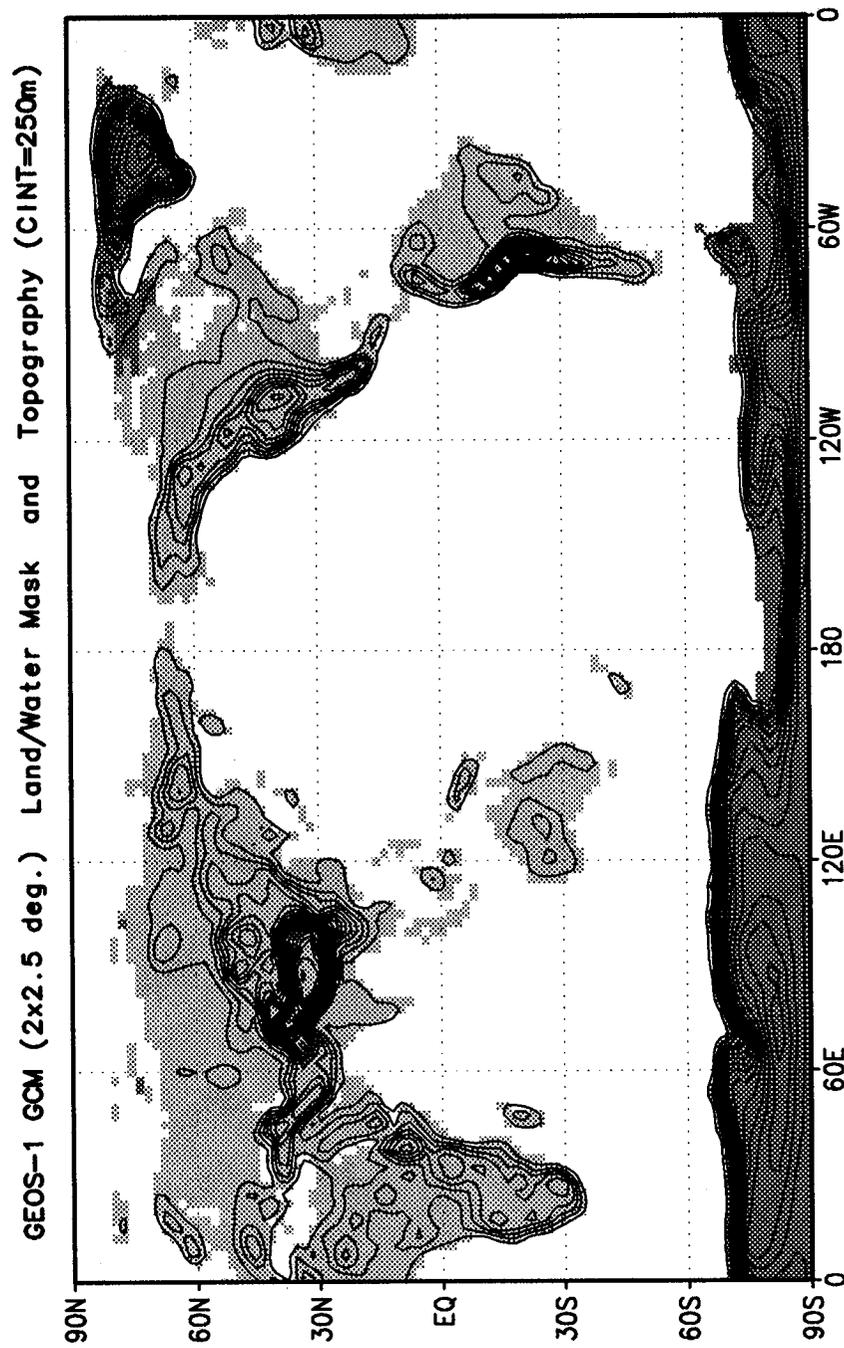
Figure 5: GEOS-1 GCM Land/Water Mask and Topography used at 2° x 2.5° resolution. Light grey shading denotes land surfaces, while dark grey denotes permanent glacier.

4.4 Sea Surface Roughness

Ocean surface roughness is computed iteratively as a function of wind stress in the Turbulence Scheme.

4.5 Albedo

Monthly mean albedos over land are data of Posey and Clapp (1964), with modifications as described in Kitzmiller (1979). Over oceans the albedo is specified as 0.07, and over ice (sea ice or glaciers) 0.80. Monthly mean values are linearly interpolated to the current time.

4.6 Sea Ice

Monthly mean sea ice extent were interpolated to the model's 4° x 5° and 2° x 2.5° grid resolutions from the AMIP monthly mean fields. Monthly mean data are linearly interpolated to the current time. Any sea ice is assumed to be three meters thick, and the conduction through sea ice is accounted for in the Turbulence Parameterization as part of the surface energy budget.

4.7 Snow Cover

Snow cover is assumed to occur when the ground temperature over the land is less than freezing in conjunction with climatological albedo values greater than 0.4. Surface conductive characteristics are adjusted accordingly.

4.8 Land Surface

Monthly varying climatological roughness lengths are specified for each land surface vegetation type from Dorman and Sellers (1989). A gridded surface vegetation type designation is from Sud, et al. (1990). Monthly mean values are interpolated linearly to the model's current time. The soil wetness climatology and yearly varying fields are from the monthly estimates of Schemm, et al. (1992) based on the procedure developed by Mintz and Serafini (1984) using an inverted single layer "bucket" model together with observed fields of surface air temperature and precipitation. Values are interpolated linearly to the model's current time. Ground temperature over land is predicted from a surface energy balance equation.

Part II

GEOS-1 GCM: Diagnostics

5 Introduction

This section of the documentation describes the Diagnostics Utilities available within the Goddard Earth Observing Systems (GEOS) General Circulation Model (GCM). In addition to a description on how to set and extract diagnostic quantities, this document also provides a comprehensive list of all available diagnostic quantities and a short description of how they are computed. It should be noted that this document is not intended to be a complete documentation of the various physical parameterization schemes used in the GEOS GCM, and the reader should refer to original publications for further insight.

6 Diagnostic Overview

A large selection of model diagnostics is available in the GEOS GCM. At the time of this writing there are 119 different diagnostic quantities which can be enabled for an experiment. As a matter of philosophy, no diagnostic is enabled as default, thus each user must specify the exact diagnostic information required for an experiment. This is accomplished by enabling the specific diagnostic of interest cataloged in the Diagnostic Menu (see Section 7). The Diagnostic Menu is a hard-wired enumeration of diagnostic quantities available within the GEOS GCM. Diagnostics are internally referred to by their associated number in the Diagnostic Menu. Once a diagnostic is enabled, the GEOS GCM will continually increment an array specifically allocated for that diagnostic whenever the associated process for the diagnostic is computed. Separate arrays are used both for the diagnostic quantity and its diagnostic counter which records how many times each diagnostic quantity has been computed.

There are several utilities within the GEOS GCM available to users to enable, disable, clear, and retrieve model diagnostics, and may be called from any user-supplied application and/or output routine. The available utilities and the CALL sequences are listed below.

SETDIAG: This subroutine enables a diagnostic from the Diagnostic Menu, meaning that space is allocated for the diagnostic and the model routines will increment the diagnostic value during execution. This routine is useful when called from either user application routines or user output routines, and is the underlying interface between the user and the desired diagnostic. The diagnostic is referenced by its diagnostic number from the menu, and its calling sequence is given by:

PROCEDING PAGE BLANK NOT FILMED

CALL SETDIAG (NUM)

where   NUM   = Diagnostic number from menu

GETDIAG: This subroutine retrieves the value of a model diagnostic. This routine is particulary useful when called from a user output routine, although it can be called from an application routine as well. This routine returns the time-averaged value of the diagnostic by dividing the current accumulated diagnostic value by its corresponding counter. This routine does not change the value of the diagnostic itself, that is, it does not replace the diagnostic with its time-average. The calling sequence for this routine is givin by:

CALL GETDIAG (LEV,NUM,QTMP,UNDEF)

where   LEV   = Sigma Level at which the diagnostic is desired
               NUM   = Diagnostic number from menu
               QTMP   = Time-Averaged Diagnostic Output
               UNDEF   = Fill value to be used when diagnostic is undefined

CLRDIAG: This subroutine initializes the values of model diagnostics to zero, and is particularly useful when called from user output routines to re-initialize diagnostics during the run. The calling sequence is:

CALL CLRDIAG (NUM)

where   NUM   = Diagnostic number from menu

ZAPDIAG: This entry into subroutine SETDIAG disables model diagnostics, meaning that the diagnostic is no longer available to the user. The memory previously allocated to the diagnostic is released when ZAPDIAG is invoked. The calling sequence is given by:

CALL ZAPDIAG (NUM)

where   NUM   = Diagnostic number from menu

DIAGSIZE: We end this section with a discussion on the manner in which computer memory is allocated for GEOS diagnostics. All GEOS GCM diagnostic quantities are

stored in the single diagnostic array QDIAG which is located in the DIAG COMMON, having the form:

COMMON /DIAG/ NDIAG_MAX,QDIAG(IM,JM,1)

where NDIAG_MAX is an Integer variable which should be set equal to the number of enabled diagnostics, and QDIAG is a three-dimensional array. The first two-dimensions of QDIAG correspond to the horizontal dimension of a given diagnostic, while the third dimension of QDIAG is used to identify specific diagnostic types. In order to minimize the maximum memory requirement used by the model, the GEOS GCM libraries are compiled with room for only one horizontal diagnostic array, as shown in the above example. In order for the User to enable more than 1 two-dimensional diagnostic, the size of the DIAG COMMON must be expanded to accomodate the desired diagnostics. This can be accomplished by including the COMMON DIAG in the User's Application program, with the QDIAG array properly dimensioned. Another method, currently used by DAO production routines, involves the use of the DIAGSIZE subroutine. Using the DIAGSIZE subroutine is a convenient method to allocate just enough permanent memory during a run to be used for diagnostic storage. All production DAO applications contain a call to subroutine DIAGSIZE, which expands the size of the DIAG COMMON to include the total number of surface and upper-air diagnostics the User has enabled. An example of the DIAGSIZE subroutine is shown below:

```
subroutine diagsize
parameter (   IM   = 144 )
parameter (   JM   = 91  )
parameter ( NLAY   = 20  )
parameter ( ndiags = 11  )
parameter ( ndiagu =  4  )
common /diag/ ndiag_max,qdiag(im,jm,ndiags+ndiagu*nlay)
ndiag_max = ndiags + ndiagu*nlay
return
end
```

7 GEOS GCM Diagnostic Menu

N	NAME	UNITS	LEVELS	DESCRIPTION
1	UFLUX	$Newton/m^2$	1	Surface U-Wind Stress on the atmosphere
2	VFLUX	$Newton/m^2$	1	Surface V-Wind Stress on the atmosphere
3	HFLUX	$Watts/m^2$	1	Surface Flux of Sensible Heat
4	EFLUX	$Watts/m^2$	1	Surface Flux of Latent Heat
5	QICE	$Watts/m^2$	1	Heat Conduction through Sea-Ice
6	RADLWG	$Watts/m^2$	1	Net upward LW flux at the ground
7	RADSWG	$Watts/m^2$	1	Net downward SW flux at the ground
8	RI	deg/day	NLAY	Richardson Number
9	CT	m/sec	1	Surface Drag coefficient for T and Q
10	CU	m/sec	1	Surface Drag coefficient for U and V
11	ET	m^2/sec	NLAY	Diffusivity coefficient for T and Q
12	EU	m^2/sec	NLAY	Diffusivity coefficient for U and V
13	TURBU	$m/sec/day$	NLAY	U-Momentum Changes due to Turbulence
14	TURBV	$m/sec/day$	NLAY	V-Momentum Changes due to Turbulence
15	TURBT	deg/day	NLAY	Temperature Changes due to Turbulence
16	TURBQ	$g/kg/day$	NLAY	Specific Humidity Changes due to Turbulence
17	MOISTT	deg/day	NLAY	Temperature Changes due to Moist Processes
18	MOISTQ	$g/kg/day$	NLAY	Specific Humidity Changes due to Moist Processes
19	RADLW	deg/day	NLAY	Net Longwave heating rate for each level
20	RADSW	deg/day	NLAY	Net Shortwave heating rate for each level
21	PREACC	mm/day	1	Total Precipitation
22	PRECON	mm/day	1	Convective Precipitation
23	TUFLUX	$Newton/m^2$	NLAY	Turbulent Flux of U-Momentum
24	TVFLUX	$Newton/m^2$	NLAY	Turbulent Flux of V-Momentum
25	TTFLUX	$Watts/m^2$	NLAY	Turbulent Flux of Sensible Heat
26	TQFLUX	$Watts/m^2$	NLAY	Turbulent Flux of Latent Heat
27	CN	m/sec	1	Neutral Drag Coefficient
28	WINDS	m/sec	1	Surface Wind Speed
29	DTSRF	deg	1	Air/Surface virtual temperature difference
30	TG	deg	1	Ground temperature
31	TS	deg	1	Surface air temperature (Adiabatic from lowest model layer)
32	DTG	deg	1	Ground temperature adjustment

N	NAME	UNITS	LEVELS	DESCRIPTION
33	QG	g/kg	1	Ground specific humidity
34	QS	g/kg	1	Saturation surface specific humidity
35	TGRLW	deg	1	Instantaneous ground temperature used as input to the Longwave radiation subroutine
36	ST4	$Watts/m^2$	1	Upward Longwave flux at the ground (σT^4)
37	OLR	$Watts/m^2$	1	Net upward Longwave flux at the top of the model
38	OLRCLR	$Watts/m^2$	1	Net upward clearsky Longwave flux at the top of the model
39	LWGCLR	$Watts/m^2$	1	Net upward clearsky Longwave flux at the ground
40	LWCLR	deg/day	NLAY	Net clearsky Longwave heating rate for each level
41	TLW	deg	NLAY	Instantaneous temperature used as input to the Longwave radiation subroutine
42	SHLW	g/g	NLAY	Instantaneous specific humidity used as input to the Longwave radiation subroutine
43	OZLW	g/g	NLAY	Instantaneous ozone used as input to the Longwave radiation subroutine
44	CLMOLW	$0-1$	NLAY	Maximum overlap cloud fraction used in the Longwave radiation subroutine
45	CLROLW	$0-1$	NLAY	Random overlap cloud fraction used in the Longwave radiation subroutine
46	CLMOSW	$0-1$	NLAY	Maximum overlap cloud fraction used in the Shortwave radiation subroutine
47	CLROSW	$0-1$	NLAY	Random overlap cloud fraction used in the Shortwave radiation subroutine
48	RADSWT	$Watts/m^2$	1	Incident Shortwave radiation at the top of the atmosphere
49				Disabled
50				Disabled
51				Disabled
52	EVAP	mm/day	1	Surface evaporation
53	DPDT	mm/day	1	Total surface pressure tendency
54	ANALU	$m/sec/sec$	NLAY	Analysis $u-Wind$ increment
55	ANALV	$m/sec/sec$	NLAY	Analysis $v-Wind$ increment
56	ANALT	$mb\,deg/mb^\kappa/sec$	NLAY	Analysis $\pi\theta$ increment, $\theta = \frac{T}{p^\kappa}$
57	ANALQ	$mb*g/g/sec$	NLAY	Analysis πq increment
58	OMEGA	mb/day	NLAY	Vertical (Omega) velocity

N	NAME	UNITS	LEVELS	DESCRIPTION
59	DUDT	$m/sec/day$	NLAY	Total U-Wind tendency
60	DVDT	$m/sec/day$	NLAY	Total V-Wind tendency
61	DTDT	deg/day	NLAY	Total Temperature tendency
62	DQDT	$g/kg/day$	NLAY	Total Specific Humidity tendency
63	VORT	sec^{-1}	NLAY	Relative Vorticity
64				Disabled
65				Disabled
66				Disabled
67	USTAR	m/sec	1	Surface USTAR wind
68	Z0	m	1	Surface roughness
69	FRQTRB	$0-1$	NLAY-1	Frequency of Turbulence
70	PBL	mb	1	Planetary Boundary Layer depth
71	SWCLR	deg/day	NLAY	Net clearsky Shortwave heating rate for each level
72	OSR	$Watts/m^2$	1	Net downward Shortwave flux at the top of the model
73	OSRCLR	$Watts/m^2$	1	Net downward clearsky Shortwave flux at the top of the model
74	CLDMAS	$kg\,m/sec$	NLAY	Convective cloud mass flux
75	UAVE	m/sec	NLAY	Time-averaged $u - Wind$
76	VAVE	m/sec	NLAY	Time-averaged $v - Wind$
77	TAVE	deg	NLAY	Time-averaged $Temperature$
78	QAVE	g/g	NLAY	Time-averaged $Specific\,Humidity$
79				Disabled
80	PAVE	mb	1	Time-averaged $p_{surf} - p_{top}$
81	QQAVE	$(m/sec)^2$	NLAY	Time-averaged $Turbulent Kinetic Energy$
82	SWGCLR	$Watts/m^2$	1	Net downward clearsky Shortwave flux at the ground
83	ANALP	mb/sec	1	Analysis $Surface Pressure$ increment
84	SDIAG1		1	User-Defined Surface Diagnostic-1
85	SDIAG2		1	User-Defined Surface Diagnostic-2
86	UDIAG1		NLAY	User-Defined Upper-Air Diagnostic-1
87	UDIAG2		NLAY	User-Defined Upper-Air Diagnostic-2
88	DIABU	$m/sec/day$	NLAY	Total Diabatic forcing on $u - Wind$
89	DIABV	$m/sec/day$	NLAY	Total Diabatic forcing on $v - Wind$
90	DIABT	deg/day	NLAY	Total Diabatic forcing on $Temperature$
91	DIABQ	$g/kg/day$	NLAY	Total Diabatic forcing on $Specific\,Humidity$

N	NAME	UNITS	LEVELS	DESCRIPTION
92				Disabled
93				Disabled
94				Disabled
95				Disabled
96				Disabled
97				Disabled
98				Disabled
99				Disabled
100				Disabled
101				Disabled
102	VINTUQ	$m/sec \cdot g/kg$	1	Vertically integrated $u\,q$
103	VINTVQ	$m/sec \cdot g/kg$	1	Vertically integrated $v\,q$
104	VINTUT	$m/sec \cdot deg$	1	Vertically integrated $u\,T$
105	VINTVT	$m/sec \cdot deg$	1	Vertically integrated $v\,T$
106	CLDFRC	$0-1$	1	Total Cloud Fraction
107	QINT	gm/cm^2	1	Precipitable water
108	U2M	m/sec	1	U-Wind at 2 meters
109	V2M	m/sec	1	V-Wind at 2 meters
110	T2M	deg	1	Temperature at 2 meters
111	Q2M	g/kg	1	Specific Humidity at 2 meters
112	U10M	m/sec	1	U-Wind at 10 meters
113	V10M	m/sec	1	V-Wind at 10 meters
114	T10M	deg	1	Temperature at 10 meters
115	Q10M	g/kg	1	Specific Humidity at 10 meters
116	DTRAIN	$kg * m/sec$	NLAY	Convective Cloud Detrainment
117	QFILL	$g/kg/day$	NLAY	Filling of negative specific humidity
118	VINTQANA	mm/day	1	Vertically integrated analysis specific humidity increment
119	VINTQFIL	mm/day	1	Vertically integrated **QFILL**

8 Diagnostic Description

In this section we list and describe the diagnostic quantities available within the GEOS GCM. The diagnostics are listed in the order that they appear in the Diagnostic Menu, Section 7. In all cases, each diagnostic as currently archived on DAO production output datasets is time-averaged over its diagnostic output frequency:

$$\textbf{DIAGNOSTIC} = \frac{1}{TTOT} \sum_{t=1}^{t=TTOT} diag(t)$$

where $TTOT = \frac{\textbf{NQDIAG}}{\Delta t}$, **NQDIAG** is the output frequency of the diagositc, and Δt is the timestep over which the diagnostic is updated. For further information on how to set the diagnostic output frequency **NQDIAG**, please see Part III, A User's Guide. Also, note that several Diagnostic Index locations are currently disabled due to changes which have occured from previous GCM versions.

A word of caution: The Arakawa C-grid stencil used in the GEOS GCM employs a "stretched" coordinate near the poles due to conservation requirements. As a result, a well-defined vorticity is is located at the poles, while the first mass point is located one $\Delta\phi$ away from the poles. Since all Physical (diabatic) processes of the model are computed at mass points, all Physics diagnostics are only truely defined at latitudes $-90 + \Delta\phi$ to $90 - \Delta\phi$. While an attempt was made to "diagnose" some pole value diagnostics through interpolation over the poles, others have been left unfilled.

1) <u>UFLUX</u> Surface Zonal Wind Stress on the Atmosphere ($Newton/m^2$)

The zonal wind stress is the turbulent flux of zonal momentum from the surface. See section 3.3 for a description of the surface layer parameterization.

$$\textbf{UFLUX} = -\rho C_D W_s u \qquad where: \quad C_D = C_u^2$$

where $\rho =$ the atmospheric density at the surface, C_D is the surface drag coefficient, C_u is the dimensionless surface exchange coefficient for momentum (see diagnostic number 10), W_s is the magnitude of the surface layer wind, and u is the zonal wind in the lowest model layer.

2) <u>VFLUX</u> Surface Meridional Wind Stress on the Atmosphere ($Newton/m^2$)

The meridional wind stress is the turbulent flux of meridional momentum from the surface. See section 3.3 for a description of the surface layer parameterization.

$$\textbf{VFLUX} = -\rho C_D W_s v \qquad where: \quad C_D = C_u^2$$

where ρ = the atmospheric density at the surface, C_D is the surface drag coefficient, C_u is the dimensionless surface exchange coefficient for momentum (see diagnostic number 10), W_s is the magnitude of the surface layer wind, and v is the meridional wind in the lowest model layer.

3) HFLUX Surface Flux of Sensible Heat ($Watts/m^2$)

The turbulent flux of sensible heat from the surface to the atmosphere is a function of the gradient of virtual potential temperature and the eddy exchange coefficient:

$$\mathbf{HFLUX} = P^\kappa \rho c_p C_H W_s (\theta_{surface} - \theta_{NLAY}) \qquad where: \quad C_H = C_u C_t$$

where ρ = the atmospheric density at the surface, c_p is the specific heat of air, C_H is the dimensionless surface heat transfer coefficient, W_s is the magnitude of the surface layer wind, C_u is the dimensionless surface exchange coefficient for momentum (see diagnostic number 10), C_t is the dimensionless surface exchange coefficient for heat and moisture (see diagnostic number 9), and θ is the potential temperature at the surface and at the bottom σ-level.

4) EFLUX Surface Flux of Latent Heat ($Watts/m^2$)

The turbulent flux of latent heat from the surface to the atmosphere is a function of the gradient of moisture, the potential evapotranspiration fraction and the eddy exchange coefficient:

$$\mathbf{EFLUX} = \rho \beta L C_H W_s (q_{surface} - q_{NLAY}) \qquad where: \quad C_H = C_u C_t$$

where ρ = the atmospheric density at the surface, β is the fraction of the potential evapotranspiration actually evaporated, L is the latent heat of evaporation, C_H is the dimensionless surface heat transfer coefficient, W_s is the magnitude of the surface layer wind, C_u is the dimensionless surface exchange coefficient for momentum (see diagnostic number 10), C_t is the dimensionless surface exchange coefficient for heat and moisture (see diagnostic number 9), and $q_{surface}$ and q_{NLAY} are the specific humidity at the surface and at the bottom σ-level, respectively.

5) QICE Heat Conduction Through Sea Ice ($Watts/m^2$)

Over sea ice there is an additional source of energy at the surface due to the heat conduction from the relatively warm ocean through the sea ice. The heat conduction through sea ice represents an additional energy source term for the ground temperature equation.

$$\mathbf{QICE} = \frac{C_{ti}}{H_i}(T_i - T_g)$$

where C_{ti} is the thermal conductivity of ice, H_i is the ice thickness, assumed to be 3 m where sea ice is present, T_i is 273 degrees Kelvin, and T_g is the temperature of the sea ice.

NOTE: QICE is not available through model version 5.3, but is available in subsequent versions.

6) <u>RADLWG</u> Net upward Longwave Flux at the surface ($Watts/m^2$)

$$\begin{aligned} \mathbf{RADLWG} &= F^{Net}_{LW,nlay+1} \\ &= F^{\uparrow}_{LW,nlay+1} - F^{\downarrow}_{LW,nlay+1} \end{aligned}$$

where nlay+1 indicates the lowest model edge-level, or $p = p_{surf}$. $F^{\uparrow}_{LW}$ is the upward Longwave flux and $F^{\downarrow}_{LW}$ is the downward Longwave flux.

7) <u>RADSWG</u> Net downard shortwave Flux at the surface ($Watts/m^2$)

$$\begin{aligned} \mathbf{RADSWG} &= F^{Net}_{SW,nlay+1} \\ &= F^{\downarrow}_{SW,nlay+1} - F^{\uparrow}_{SW,nlay+1} \end{aligned}$$

where nlay+1 indicates the lowest model edge-level, or $p = p_{surf}$. $F^{\downarrow}_{SW}$ is the downward Shortwave flux and $F^{\uparrow}_{SW}$ is the upward Shortwave flux.

8) <u>RI</u> Richardson Number (*dimensionless*)

The non-dimensional stability indicator is the ratio of the buoyancy to the shear:

$$\mathbf{RI} = \frac{\frac{g}{\theta_v}\frac{\partial \theta_v}{\partial z}}{\left(\frac{\partial u}{\partial z}\right)^2 + \left(\frac{\partial v}{\partial z}\right)^2} = \frac{c_p \frac{\partial \theta_v}{\partial z}\frac{\partial P^\kappa}{\partial z}}{\left(\frac{\partial u}{\partial z}\right)^2 + \left(\frac{\partial v}{\partial z}\right)^2}$$

where we used the hydrostatic equation:

$$\frac{\partial \Phi}{\partial P^\kappa} = c_p \theta_v$$

Negative values indicate unstable buoyancy **AND** shear, small positive values (< 0.4) indicate dominantly unstable shear, and large positive values indicate dominantly stable stratification.

9) <u>CT</u> Surface Exchange Coefficient for Temperature and Moisture (*dimensionless*)

The surface exchange coefficient is obtained from the similarity functions for the stability dependant flux profile relationships:

$$\mathbf{CT} = -\frac{\overline{(w'\theta')}}{u_*\Delta\theta} = -\frac{\overline{(w'q')}}{u_*\Delta q} = \frac{k}{(\psi_h + \psi_g)}$$

where ψ_h is the surface layer non-dimensional temperature change and ψ_g is the viscous sublayer non-dimensional temperature or moisture change:

$$\psi_h = \int_{\zeta_0}^{\zeta} \frac{\phi_h}{\zeta} d\zeta \qquad and \qquad \psi_g = \frac{0.55(Pr^{2/3} - 0.2)}{\nu^{1/2}}(h_0 u_* - h_{0_{ref}} u_{*_{ref}})^{1/2}$$

and: $h_0 = 30 z_0$ with a maximum value over land of 0.01

ϕ_h is the similarity function of ζ, which expresses the stability dependance of the temperature and moisture gradients, specified differently for stable and unstable layers according to Helfand and Schubert, 1993. k is the Von Karman constant, ζ is the non-dimensional stability parameter, Pr is the Prandtl number for air, ν is the molecular viscosity, z_0 is the surface roughness length, u_* is the surface stress velocity (see diagnostic number 67), and the subscript ref refers to a reference value.

10) <u>CU</u> Surface Exchange Coefficient for Momentum (*dimensionless*)

The surface exchange coefficient is obtained from the similarity functions for the stability dependant flux profile relationships:

$$\mathbf{CU} = \frac{u_*}{W_s} = \frac{k}{\psi_m}$$

where ψ_m is the surface layer non-dimensional wind shear:

$$\psi_m = \int_{\zeta_0}^{\zeta} \frac{\phi_m}{\zeta} d\zeta$$

ϕ_m is the similarity function of ζ, which expresses the stability dependance of the temperature and moisture gradients, specified differently for stable and unstable layers according to Helfand and Schubert, 1993. k is the Von Karman constant, ζ is the non-dimensional stability parameter, u_* is the surface stress velocity (see diagnostic number 67), and W_s is the magnitude of the surface layer wind.

11) <u>ET</u> Diffusivity Coefficient for Temperature and Moisture (m^2/sec)

In the level 2.5 version of the Mellor-Yamada (1974) hierarchy, the turbulent heat or moisture flux for the atmosphere above the surface layer can be expressed as a turbulent diffusion coefficient K_h times the negative of the gradient of potential temperature or moisture. In the Helfand and Labraga (1988) adaptation of this closure, K_h takes the form:

$$\mathbf{ET} = K_h = -\frac{(\overline{w'\theta'_v})}{\frac{\partial \theta_v}{\partial z}} = \begin{cases} q\,\ell\,S_H(G_M, G_H) & \text{for decaying turbulence} \\ \frac{q^2}{q_e}\ell\,S_H(G_{M_e}, G_{H_e}) & \text{for growing turbulence} \end{cases}$$

where q is the turbulent velocity, or $\sqrt{2 * turbulent\ kinetic\ energy}$, q_e is the turbulence velocity derived from the more simple level 2.0 model, which describes equilibrium turbulence, ℓ is the master length scale related to the layer depth, S_H is a function of G_H and G_M, the dimensionless buoyancy and wind shear parameters, respectively, or a function of G_{H_e} and G_{M_e}, the equilibrium dimensionless buoyancy and wind shear parameters. Both G_H and G_M, and their equilibrium values G_{H_e} and G_{M_e}, are functions of the Richardson number.

For the detailed equations and derivations of the modified level 2.5 closure scheme, see Helfand and Labraga, 1988.

In the surface layer, **ET** is the exchange coefficient for heat and moisture, in units of m/sec, given by:

$$\mathbf{ET}_{\mathbf{NLAY}} = C_t * u_* = C_H W_s$$

where C_t is the dimensionless exchange coefficient for heat and moisture from the surface layer similarity functions (see diagnostic number 9), u_* is the surface friction velocity (see diagnostic number 67), C_H is the heat transfer coefficient, and W_s is the magnitude of the surface layer wind.

12) <u>EU</u> Diffusivity Coefficient for Momentum (m^2/sec)

In the level 2.5 version of the Mellor-Yamada (1974) hierarchy, the turbulent heat momentum flux for the atmosphere above the surface layer can be expressed as a turbulent diffusion coefficient K_m times the negative of the gradient of the u-wind. In the Helfand and Labraga (1988) adaptation of this closure, K_m takes the form:

$$\mathbf{EU} = K_m = -\frac{(\overline{u'w'})}{\frac{\partial U}{\partial z}} = \begin{cases} q\,\ell\,S_M(G_M, G_H) & \text{for decaying turbulence} \\ \frac{q^2}{q_e}\ell\,S_M(G_{M_e}, G_{H_e}) & \text{for growing turbulence} \end{cases}$$

where q is the turbulent velocity, or $\sqrt{2 * turbulent\ kinetic\ energy}$, q_e is the turbulence velocity derived from the more simple level 2.0 model, which describes equilibrium turbulence, ℓ is the master length scale related to the layer depth, S_M is a function of G_H and G_M, the dimensionless buoyancy and wind shear parameters, respectively, or a function of G_{H_e} and G_{M_e}, the equilibrium dimensionless buoyancy and wind shear parameters. Both

G_H and G_M, and their equilibrium values G_{H_e} and G_{M_e}, are functions of the Richardson number.

For the detailed equations and derivations of the modified level 2.5 closure scheme, see Helfand and Labraga, 1988.

In the surface layer, **EU** is the exchange coefficient for momentum, in units of m/sec, given by:

$$\mathbf{EU}_{\mathbf{NLAY}} = C_u * u_* = C_D W_s$$

where C_u is the dimensionless exchange coefficient for momentum from the surface layer similarity functions (see diagnostic number 10), u_* is the surface friction velocity (see diagnostic number 67), C_D is the surface drag coefficient, and W_s is the magnitude of the surface layer wind.

13) <u>TURBU</u> Zonal U-Momentum changes due to Turbulence $(m/sec/day)$

The tendency of U-Momentum due to turbulence is written:

$$\mathbf{TURBU} = \left.\frac{\partial u}{\partial t}\right|_{turb} = \frac{\partial}{\partial z}(-\overline{u'w'}) = \frac{\partial}{\partial z}(K_m \frac{\partial u}{\partial z})$$

The Helfand and Labraga level 2.5 scheme models the turbulent flux of u-momentum in terms of K_m, and the equation has the form of a diffusion equation.

14) <u>TURBV</u> Meridional V-Momentum changes due to Turbulence $(m/sec/day)$

The tendency of V-Momentum due to turbulence is written:

$$\mathbf{TURBV} = \left.\frac{\partial v}{\partial t}\right|_{turb} = \frac{\partial}{\partial z}(-\overline{v'w'}) = \frac{\partial}{\partial z}(K_m \frac{\partial v}{\partial z})$$

The Helfand and Labraga level 2.5 scheme models the turbulent flux of v-momentum in terms of K_m, and the equation has the form of a diffusion equation.

15) <u>TURBT</u> Temperature changes due to Turbulence (deg/day)

The tendency of temperature due to turbulence is written:

$$\mathbf{TURBT} = \frac{\partial T}{\partial t} = P^\kappa \left.\frac{\partial \theta}{\partial t}\right|_{turb} = P^\kappa \frac{\partial}{\partial z}(-\overline{w'\theta'}) = P^\kappa \frac{\partial}{\partial z}(K_h \frac{\partial \theta_v}{\partial z})$$

The Helfand and Labraga level 2.5 scheme models the turbulent flux of temperature in terms of K_h, and the equation has the form of a diffusion equation.

16) TURBQ Specific Humidity changes due to Turbulence ($g/kg/day$)

The tendency of specific humidity due to turbulence is written:

$$\mathbf{TURBQ} = \frac{\partial q}{\partial t}\bigg|_{turb} = \frac{\partial}{\partial z}(-\overline{w'q'}) = \frac{\partial}{\partial z}(K_h\frac{\partial q}{\partial z})$$

The Helfand and Labraga level 2.5 scheme models the turbulent flux of temperature in terms of K_h, and the equation has the form of a diffusion equation.

17) MOISTT Temperature Changes Due to Moist Processes (deg/day)

$$\mathbf{MOISTT} = \frac{\partial T}{\partial t}\bigg|_c + \frac{\partial T}{\partial t}\bigg|_{ls}$$

where:

$$\frac{\partial T}{\partial t}\bigg|_c = R\sum_i\left(\alpha\frac{m_B}{c_p}\Gamma_s\right)_i \quad and \quad \frac{\partial T}{\partial t}\bigg|_{ls} = \frac{L}{c_p}(q^* - q)$$

and

$$\Gamma_s = g\eta\frac{\partial s}{\partial p}$$

The subscript c refers to convective processes, while the subscript ls refers to large scale precipitation processes, or supersaturation rain. The summation refers to contributions from each cloud type called by RAS. The dry static energy is given as s, the convective cloud base mass flux is given as m_B, and the cloud entrainment is given as η, which are explicitly defined in Section 3.1.1, the description of the convective parameterization. The fractional adjustment, or relaxation parameter, for each cloud type is given as α, while R is the rain re-evaporation adjustment.

18) MOISTQ Specific Humidity Changes Due to Moist Processes ($g/kg/day$)

$$\mathbf{MOISTQ} = \frac{\partial q}{\partial t}\bigg|_c + \frac{\partial q}{\partial t}\bigg|_{ls}$$

where:

$$\frac{\partial q}{\partial t}\bigg|_c = R\sum_i\left(\alpha\frac{m_B}{L}(\Gamma_h - \Gamma_s)\right)_i \quad and \quad \frac{\partial q}{\partial t}\bigg|_{ls} = (q^* - q)$$

and

$$\Gamma_s = g\eta\frac{\partial s}{\partial p} \quad and \quad \Gamma_h = g\eta\frac{\partial h}{\partial p}$$

The subscript c refers to convective processes, while the subscript ls refers to large scale precipitation processes, or supersaturation rain. The summation refers to contributions

from each cloud type called by RAS. The dry static energy is given as s, the moist static energy is given as h, the convective cloud base mass flux is given as m_B, and the cloud entrainment is given as η, which are explicitly defined in Section 3.1.1, the description of the convective parameterization. The fractional adjustment, or relaxation parameter, for each cloud type is given as α, while R is the rain re-evaporation adjustment.

19) <u>RADLW</u> Heating Rate due to Longwave Radiation (deg/day)

The net longwave heating rate is calculated as the vertical divergence of the net terrestrial radiative fluxes. Both the clear-sky and cloudy-sky longwave fluxes are computed within the longwave routine. The subroutine calculates the clear-sky flux, $F_{LW}^{clearsky}$, first. For a given cloud fraction, the clear line-of-sight probability $C(p, p')$ is computed from the current level pressure p to the model top pressure, $p' = p_{top}$, and the model surface pressure, $p' = p_{surf}$, for the upward and downward radiative fluxes. (see Section 3.2.3). The cloudy-sky flux is then obtained as:

$$F_{LW} = C(p, p') \cdot F_{LW}^{clearsky},$$

Finally, the net longwave heating rate is calculated as the vertical divergence of the net terrestrial radiative fluxes:

$$\frac{\partial \rho c_p T}{\partial t} = -\frac{\partial}{\partial z} F_{LW}^{NET},$$

or

$$\textbf{RADLW} = \frac{g}{c_p \pi} \frac{\partial}{\partial \sigma} F_{LW}^{NET}.$$

where g is the accelation due to gravity, c_p is the heat capacity of air at constant pressure, and

$$F_{LW}^{NET} = F_{LW}^{\uparrow} - F_{LW}^{\downarrow}$$

20) <u>RADSW</u> Heating Rate due to Shortwave Radiation (deg/day)

The net Shortwave heating rate is calculated as the vertical divergence of the net solar radiative fluxes. The clear-sky and cloudy-sky shortwave fluxes are calculated separately. For the clear-sky case, the shortwave fluxes and heating rates are computed with both CLMO (maximum overlap cloud fraction) and CLRO (random overlap cloud fraction) set to zero (see Section 3.2.3). The shortwave routine is then called a second time, for the cloudy-sky case, with the true time-averaged cloud fractions CLMO and CLRO being used. In all cases, a normalized incident shortwave flux is used as input at the top of the atmosphere.

The heating rate due to Shortwave Radiation under cloudy skies is defined as:

$$\frac{\partial \rho c_p T}{\partial t} = -\frac{\partial}{\partial z} F(cloudy)_{SW}^{NET} \cdot \text{RADSWT},$$

or

$$\textbf{RADSW} = \frac{g}{c_p \pi} \frac{\partial}{\partial \sigma} F(cloudy)_{SW}^{NET} \cdot \text{RADSWT}.$$

where g is the acceleration due to gravity, c_p is the heat capacity of air at constant pressure, RADSWT is the true incident shortwave radiation at the top of the atmosphere (See Diagnostic #48), and

$$F(cloudy)_{SW}^{Net} = F(cloudy)_{SW}^{\uparrow} - F(cloudy)_{SW}^{\downarrow}$$

21) <u>PREACC</u> Total (Large-scale + Convective) Accumulated Precipition (mm/day)

For a change in specific humidity due to moist processes, Δq_{moist}, the vertical integral or total precipitable amount is given by:

$$\textbf{PREACC} = \int_{surf}^{top} \rho \Delta q_{moist} dz = -\int_{surf}^{top} \Delta q_{moist} \frac{dp}{g} = \frac{\pi}{g} \int_0^1 \Delta q_{moist} d\sigma$$

A precipitation rate is defined as the vertically integrated moisture adjustment per Moist Processes time step, scaled to mm/day.

22) <u>PRECON</u> Convective Precipition (mm/day)

For a change in specific humidity due to sub-grid scale cumulus convective processes, Δq_{cum}, the vertical integral or total precipitable amount is given by:

$$\textbf{PRECON} = \int_{surf}^{top} \rho \Delta q_{cum} dz = -\int_{surf}^{top} \Delta q_{cum} \frac{dp}{g} = \frac{\pi}{g} \int_0^1 \Delta q_{cum} d\sigma$$

A precipitation rate is defined as the vertically integrated moisture adjustment per Moist Processes time step, scaled to mm/day.

23) <u>TUFLUX</u> Turbulent Flux of U-Momentum ($Newton/m^2$)

The turbulent flux of u-momentum is calculated for *diagnostic purposes only* from the eddy coefficient for momentum:

$$\textbf{TUFLUX} = \rho(\overline{u'w'}) = \rho(-K_m\frac{\partial U}{\partial z})$$

where ρ is the air density, and K_m is the eddy coefficient.

24) <u>TVFLUX</u> Turbulent Flux of V-Momentum ($Newton/m^2$)

The turbulent flux of v-momentum is calculated for *diagnostic purposes only* from the eddy coefficient for momentum:

$$\textbf{TVFLUX} = \rho(\overline{v'w'}) = \rho(-K_m\frac{\partial V}{\partial z})$$

where ρ is the air density, and K_m is the eddy coefficient.

25) <u>TTFLUX</u> Turbulent Flux of Sensible Heat ($Watts/m^2$)

The turbulent flux of sensible heat is calculated for *diagnostic purposes only* from the eddy coefficient for heat and moisture:

$$\textbf{TTFLUX} = c_p\rho P^\kappa(\overline{w'\theta'}) = c_p\rho P^\kappa(-K_h\frac{\partial \theta_v}{\partial z})$$

where ρ is the air density, and K_h is the eddy coefficient.

26) <u>TQFLUX</u> Turbulent Flux of Latent Heat ($Watts/m^2$)

The turbulent flux of latent heat is calculated for *diagnostic purposes only* from the eddy coefficient for heat and moisture:

$$\textbf{TQFLUX} = L\rho(\overline{w'q'}) = L\rho(-K_h\frac{\partial q}{\partial z})$$

where ρ is the air density, and K_h is the eddy coefficient.

27) <u>CN</u> Neutral Drag Coefficient (*dimensionless*)

The drag coefficient for momentum obtained by assuming a neutrally stable surface layer:

$$CN = \frac{k}{\ln(\frac{h}{z_0})}$$

where k is the Von Karman constant, h is the height of the surface layer, and z_0 is the surface roughness.

NOTE: CN is not available through model version 5.3, but is available in subsequent versions.

28) <u>WINDS</u> Surface Wind Speed (*meter/sec*)

The surface wind speed is calculated for the last internal turbulence time step:

$$WINDS = \sqrt{u_{NLAY}^2 + v_{NLAY}^2}$$

where the subscript $NLAY$ refers to the lowest model $\sigma - level$.

29) <u>DTSRF</u> Air/Surface Virtual Temperature Difference (*deg K*)

The air/surface virtual temperature difference measures the stability of the surface layer:

$$DTSRF = (\theta_{vNLAY+1} - \theta_{vNLAY})P_{surf}^{\kappa}$$

where

$$\theta_{vNLAY+1} = \frac{T_g}{P_{surf}^{\kappa}}(1+.609q_{NLAY+1}) \qquad and \qquad q_{NLAY+1} = q_{NLAY}+\beta(q^*(T_g,P_s)-q_{NLAY})$$

β is the surface potential evapotranspiration coefficient ($\beta = 1$ over oceans), $q^*(T_g, P_s)$ is the saturation specific humidity at the ground temperature and surface pressure, level $NLAY$ refers to the lowest model level and level $NLAY + 1$ refers to the surface.

30) <u>TG</u> Ground Temperature (*deg K*)

The ground temperature equation is solved as part of the turbulence package using a backward implicit time differencing scheme:

$$TG \; is \; obtained \; from: \; C_g\frac{\partial T_g}{\partial t} = R_{sw} - R_{lw} + Q_{ice} - H - LE$$

where R_{sw} is the net surface downward shortwave radiative flux, R_{lw} is the net surface upward longwave radiative flux, Q_{ice} is the heat conduction through sea ice, H is the upward sensible heat flux, LE is the upward latent heat flux, and C_g is the total heat capacity of the ground. C_g is obtained by solving a heat diffusion equation for the penetration of the diurnal cycle into the ground (Blackadar, 1977), and is given by:

$$C_g = \sqrt{\frac{\lambda C_s}{2\omega}} = \sqrt{(0.386 + 0.536W + 0.15W^2)2x10^{-3}\frac{86400.}{2\pi}} \ .$$

Here, the thermal conductivity, λ, is equal to $2x10^{-3} \frac{ly}{sec} \frac{cm}{{}^\circ K}$, the angular velocity of the earth, ω, is written as 86400 sec/day divided by 2π $radians/day$, and the expression for C_s, the heat capacity per unit volume at the surface, is a function of the ground wetness, W.

31) <u>TS</u> Surface Temperature (deg K)

The surface temperature estimate is made by assuming that the model's lowest layer is well-mixed, and therefore that θ is constant in that layer. The surface temperature is therefore:

$$\textbf{TS} = \theta_{NLAY} P_{surf}^\kappa$$

32) <u>DTG</u> Surface Temperature Adjustment (deg K)

The change in surface temperature from one turbulence time step to the next, solved using the Ground Temperature Equation (see diagnostic number 30) is calculated:

$$\textbf{DTG} = T_g{}^n - T_g{}^{n-1}$$

where superscript n refers to the new, updated time level, and the superscript $n - 1$ refers to the value at the previous turbulence time level.

33) <u>QG</u> Ground Specific Humidity (g/kg)

The ground specific humidity is obtained by interpolating between the specific humidity at the lowest model level and the specific humidity of a saturated ground. The interpolation is performed using the potential evapotranspiration function:

$$\textbf{QG} = q_{NLAY+1} = q_{NLAY} + \beta(q^*(T_g, P_s) - q_{NLAY})$$

where β is the surface potential evapotranspiration coefficient ($\beta = 1$ over oceans), and $q^*(T_g, P_s)$ is the saturation specific humidity at the ground temperature and surface pres-

41

sure.

34) <u>QS</u> Saturation Surface Specific Humidity (g/kg)

The surface saturation specific humidity is the saturation specific humidity at the ground temprature and surface pressure:

$$QS = q^*(T_g, P_s)$$

35) <u>TGRLW</u> Instantaneous ground temperature used as input to the Longwave radiation subroutine (deg)

$$TGRLW = T_g(\lambda, \phi, n)$$

where T_g is the model ground temperature at the current time step n.

36) <u>ST4</u> Upward Longwave flux at the surface ($Watts/m^2$)

$$ST4 = \sigma T^4$$

where σ is the Stefan-Boltzmann constant and T is the temperature.

37) <u>OLR</u> Net upward Longwave flux at $p = p_{top}$ ($Watts/m^2$)

$$OLR = F_{LW,top}^{NET}$$

where top indicates the top of the first model layer. In the GEOS-1 GCM, $p_{top} = 10$ mb.

38) <u>OLRCLR</u> Net upward clearsky Longwave flux at $p = p_{top}$ ($Watts/m^2$)

$$OLRCLR = F(clearsky)_{LW,top}^{NET}$$

where top indicates the top of the first model layer. In the GEOS-1 GCM, $p_{top} = 10$ mb.

39) <u>LWGCLR</u> Net upward clearsky Longwave flux at the surface ($Watts/m^2$)

$$
\begin{aligned}
LWGCLR &= F(clearsky)_{LW,nlay+1}^{Net} \\
&= F(clearsky)_{LW,nlay+1}^{\uparrow} - F(clearsky)_{LW,nlay+1}^{\downarrow}
\end{aligned}
$$

where nlay+1 indicates the lowest model edge-level, or $p = p_{surf}$. $F(clearsky)^{\uparrow}_{LW}$ is the upward clearsky Longwave flux and the $F(clearsky)^{\downarrow}_{LW}$ is the downward clearsky Longwave flux.

40) <u>LWCLR</u> Heating Rate due to Clearsky Longwave Radiation (deg/day)

The net longwave heating rate is calculated as the vertical divergence of the net terrestrial radiative fluxes. Both the clear-sky and cloudy-sky longwave fluxes are computed within the longwave routine. The subroutine calculates the clear-sky flux, $F_{LW}^{clearsky}$, first. For a given cloud fraction, the clear line-of-sight probability $C(p, p')$ is computed from the current level pressure p to the model top pressure, $p' = p_{top}$, and the model surface pressure, $p' = p_{surf}$, for the upward and downward radiative fluxes. (see Section 3.2.3). The cloudy-sky flux is then obtained as:

$$F_{LW} = C(p, p') \cdot F_{LW}^{clearsky},$$

Thus, **LWCLR** is defined as the net longwave heating rate due to the vertical divergence of the clear-sky longwave radiative flux:

$$\frac{\partial \rho c_p T}{\partial t}_{clearsky} = -\frac{\partial}{\partial z} F(clearsky)^{NET}_{LW},$$

or

$$\textbf{LWCLR} = \frac{g}{c_p \pi} \frac{\partial}{\partial \sigma} F(clearsky)^{NET}_{LW}.$$

where g is the accelation due to gravity, c_p is the heat capacity of air at constant pressure, and

$$F(clearsky)^{Net}_{LW} = F(clearsky)^{\uparrow}_{LW} - F(clearsky)^{\downarrow}_{LW}$$

41) <u>TLW</u> Instantaneous temperature used as input to the Longwave radiation subroutine (deg)

$$\textbf{TLW} = T(\lambda, \phi, \sigma, n)$$

where T is the model temperature at the current time step n.

42) <u>SHLW</u> Instantaneous specific humidity used as input to the Longwave radiation subroutine (kg/kg)

$$\textbf{SHLW} = q(\lambda, \phi, \sigma, n)$$

where q is the model specific humidity at the current time step n.

43) OZLW Instantaneous ozone used as input to the Longwave radiation subroutine (kg/kg)

$$OZLW = OZ(\lambda, \phi, \sigma, n)$$

where OZ is the interpolated ozone data set from the climatological monthly mean zonally averaged ozone data set.

44) CLMOLW Maximum Overlap cloud fraction used in LW Radiation $(0-1)$

CLMOLW is the time-averaged maximum overlap cloud fraction that has been filled by the Relaxed Arakawa/Schubert Convection scheme and will be used in the Longwave Radiation algorithm. These are convective clouds whose radiative characteristics are assumed to be correlated in the vertical. For a complete description of cloud/radiative interactions, see Section 3.2.3.

$$\mathbf{CLMOLW} = CLMO_{RAS,LW}(\lambda, \phi, \sigma)$$

Note, in Version 1 of the GEOS GCM, shortwave and longwave cloud fields are computed identically, ie.

$$\mathbf{CLMOLW} = \mathbf{CLMOSW}$$

45) CLROLW Random Overlap cloud fraction used in LW Radiation $(0-1)$

CLROLW is the time-averaged random overlap cloud fraction that has been filled by the Relaxed Arakawa/Schubert and Large-scale Convection schemes and will be used in the Longwave Radiation algorithm. These are convective and large-scale clouds whose radiative characteristics are not assumed to be correlated in the vertical. For a complete description of cloud/radiative interactions, see Section 3.2.3.

$$\mathbf{CLROLW} = CLRO_{RAS,LargeScale,LW}(\lambda, \phi, \sigma)$$

Note, in Version 1 of the GEOS GCM, shortwave and longwave cloud fields are computed identically, ie.

$$\mathbf{CLROLW} = \mathbf{CLROSW}$$

46) CLMOSW Maximum Overlap cloud fraction used in SW Radiation $(0-1)$

CLMOSW is the time-averaged maximum overlap cloud fraction that has been filled by the Relaxed Arakawa/Schubert Convection scheme and will be used in the Shortwave Radiation algorithm. These are convective clouds whose radiative characteristics are assumed to be correlated in the vertical. For a complete description of cloud/radiative interactions, see Section 3.2.3.

$$\text{CLMOSW} = CLMO_{RAS,SW}(\lambda, \phi, \sigma)$$

Note, in Version 1 of the GEOS GCM, shortwave and longwave cloud fields are computed identically, ie.

$$\text{CLMOSW} = \text{CLMOLW}$$

47) <u>CLROSW</u> Random Overlap cloud fraction used in SW Radiation (0 – 1)

CLROSW is the time-averaged random overlap cloud fraction that has been filled by the Relaxed Arakawa/Schubert and Large-scale Convection schemes and will be used in the Shortwave Radiation algorithm. These are convective and large-scale clouds whose radiative characteristics are not assumed to be correlated in the vertical. For a complete description of cloud/radiative interactions, see Section 3.2.3.

$$\text{CLROSW} = CLRO_{RAS,LargeScale,SW}(\lambda, \phi, \sigma)$$

Note, in Version 1 of the GEOS GCM, shortwave and longwave cloud fields are computed identically, ie.

$$\text{CLROSW} = \text{CLROLW}$$

48) <u>RADSWT</u> Incident Shortwave radiation at the top of the atmosphere ($Watts/m^2$)

$$\text{RADSWT} = \frac{S_0}{R_a^2} \cdot cos\phi_z$$

where S_0, is the extra-terrestial solar contant, R_a is the earth-sun distance in Astronomical Units, and $cos\phi_z$ is the cosine of the zenith angle. It should be noted that **RADSWT**, as well as **OSR** and **OSRCLR**, are calculated at the top of the atmosphere (p=0 mb). However, the **OLR** and **OLRCLR** diagnostics are currently calculated at $p = p_{top}$ (10 mb for the 20-level GEOS-1 GCM).

49) Disabled

50) Disabled

51) Disabled

52) <u>EVAP</u> Surface Evaporation (mm/day)

The surface evaporation is a function of the gradient of moisture, the potential evapotranspiration fraction and the eddy exchange coefficient:

$$\textbf{EVAP} = \rho\beta K_h(q_{surface} - q_{NLAY})$$

where ρ = the atmospheric density at the surface, β is the fraction of the potential evapotranspiration actually evaporated ($\beta = 1$ over oceans), K_h is the turbulent eddy exchange coefficient for heat and moisture at the surface in m/sec and $qsurface$ and q_{NLAY} are the specific humidity at the surface (see diagnostic number 34) and at the bottom σ-level, respectively.

53) <u>DPDT</u> Total Surface Pressure Tendency (mb/day)

DPDT is the total time-tendency of the surface pressure due to Hydrodynamic and Analysis forcing. There are no surface pressure changes due to physical diabatic processes, such as changes in total precipitable water amounts.

$$\textbf{DPDT} = \frac{\partial\pi}{\partial t}_{Dynamics} + \frac{\partial\pi}{\partial t}_{Analysis},$$

where $\pi = p_{surf} - p_{top}$. In forecast simulations $\frac{\partial\pi}{\partial t}_{Analysis} = 0$.

54) <u>ANALU</u> Analysis Zonal U-Wind Tendency ($m/sec/sec$)

ANALU is the Zonal U-Wind tendency created during the assimilation cycle which is used in the Incremental Analysis Updating (IAU) procedure.

$$\textbf{ANALU} = \left(u^A(\lambda, \phi, \sigma, t) - u^{FG}(\lambda, \phi, \sigma, t)\right)/\Delta t_{Analysis}$$

where u^A corresponds to the u-wind after the analysis, u^{FG} corresponds to the u-wind first guess, and $\Delta t_{Analysis}$ is the time-step between analyses (6 hours). Note, **ANALU** is stored on the staggered C-grid.

55) <u>ANALV</u> Analysis Meridional V-Wind Tendency ($m/sec/sec$)

ANALV is the Meridional V-Wind tendency created during the assimilation cycle which is used in the Incremental Analysis Updating (IAU) procedure.

$$\mathbf{ANALV} = \left(v^A(\lambda, \phi, \sigma, t) - v^{FG}(\lambda, \phi, \sigma, t) \right) / \Delta t_{Analysis}$$

where v^A corresponds to the v-wind after the analysis, v^{FG} corresponds to the v-wind first guess, and $\Delta t_{Analysis}$ is the time-step between analyses (6 hours). Note, **ANALV** is stored on the staggered C-grid.

56) <u>ANALT</u> Analysis Temperature Tendency ($mb\,deg/mb^\kappa/sec$)

ANALT is the pressure weighted Potential Temperature tendency created during the assimilation cycle which is used in the Incremental Analysis Updating (IAU) procedure.

$$\mathbf{ANALT} = \left((\pi\theta)^A(\lambda, \phi, \sigma, t) - (\pi\theta)^{FG}(\lambda, \phi, \sigma, t) \right) / \Delta t_{Analysis}$$

where $(\pi\theta)^A$ corresponds to the pressure weighted Potential Temperature after the analysis, $(\pi\theta)^{FG}$ corresponds to the pressure weighted Potential Temperature first guess, $\theta = T/p^\kappa$, and $\Delta t_{Analysis}$ is the time-step between analyses (6 hours).

57) <u>ANALQ</u> Analysis Temperature Tendency ($mb \cdot g/g/sec$)

ANALQ is the pressure weighted Specific Humidity tendency created during the assimilation cycle which is used in the Incremental Analysis Updating (IAU) procedure.

$$\mathbf{ANALQ} = \left((\pi q)^A(\lambda, \phi, \sigma, t) - (\pi q)^{FG}(\lambda, \phi, \sigma, t) \right) / \Delta t_{Analysis}$$

where $(\pi q)^A$ corresponds to the pressure weighted Specific Humidity after the analysis, $(\pi q)^{FG}$ corresponds to the pressure weighted Specific Humidity first guess, and $\Delta t_{Analysis}$ is the time-step between analyses (6 hours).

58) <u>OMEGA</u> Pressure Coordinate Vertical Velocity (mb/day)

OMEGA, which is the change in pressure in time following the parcel, is diagnostically obtained by integrating the GCM's continuity equation. We have

$$\mathbf{OMEGA} \equiv \frac{dp}{dt} = (\pi\dot{\sigma} + \dot{\pi}\sigma)$$

since $p = \pi\sigma + p_{Top}$. Now,

$$\dot{\pi} = \frac{\partial\pi}{\partial t} + \mathbf{V} \cdot \nabla\pi$$

$$\frac{\partial\pi}{\partial t} = -\nabla \cdot (\pi\mathbf{V}) - \frac{\partial\pi\dot{\sigma}}{\partial\sigma}$$

Integrating the continuity equation from the top of the model to a given model edge-level, σ_e, and using the boundary condition $\dot{\sigma}\mid_{\sigma=0}= 0$, we have

$$\pi\dot{\sigma}_e = -\int_0^{\sigma_e} \nabla \cdot (\pi\mathbf{V})d\sigma - \sigma_e\frac{\partial\pi}{\partial t}$$

Combining the above equations, we have

$$\mathbf{OMEGA} = -\int_0^{\sigma_e} \nabla \cdot (\pi\mathbf{V})d\sigma + \sigma_e\mathbf{V} \cdot \nabla\pi$$

Note that in this formulation, **OMEGA** is computed at GCM model edge-levels. **OMEGA** at the model top edge is taken to be 0, thus the first computed value of **OMEGA** is at sigma edge 2, or the bottom edge of the top model sigma layer.

59) <u>DUDT</u> Total Zonal U-Wind Tendency $(m/sec/day)$

DUDT is the total time-tendency of the Zonal U-Wind due to Hydrodynamic, Diabatic, and Analysis forcing.

$$\mathbf{DUDT} = \frac{\partial u}{\partial t}_{Dynamics} + \frac{\partial u}{\partial t}_{Moist} + \frac{\partial u}{\partial t}_{Turbulence} + \frac{\partial u}{\partial t}_{Analysis}$$

Note, in Version 1 of the GEOS GCM there are no u-wind tendencies due to cumulus friction, (ie. $\frac{\partial u}{\partial t}_{Moist} = 0$). Also, in forecast simulations $\frac{\partial u}{\partial t}_{Analysis} = 0$.

60) <u>DVDT</u> Total Zonal V-Wind Tendency $(m/sec/day)$

DVDT is the total time-tendency of the Meridional V-Wind due to Hydrodynamic, Diabatic, and Analysis forcing.

$$\mathbf{DVDT} = \frac{\partial v}{\partial t}_{Dynamics} + \frac{\partial v}{\partial t}_{Moist} + \frac{\partial v}{\partial t}_{Turbulence} + \frac{\partial v}{\partial t}_{Analysis}$$

Note, in Version 1 of the GEOS GCM there are no v-wind tendencies due to cumulus friction, (ie. $\frac{\partial v}{\partial t}_{Moist} = 0$). Also, in forecast simulations $\frac{\partial v}{\partial t}_{Analysis} = 0$.

61) <u>DTDT</u> Total Temperature Tendency (deg/day)

DTDT is the total time-tendency of Temperature due to Hydrodynamic, Diabatic, and Analysis forcing.

$$\begin{aligned}\mathbf{DTDT} = {} & \frac{\partial T}{\partial t}_{Dynamics} + \frac{\partial T}{\partial t}_{MoistProcesses} + \frac{\partial T}{\partial t}_{ShortwaveRadiation} \\ & + \frac{\partial T}{\partial t}_{LongwaveRadiation} + \frac{\partial T}{\partial t}_{Turbulence} + \frac{\partial T}{\partial t}_{Analysis}\end{aligned}$$

Note, this diagnostic is obtained through differentiation by parts and re-arranging the model prognostic equations. Since the thermodynamic equation is written in the mass-weighted flux form, we have

$$\frac{\partial T}{\partial t} = \frac{p^\kappa}{\pi} \left(\frac{\partial \pi \theta}{\partial t} + \theta \frac{\partial \pi}{\partial t} \left[\frac{\sigma \pi \kappa}{p} - 1 \right] \right)$$

where $\theta = T/p^\kappa$. Also, in forecast simulations, $\frac{\partial T}{\partial t}_{Analysis} = 0$.

62) <u>DQDT</u> Total Specific Humidity Tendency $(g/kg/day)$

DQDT is the total time-tendency of Specific Humidity due to Hydrodynamic, Diabatic, and Analysis forcing.

$$\mathbf{DQDT} = \frac{\partial q}{\partial t}_{Dynamics} + \frac{\partial q}{\partial t}_{MoistProcesses} + \frac{\partial q}{\partial t}_{Turbulence} + \frac{\partial q}{\partial t}_{Analysis}$$

Note, this diagnostic is obtained through differentiation by parts and re-arranging the model prognostic equations. Since the moisture equation is written in the mass-weighted flux form, we have

$$\frac{\partial q}{\partial t} = \left(\frac{\partial \pi q}{\partial t} - q \frac{\partial \pi}{\partial t} \right) / \pi$$

Also, in forecast simulations, $\frac{\partial q}{\partial t}_{Analysis} = 0$.

63) <u>VORT</u> Relative Vorticity (sec^{-1})

The relative vorticity used in the formulation of the potential energy and enstrophy conserving scheme described in Section 2 is stored as the diagnostic **VORT**. The relative vorticity is given as:

$$\mathbf{VORT} = \frac{1}{a \cos \phi} \left[\frac{\partial v}{\partial \lambda} - \frac{\partial (u \cos \phi)}{\partial \phi} \right]$$

This diagnostic is stored on the Arakawa C-grid used in the GEOS GCM at the "vorticity-point" locations, ie., centered between the u-points and v-points, including values well defined at both poles.

64) Disabled

65) Disabled

66) Disabled

67) <u>USTAR</u> Surface-Stress Velocity (m/sec)

The surface stress velocity, or the friction velocity, is the wind speed at the surface layer top impeded by the surface drag:

$$\textbf{USTAR} = C_u W_s \qquad where: \quad C_u = \frac{k}{\psi_m}$$

C_u is the non-dimensional surface drag coefficient (see diagnostic number 10), and W_s is the surface wind speed (see diagnostic number 28).

68) <u>Z0</u> Surface Roughness Length (m)

Over the land surface, the surface roughness length is interpolated to the local time from the monthly mean data of Dorman and Sellers (1989). Over the ocean, the roughness length is a function of the surface-stress velocity, u_*.

$$\textbf{Z0} = c_1 u_*^3 + c_2 u_*^2 + c_3 u_* + c_4 + \frac{c_5}{u_*}$$

where the constants are chosen to interpolate between the reciprocal relation of Kondo(1975) for weak winds, and the piecewise linear relation of Large and Pond(1981) for moderate to large winds.

69) <u>FRQTRB</u> Frequency of Turbulence ($0 - 1$)

The fraction of time when turbulence is present is defined as the fraction of time when the turbulent kinetic energy exceeds some minimum value, defined here to be $0.005\, m^2/sec^2$. When this criterion is met, a counter is incremented. The fraction over the averaging interval is reported.

70) <u>PBL</u> Planetary Boundary Layer Depth (mb)

The depth of the PBL is defined by the turbulence parameterization to be the depth at which the turbulent kinetic energy reduces to ten percent of its surface value.

$$\textbf{PBL} = P_{PBL} - P_{surface}$$

where P_{PBL} is the pressure in mb at which the turbulent kinetic energy reaches one tenth

of its surface value, and P_s is the surface pressure.

71) <u>SWCLR</u> Clear sky Heating Rate due to Shortwave Radiation (deg/day)

The net Shortwave heating rate is calculated as the vertical divergence of the net solar radiative fluxes. The clear-sky and cloudy-sky shortwave fluxes are calculated separately. For the clear-sky case, the shortwave fluxes and heating rates are computed with both CLMO (maximum overlap cloud fraction) and CLRO (random overlap cloud fraction) set to zero (see Section 3.2.3). The shortwave routine is then called a second time, for the cloudy-sky case, with the true time-averaged cloud fractions CLMO and CLRO being used. In all cases, a normalized incident shortwave flux is used as input at the top of the atmosphere.

The heating rate due to Shortwave Radiation under clear skies is defined as:

$$\frac{\partial \rho c_p T}{\partial t} = -\frac{\partial}{\partial z} F(clear)_{SW}^{NET} \cdot \text{RADSWT},$$

or

$$\text{SWCLR} = \frac{g}{c_p \pi} \frac{\partial}{\partial \sigma} F(clear)_{SW}^{NET} \cdot \text{RADSWT}.$$

where g is the accelation due to gravity, c_p is the heat capacity of air at constant pressure, RADSWT is the true incident shortwave radiation at the top of the atmosphere (See Diagnostic #48), and

$$F(clear)_{SW}^{Net} = F(clear)_{SW}^{\uparrow} - F(clear)_{SW}^{\downarrow}$$

72) <u>OSR</u> Net upward Shortwave flux at the top of the model ($Watts/m^2$)

$$\text{OSR} = F_{SW,top}^{NET}$$

where top indicates the top of the first model layer used in the shortwave radiation routine. In the GEOS-1 GCM, $p_{SW_{top}} = 0$ mb.

73) <u>OSRCLR</u> Net upward clearsky Shortwave flux at the top of the model ($Watts/m^2$)

$$\text{OSRCLR} = F(clearsky)_{SW,top}^{NET}$$

where top indicates the top of the first model layer used in the shortwave radiation routine. In the GEOS-1 GCM, $p_{SW_{top}} = 0$ mb.

51

74) CLDMAS Convective Cloud Mass Flux ($kg\,m/sec$)

The cumulative cloud mass flux per unit time, from all convective clouds generated during the output interval, is written:

$$\mathbf{CLDMAS} = \eta m_B$$

where η is the entrainment, normalized by the cloud base mass flux, and m_B is the cloud base mass flux. m_B and η are defined explicitly in Section 3.1.1, the description of the convective parameterization.

75) UAVE Time-Averaged Zonal U-Wind (m/sec)

The diagnostic **UAVE** is simply the time-averaged Zonal U-Wind over the **NUAVE** output frequency. This is contrasted to the instantanious Zonal U-Wind which is archived on the Prognostic Output data stream.

$$\mathbf{UAVE} = u(\lambda, \phi, \sigma, t)$$

Note, **UAVE** is computed and stored on the staggered C-grid.

76) VAVE Time-Averaged Meridional V-Wind (m/sec)

The diagnostic **VAVE** is simply the time-averaged Meridional V-Wind over the **NVAVE** output frequency. This is contrasted to the instantanious Meridional V-Wind which is archived on the Prognostic Output data stream.

$$\mathbf{VAVE} = v(\lambda, \phi, \sigma, t)$$

Note, **VAVE** is computed and stored on the staggered C-grid.

77) TAVE Time-Averaged Temperature ($Kelvin$)

The diagnostic **TAVE** is simply the time-averaged Temperature over the **NTAVE** output frequency. This is contrasted to the instantanious Temperature which is archived on the Prognostic Output data stream.

$$\mathbf{TAVE} = T(\lambda, \phi, \sigma, t)$$

78) QAVE Time-Averaged Specific Humidity (g/kg)

The diagnostic **QAVE** is simply the time-averaged Specific Humidity over the **NQAVE** output frequency. This is contrasted to the instantanious Specific Humidity which is archived on the Prognostic Output data stream.

$$\textbf{QAVE} = q(\lambda, \phi, \sigma, t)$$

79) Disabled

80) <u>PAVE</u> Time-Averaged Surface Pressure - PTOP (mb)

The diagnostic **PAVE** is simply the time-averaged Surface Pressure - PTOP over the **NPAVE** output frequency. This is contrasted to the instantanious Surface Pressure - PTOP which is archived on the Prognostic Output data stream.

$$
\begin{aligned}
\textbf{PAVE} &= \pi(\lambda, \phi, \sigma, t) \\
&= p_s(\lambda, \phi, \sigma, t) - p_T
\end{aligned}
$$

81) <u>QQAVE</u> Time-Averaged Turbulent Kinetic Energy $(m/sec)^2$

The diagnostic **QQAVE** is simply the time-averaged prognostic Turbulent Kinetic Energy produced by the GEOS-1 GCM Turbulence parameterization over the **NQQAVE** output frequency. This is contrasted to the instantanious Turbulent Kinetic Energy which is archived on the Prognostic Output data stream.

$$\textbf{QQAVE} = qq(\lambda, \phi, \sigma, t)$$

Note, **QQAVE** is computed and stored at the "mass-point" locations on the staggered C-grid.

82) <u>SWGCLR</u> Net downward clearsky Shortwave flux at the surface $(Watts/m^2)$

$$
\begin{aligned}
\textbf{SWGCLR} &= F(clearsky)^{Net}_{SW,nlay+1} \\
&= F(clearsky)^{\downarrow}_{SW,nlay+1} - F(clearsky)^{\uparrow}_{SW,nlay+1}
\end{aligned}
$$

where nlay+1 indicates the lowest model edge-level, or $p = p_{surf}$. $F(clearsky)SW^{\downarrow}$ is the

downward clearsky Shortwave flux and $F(clearsky)^{\uparrow}_{SW}$ is the upward clearsky Shortwave flux.

83) <u>ANALP</u> Analysis Surface Pressure Tendency (mb/sec)

ANALP is the surface pressure tendency created during the assimilation cycle which is used in the Incremental Analysis Updating (IAU) procedure.

$$\textbf{ANALP} = \left(\pi^A(\lambda, \phi, \sigma, t) - \pi^{FG}(\lambda, \phi, \sigma, t)\right) / \Delta t_{Analysis}$$

where π^A corresponds to the surface pressure after the analysis, π^{FG} corresponds to the surface pressure first guess, and $\Delta t_{Analysis}$ is the time-step between analyses (6 hours).

84) <u>SDIAG1</u> User-Defined Surface Diagnostic-1

The GEOS GCM provides Users with a built-in mechanism for archiving user-defined diagnostics. The generic diagnostic array QDIAG located in COMMON /DIAG/, and the associated diagnostic counters and pointers located in COMMON /DIAGP/, must be accessable in order to use the user-defined diagnostics (see Section 6). A convenient method for incorporating all necessary COMMON files is to include the GEOS GCM *vstate.com* file in the routine which employs the user-defined diagnostics.

In addition to enabling the user-defined diagnostic (ie., CALL SETDIAG(84)), the User must fill the QDIAG array with the desired quantity within the User's application program or within modified GEOS GCM subroutines, as well as increment the diagnostic counter at the time when the diagnostic is updated. The QDIAG location index for **SDIAG1** and its corresponding counter is automatically defined as **ISDIAG1** and **NSDIAG1**, respectively, after the diagnostic has been enabled. The syntax for its use is given by

```
do j=1,jm
do i=1,im
qdiag(i,j,ISDIAG1) = qdiag(i,j,ISDIAG1) + ...
enddo
enddo

NSDIAG1 = NSDIAG1 + 1
```

The diagnostics defined in this manner will automatically be archived by the production output programs (see Section 11).

85) <u>SDIAG2</u> User-Defined Surface Diagnostic-2

The GEOS GCM provides Users with a built-in mechanism for archiving user-defined diagnostics. For a complete description refer to Diagnostic #84. The syntax for using the surface SDIAG2 diagnostic is given by

```
do j=1,jm
do i=1,im
qdiag(i,j,ISDIAG2) = qdiag(i,j,ISDIAG2) + ...
enddo
enddo

NSDIAG2 = NSDIAG2 + 1
```

The diagnostics defined in this manner will automatically be archived by the production output programs (see Section 11).

86) <u>UDIAG1</u> User-Defined Upper-Air Diagnostic-1

The GEOS GCM provides Users with a built-in mechanism for archiving user-defined diagnostics. For a complete description refer to Diagnostic #84. The syntax for using the upper-air UDIAG1 diagnostic is given by

```
do L=1,nlay
do j=1,jm
do i=1,im
qdiag(i,j,IUDIAG1+L-1) = qdiag(i,j,IUDIAG1+L-1) + ...
enddo
enddo
enddo

NUDIAG1 = NUDIAG1 + 1
```

The diagnostics defined in this manner will automatically be archived by the production output programs (see Section 11).

87) <u>UDIAG2</u> User-Defined Upper-Air Diagnostic-2

The GEOS GCM provides Users with a built-in mechanism for archiving user-defined diagnostics. For a complete description refer to Diagnostic #84. The syntax for using the upper-air UDIAG2 diagnostic is given by

```
do L=1,nlay
do j=1,jm
do i=1,im
qdiag(i,j,IUDIAG2+L-1) = qdiag(i,j,IUDIAG2+L-1) + ...
enddo
enddo
enddo

NUDIAG2 = NUDIAG2 + 1
```

The diagnostics defined in this manner will automatically be archived by the production output programs (see Section 11).

88) <u>DIABU</u> Total Diabatic Zonal U-Wind Tendency $(m/sec/day)$

DIABU is the total time-tendency of the Zonal U-Wind due to Diabatic processes and the Analysis forcing.

$$\textbf{DIABU} = \frac{\partial u}{\partial t}_{Moist} + \frac{\partial u}{\partial t}_{Turbulence} + \frac{\partial u}{\partial t}_{Analysis}$$

Note, in Version 1 of the GEOS GCM there are no u-wind tendencies due to cumulus friction, (ie. $\frac{\partial u}{\partial t}_{Moist} = 0$). Also, in forecast simulations $\frac{\partial u}{\partial t}_{Analysis} = 0$.

89) <u>DIABV</u> Total Diabatic Meridional V-Wind Tendency $(m/sec/day)$

DIABV is the total time-tendency of the Meridional V-Wind due to Diabatic processes and the Analysis forcing.

$$\textbf{DIABV} = \frac{\partial v}{\partial t}_{Moist} + \frac{\partial v}{\partial t}_{Turbulence} + \frac{\partial v}{\partial t}_{Analysis}$$

Note, in Version 1 of the GEOS GCM there are no v-wind tendencies due to cumulus friction, (ie. $\frac{\partial v}{\partial t}_{Moist} = 0$). Also, in forecast simulations $\frac{\partial v}{\partial t}_{Analysis} = 0$.

90) <u>DIABT</u> Total Diabatic Temperature Tendency (deg/day)

DIABT is the total time-tendency of Temperature due to Diabatic processes and the Analysis forcing.

$$\textbf{DIABT} = \frac{\partial T}{\partial t}_{MoistProcesses} + \frac{\partial T}{\partial t}_{ShortwaveRadiation}$$
$$+ \frac{\partial T}{\partial t}_{LongwaveRadiation} + \frac{\partial T}{\partial t}_{Turbulence} + \frac{\partial T}{\partial t}_{Analysis}$$

If we define the time-tendency of Temperature due to Diabatic processes as

$$\frac{\partial T}{\partial t}_{Diabatic} = \frac{\partial T}{\partial t}_{MoistProcesses} + \frac{\partial T}{\partial t}_{ShortwaveRadiation}$$
$$+ \frac{\partial T}{\partial t}_{LongwaveRadiation} + \frac{\partial T}{\partial t}_{Turbulence}$$

then, since there are no surface pressure changes due to Diabatic processes, we may write

$$\frac{\partial T}{\partial t}_{Diabatic} = \frac{p^\kappa}{\pi} \frac{\partial \pi \theta}{\partial t}_{Diabatic}$$

where $\theta = T/p^\kappa$. Thus, **DIABT** may be written as

$$\textbf{DIABT} = \frac{p^\kappa}{\pi} \left(\frac{\partial \pi \theta}{\partial t}_{Diabatic} + \frac{\partial \pi \theta}{\partial t}_{Analysis} \right)$$

Note, this diagnostic is only approximate since we have neglected the affect of the analysis on the surface pressure, ie.

$$\frac{\partial T}{\partial t}_{Analysis} = \frac{p^\kappa}{\pi} \left(\frac{\partial \pi \theta}{\partial t}_{Analysis} + \theta \frac{\partial \pi}{\partial t}_{Analysis} \left[\frac{\sigma \pi \kappa}{p} - 1 \right] \right)$$

This term will be added in subsequent versions of the GEOS GCM. In forecast simulations there is no error since $\frac{\partial T}{\partial t}_{Analysis} = 0$.

91) <u>DIABQ</u> Total Diabatic Specific Humidity Tendency ($g/kg/day$)

DIABQ is the total time-tendency of Specific Humidity due to Diabatic processes and the Analysis forcing.

$$\textbf{DIABQ} = \frac{\partial q}{\partial t}_{MoistProcesses} + \frac{\partial q}{\partial t}_{Turbulence} + \frac{\partial q}{\partial t}_{Analysis}$$

If we define the time-tendency of Specific Humidity due to Diabatic processes as

$$\frac{\partial q}{\partial t}_{Diabatic} = \frac{\partial q}{\partial t}_{MoistProcesses} + \frac{\partial q}{\partial t}_{Turbulence}$$

then, since there are no surface pressure changes due to Diabatic processes, we may write

$$\frac{\partial q}{\partial t}_{Diabatic} = \frac{1}{\pi} \frac{\partial \pi q}{\partial t}_{Diabatic}$$

Thus, **DIABQ** may be written as

$$\textbf{DIABQ} = \frac{1}{\pi} \left(\frac{\partial \pi q}{\partial t}_{Diabatic} + \frac{\partial \pi q}{\partial t}_{Analysis} \right)$$

Note, this diagnostic is only approximate since we have neglected the affect of the analysis on the surface pressure, ie.

$$\frac{\partial q}{\partial t}_{Analysis} = \frac{1}{\pi}\left(\frac{\partial \pi q}{\partial t}_{Analysis} - q\frac{\partial \pi}{\partial t}_{Analysis}\right)$$

This term will be added in subsequent versions of the GEOS GCM. In forecast simulations there is no error since $\frac{\partial q}{\partial t}_{Analysis} = 0$.

92) Disabled

93) Disabled

94) Disabled

95) Disabled

96) Disabled

97) Disabled

98) Disabled

99) Disabled

100) Disabled

101) Disabled

102) <u>VINTUQ</u> Vertically Integrated Moisture Flux $(m/sec \cdot g/kg)$

The vertically integrated moisture flux due to the zonal u-wind is obtained by integrating uq over the depth of the atmosphere at each model timestep, and dividing by the total mass

of the column.

$$\text{VINTUQ} = \frac{\int_{surf}^{top} uq\rho dz}{\int_{surf}^{top} \rho dz}$$

Using $\rho\delta z = -\frac{\delta p}{g} = -\frac{\pi}{g}\delta\sigma$, we have

$$\text{VINTUQ} = \int_0^1 uq d\sigma$$

103) VINTVQ Vertically Integrated Moisture Flux ($m/sec \cdot g/kg$)

The vertically integrated moisture flux due to the meridional v-wind is obtained by integrating vq over the depth of the atmosphere at each model timestep, and dividing by the total mass of the column.

$$\text{VINTVQ} = \frac{\int_{surf}^{top} vq\rho dz}{\int_{surf}^{top} \rho dz}$$

Using $\rho\delta z = -\frac{\delta p}{g} = -\frac{\pi}{g}\delta\sigma$, we have

$$\text{VINTVQ} = \int_0^1 vq d\sigma$$

104) VINTUT Vertically Integrated Heat Flux ($m/sec \cdot deg$)

The vertically integrated heat flux due to the zonal u-wind is obtained by integrating uT over the depth of the atmosphere at each model timestep, and dividing by the total mass of the column.

$$\text{VINTUT} = \frac{\int_{surf}^{top} uT\rho dz}{\int_{surf}^{top} \rho dz}$$

Using $\rho\delta z = -\frac{\delta p}{g} = -\frac{\pi}{g}\delta\sigma$, we have

$$\text{VINTUT} = \int_0^1 uT d\sigma$$

105) VINTVT Vertically Integrated Heat Flux ($m/sec \cdot deg$)

The vertically integrated heat flux due to the meridional v-wind is obtained by integrating vT over the depth of the atmosphere at each model timestep, and dividing by the total mass of the column.

$$\mathbf{VINTVT} = \frac{\int_{surf}^{top} vT\rho dz}{\int_{surf}^{top} \rho dz}$$

Using $\rho\delta z = -\frac{\delta p}{g} = -\frac{\pi}{g}\delta\sigma$, we have

$$\mathbf{VINTVT} = \int_0^1 vTd\sigma$$

106 <u>CLDFRC</u> Total 2-Dimensional Cloud Fracton $(0-1)$

The 2-dimensional net cloud fraction as seen from the top of the atmosphere is given by

$$\mathbf{CLDFRC} = 1 - \left(1 - MAX_{l=l_1}^{NLAY}\left[CLMO_l\right]\right) \prod_{l=l_1}^{NLAY} (1 - CLRO_l)$$

For a complete description of cloud/radiative interactions, see Section 3.2.3.

107) <u>QINT</u> Total Precipitable Water (gm/cm^2)

The Total Precipitable Water is defined as the vertical integral of the specific humidity, given by:

$$\begin{aligned}
\mathbf{QINT} &= \int_{surf}^{top} \rho q dz \\
&= \frac{\pi}{g} \int_0^1 q d\sigma
\end{aligned}$$

where we have used the hydrostatic relation $\rho\delta z = -\frac{\delta p}{g} = -\frac{\pi}{g}\delta\sigma$.

108) <u>U2M</u> Zonal U-Wind at 2 Meter Depth (m/sec)

The u-wind at the 2-meter depth is determined from the similarity theory:

$$\mathbf{U2M} = \frac{u_*}{k}\psi_{m2m}\frac{u_{sl}}{W_s} = \frac{\psi_{m2m}}{\psi_{m_{sl}}}u_{sl}$$

where $\psi_m(2m)$ is the non-dimensional wind shear at two meters, and the subscript sl refers to the height of the top of the surface layer. If the roughness height is above two meters,

U2M is undefined.

109) <u>V2M</u> Meridional V-Wind at 2 Meter Depth (m/sec)

The v-wind at the 2-meter depth is a determined from the similarity theory:

$$\mathbf{V2M} = \frac{u_*}{k}\psi_{m_{2m}}\frac{v_{sl}}{W_s} = \frac{\psi_{m_{2m}}}{\psi_{m_{sl}}}v_{sl}$$

where $\psi_m(2m)$ is the non-dimensional wind shear at two meters, and the subscript sl refers to the height of the top of the surface layer. If the roughness height is above two meters, **V2M** is undefined.

110) <u>T2M</u> Temperature at 2 Meter Depth ($deg\ K$)

The temperature at the 2-meter depth is a determined from the similarity theory:

$$\mathbf{T2M} = P^\kappa(\frac{\theta*}{k}(\psi_{h_{2m}} + \psi_g) + \theta_{surf}) = P^\kappa(\theta_{surf} + \frac{\psi_{h_{2m}} + \psi_g}{\psi_{h_{sl}} + \psi_g}(\theta_{sl} - \theta_{surf}))$$

where:

$$\theta_* = -\frac{\overline{(w'\theta')}}{u_*}$$

where $\psi_h(2m)$ is the non-dimensional temperature gradient at two meters, ψ_g is the non-dimensional temperature gradient in the viscous sublayer, and the subscript sl refers to the height of the top of the surface layer. If the roughness height is above two meters, **T2M** is undefined.

111) <u>Q2M</u> Specific Humidity at 2 Meter Depth (g/kg)

The specific humidity at the 2-meter depth is determined from the similarity theory:

$$\mathbf{Q2M} = P^\kappa(\frac{q_*}{k}(\psi_{h_{2m}} + \psi_g) + q_{surf}) = P^\kappa(q_{surf} + \frac{\psi_{h_{2m}} + \psi_g}{\psi_{h_{sl}} + \psi_g}(q_{sl} - q_{surf}))$$

where:

$$q_* = -\frac{\overline{(w'q')}}{u_*}$$

where $\psi_h(2m)$ is the non-dimensional temperature gradient at two meters, ψ_g is the non-dimensional temperature gradient in the viscous sublayer, and the subscript sl refers to the

height of the top of the surface layer. If the roughness height is above two meters, **Q2M** is undefined.

112) U10M Zonal U-Wind at 10 Meter Depth (m/sec)

The u-wind at the 10-meter depth is an interpolation between the surface wind and the model lowest level wind using the ratio of the non-dimensional wind shear at the two levels:

$$\mathbf{U10M} = \frac{u_*}{k} \psi_{m_{10m}} \frac{u_{sl}}{W_s} = \frac{\psi_{m_{10m}}}{\psi_{m_{sl}}} u_{sl}$$

where $\psi_m(10m)$ is the non-dimensional wind shear at ten meters, and the subscript sl refers to the height of the top of the surface layer.

113) V10M Meridional V-Wind at 10 Meter Depth (m/sec)

The v-wind at the 10-meter depth is an interpolation between the surface wind and the model lowest level wind using the ratio of the non-dimensional wind shear at the two levels:

$$\mathbf{V10M} = \frac{u_*}{k} \psi_{m_{10m}} \frac{v_{sl}}{W_s} = \frac{\psi_{m_{10m}}}{\psi_{m_{sl}}} v_{sl}$$

where $\psi_m(10m)$ is the non-dimensional wind shear at ten meters, and the subscript sl refers to the height of the top of the surface layer.

114) T10M Temperature at 10 Meter Depth ($deg\ K$)

The temperature at the 10-meter depth is an interpolation between the surface potential temperature and the model lowest level potential temperature using the ratio of the non-dimensional temperature gradient at the two levels:

$$\mathbf{T10M} = P^{\kappa}(\frac{\theta_*}{k}(\psi_{h_{10m}} + \psi_g) + \theta_{surf}) = P^{\kappa}(\theta_{surf} + \frac{\psi_{h_{10m}} + \psi_g}{\psi_{h_{sl}} + \psi_g}(\theta_{sl} - \theta_{surf}))$$

where:

$$\theta_* = -\frac{\overline{(w'\theta')}}{u_*}$$

where $\psi_h(10m)$ is the non-dimensional temperature gradient at two meters, ψ_g is the non-dimensional temperature gradient in the viscous sublayer, and the subscript sl refers to the height of the top of the surface layer.

115) <u>Q10M</u> Specific Humidity at 10 Meter Depth (g/kg)

The specific humidity at the 10-meter depth is an interpolation between the surface specific humidity and the model lowest level specific humidity using the ratio of the non-dimensional temperature gradient at the two levels:

$$\mathbf{Q10M} = P^\kappa(\frac{q_*}{k}(\psi_{h_{10m}} + \psi_g) + q_{surf}) = P^\kappa(q_{surf} + \frac{\psi_{h_{10m}} + \psi_g}{\psi_{h_{sl}} + \psi_g}(q_{sl} - q_{surf}))$$

where:

$$q_* = -\frac{\overline{(w'q')}}{u_*}$$

where $\psi_h(10m)$ is the non-dimensional temperature gradient at two meters, ψ_g is the non-dimensional temperature gradient in the viscous sublayer, and the subscript sl refers to the height of the top of the surface layer.

116) <u>DTRAIN</u> Convective Cloud Detrainment $(kg\,m/sec)$

The cloud mass flux at the detrainment level per unit time, from all convective clouds generated during the output interval, is written:

$$\mathbf{DTRAIN} = \eta_{\sigma_D} m_B$$

where σ_D is the detrainment σ level, m_B is the cloud base mass flux, and η is the entrainment, defined in Section 3.1.1.

117) <u>QFILL</u> Filling of negative Specific Humidity $(g/kg/day)$

Due to computational errors associated with the numerical scheme used for the advection of moisture, negative values of specific humidity may be generated. The specific humidity is checked for negative values after every dynamics timestep. If negative values have been produced, a filling algorithm is invoked which redistributes moisture from below (see Section 2.3). Diagnostic **QFILL** is equal to the net filling needed to eliminate negative specific humidity, scaled to a per-day rate:

$$\mathbf{QFILL} = q_{final}^{n+1} - q_{initial}^{n+1}$$

where

$$q^{n+1} = (\pi q)^{n+1}/\pi^{n+1}$$

118) <u>VINTQANA</u> Precipitable Moisture Adjustment from Analysis (mm/day)

For the time change in specific humidity due to the analysis increment, $\frac{\partial q}{\partial t}_{analysis}$, the vertical integral or total precipitable amount is given by:

$$\textbf{VINTQANA} = \int_{surf}^{top} \rho \frac{\partial q}{\partial t}_{analysis} dz = - \int_{surf}^{top} \frac{\partial q}{\partial t}_{analysis} \frac{dp}{g} = \frac{\pi}{g} \int_0^1 \frac{\partial q}{\partial t}_{analysis} d\sigma$$

Defining the specific humidity analysis increment, $\frac{\partial q}{\partial t}_{analysis}$, as

$$\frac{\partial q}{\partial t}_{analysis} = \frac{1}{\pi} \left(\frac{\partial \pi q}{\partial t}_{analysis} - q \frac{\partial \pi}{\partial t}_{analysis} \right)$$

we may write

$$\textbf{VINTQANA} = \frac{1}{g} \int_0^1 \left(\frac{\partial \pi q}{\partial t}_{analysis} - q \frac{\partial \pi}{\partial t}_{analysis} \right) d\sigma$$

119) <u>VINTQFIL</u> Precipitable Moisture Adjustment from Filling (mm/day)

When advective or other processes create spurious negative specific humidity, total moisture is conserved by filling the negative amounts by "borrowing" moisture from below. When there is not enough moisture in a column to adequately fill the negative values, the specific humidities are set to zero, creating an artificial source of moisture.

For a change in specific humidity due to filling, Δq_{fill}, the vertical integral or total precipitable amount is given by:

$$\textbf{VINTQFIL} = \int_{surf}^{top} \rho \Delta q_{fill} dz = - \int_{surf}^{top} \Delta q_{fill} \frac{dp}{g} = \frac{\pi}{g} \int_0^1 \Delta q_{fill} d\sigma$$

A precipitable adjustment rate is defined as the vertically integrated moisture adjustment per Dynamics time step, scaled to mm/day.

Part III

GEOS-1 GCM: User's Guide

9 Introduction

In this section we discuss the general philosophy used in the construct of the GEOS GCM system, the necessary components of the system, and a basic User's Guide on how to set-up and run experiments.

10 GEOS Superstructure

The superstructure of the GEOS GCM is designed so that the entire model may be invoked by a simple subroutine call. With each call of the main GCM driver, all model prognostic and diagnostic fields are updated by one timestep. A variety of applications may be built around the main GCM driver (GCMDRV), which allow for straight forecast simulations, assimilation cyles, and dynamic initialization procedures. It should be emphasized that what is meant by the GEOS System is simply the library of GCM subroutines which include GCMDRV and those that are subsequently called. These subroutines will be denoted as *below* GCMDRV. Those routines which are *above* GCMDRV include the Main Program, or the *Application*, and any model Output routines.

10.1 GEOS Applications

The GEOS Application can be defined as the Main Program from which the GEOS GCM and/or the GEOS Utility subroutines are called. All Applications are User-supplied, that is, they do not belong to the GEOS GCM compiled library. The purpose of the GEOS Application is a pre-determined experiment, or *application*, which the User wants to perform using the GEOS GCM library.

For example, let us create an Application which performs the following funtions:

- Read a model restart from Unit1
- Integrate the model forward in time for NMAX iterations
- Write the resulting model restart to Unit2

This could be accomplished with the following FORTRAN code:

```
        CALL RESTART (UNIT1,IREAD,...)

        DO   N = 1,NMAX
        CALL GCMDRV (Arg1, Arg2, Arg3, ...)
        ENDDO

        CALL RESTART (UNIT2,IWRITE,...)
```

Here **IREAD** and **IWRITE** are read/write IO flags used by the GEOS Utility Subroutine **RESTART** to read/write GEOS Model restarts, and $Arg1, Arg2, Arg3, ...$ are the the arguments to **GCMDRV**. Both of these argument lists are described fully in the next section.

We can easily modify this application to run forecasts from the same initial state but using different **GCMDRV** model parameters:

```
        CALL RESTART (UNIT1,IREAD,...)

        DO   N = 1,NMAX
        CALL GCMDRV (Arg1.1, Arg1.2, Arg1.3, ...)
        ENDDO

        REWIND UNIT1
        CALL RESTART (UNIT1,IREAD,...)

        DO   N = 1,NMAX
        CALL GCMDRV (Arg2.1, Arg2.2, Arg2.3, ...)
        ENDDO

        CALL RESTART (UNIT2,IWRITE,...)
```

Finally, we could run the model with the same set of **GCMDRV** model parameters but starting from two different initial states:

```
        CALL RESTART (UNIT1,IREAD,...)
```

```
DO    N = 1,NMAX
CALL GCMDRV (Arg1, Arg2, Arg3, ...)
ENDDO

CALL RESTART (UNIT2,IWRITE,...)
CALL RESTART (UNIT3,IREAD,...)

DO    N = 1,NMAX
CALL GCMDRV (Arg1, Arg2, Arg3, ...)
ENDDO

CALL RESTART (UNIT4,IWRITE,...)
```

These simple examples show the ease and flexibility of creating applications to perform experiments with the GEOS GCM. In the next section we describe fully the argument lists for subroutines **GCMDRV** and **RESTART**, and briefly describe **GCMDRV**'s flow structure.

10.2   Subroutines GCMDRV & RESTART

Subroutine **GCMDRV** is the single interface between User Application routines and the actual updating of model prognostic fields. Its flow structure can be separated into three essential parts:

- Read and refresh Boundary Conditions
- Compute time-tendencies of atmospheric state variables due to physical and hydrodynamical processes
- Integrate the atmospheric state variables forward in time by one timestep

Every call to **GCMDRV** updates the boundary conditions to the current date and time. In Version 1 of the GEOS GCM this is accomplished by a linear interpolation between monthly mean data sets. Subsequent versions of the GCM will allow for boundary condition data sets with varying frequency intervals. The boundary conditions which are currently updated are:

- Sea Surface Temperature

- Ground Wetness
- Surface Albedo
- Surface Roughness
- Sea-Ice Thickness

In addition, data is provided describing the model topography, topography variance, and the Land/Water/Glacier flags. These data are not interpolated to the current date and time since they are fixed quantities. Finally, the incident solar radiation at the top of the atmosphere is computed for the current date and time.

At prescribed time intervals, **GCMDRV** calls separate mini-drivers to update the time-tendencies of the prognostic state variables due to particular physical or hydrodynamical processes. Each mini-driver has its own timescale of operation. The mini-drivers associated with physical and hydrodynamical processes are:

- Moist Processes (Updated every 10 minutes)
- Shortwave Radiation (Updated every 3 hours using a normalized incident radiation, and adjusted every timestep using the true incident radiation)
- Longwave Radiation (Updated every 3 hours)
- Turbulence (Updated every 30 minutes)
- Eulerian Hydrodynamics (Updated every timestep)

The time-tendencies for the processes stated above are always kept in core during the GEOS GCM simulation. Thus, all prognostic fields are time-continuous while the time-tendencies of the prognostic fields due to the various processes are discontinuous at the above stated frequencies. These time-tendencies are summed together to provide a total time-tendency to be used in the time-integration scheme. Currently, the GEOS GCM can be run with either the Matsuno or the Leapfrog time scheme. The Leapfrog scheme has associated with it an Asselin (1972) time filter.

The calling sequence associated with **GCMDRV** and a description of the argument list is provided below:

CALL GCMDRV (KBC,N,NYMD,NHMS,SCHEME,NDT,ALPHA,QQINIT,QBUD)

PARAMETER	TYPE	DESCRIPTION
KBC	Integer	KBC is the unit from which Boundary Conditions are read. Every call to GCMDRV will initiate an update of the boundary conditions. Boundary conditions are updated by a linear interpolation between the two months kept in memory which strap the current date and time. Each time a new mid-month is passed or a new KBC value is encountered, two new months are read in. Setting KBC equal to zero disables all boundary condition updates.
N	Integer	N refers to the current time index, and is equal to 1 or 2. Its value always points to the updated fields and is modified by GCMDRV.
NYMD	Integer	NYMD is the current year/month/day in YYMMDD format. Its value is modified by GCMDRV.
NHMS	Integer	NHMS is the current hour/minute/second in HHMMSS format. Its value is modified by GCMDRV.
SCHEME	Character*4	SCHEME is the variable indicating the time scheme to be used for the integration. SCHEME may be set to 'MATS' for the Matsuno time scheme, or 'LEAP' for the Leapfrog time scheme. The SCHEME variable may be changed at any time during the forecast.
NDT	Integer	NDT is the timestep (in seconds) used for the forecast. NDT may be positive, zero, or negative, and may be changed at any time during the forecast.
ALPHA	Real	Asselin Filter Coefficient, α, to be used with the Leapfrog Time Scheme, where $q_n^{Filt} = q_n(1 - \alpha) + \alpha \left(\frac{q_{n+1} + q_{n-1}}{2} \right)$. ALPHA may be changed at any time during the forecast.
QQINIT	Logical	QQINIT is a Logical flag parameter used by the Turbulence parameterization scheme. QQINIT should be set to TRUE if the GEOS GCM is starting from an initial condition which does not contain Turbulent Kinetic Energy as a prognostic state variable. After one successful call to GCMDRV, QQINIT should be set to FALSE.
QBUD	Logical	Logical flag to compute budget diagnostics.

The GEOS GCM Utility subroutine **RESTART** may be used within User-Defined Applications to read and/or write a GEOS GCM Restart dataset. The calling sequence associated with **RESTART** and a description of the argument list is provided below:

CALL RESTART (KU,IOFLAG,NYMD,NHMS,N,NYMD0,NHMS0,JOB,NTYPE)

PARAMETER	TYPE	DESCRIPTION
KU	Integer	Unit number from which to read or to write the GEOS Restart
IOFLAG	Integer	IO Flag which is equal to: 1 to Read a GEOS Restart, 2 to Write a GEOS Restart.
NYMD	Integer	NYMD is the current year/month/day in YYMMDD format.
NHMS	Integer	NHMS is the current hour/minute/second in HHMMSS format.
N	Integer	N refers to the current time index, and is equal to 1 or 2. Its value always points to the most recently updated fields.
NYMD0	Integer	NYMD0 is the beginning year/month/day of the current experiment in YYMMDD format. NYMD0 is used in current Production Applications to control Output frequencies.
NHMS0	Integer	NHMS0 is the beginning hour/minute/second of the current experiment in HHMMSS format. NYMD0 is used in current Production Applications to control Output frequencies.
JOB	Character*8	An Experiment Identifier (usually a name or experiment number).
NTYPE	Integer	NTYPE is the GEOS Restart Identification index. NTYPE = -1 refers to a "First Guess" restart which was used for an analysis. NTYPE = 0 refers to the "After Analysis" or straight forecast restart. NTYPE = 1 refers to a restart from an IAU assimilation.

It should be noted that if IOFLAG = 1, the **RESTART** parameters NYMD, NHMS, N, NYMD0, NHMS0, JOB, and NTYPE are read from the GEOS Restart dataset and passed back to the calling program. If IOFLAG = 2, the parameters NYMD, NHMS, N, NYMD0, NHMS0, JOB, and NTYPE passed into subroutine **RESTART** will be written out to the GEOS Restart.

11 GEOS Production

Although the GEOS GCM system is designed to work with a User supplied "Applications" program, several application programs have been developed by the DAO which are used in standard production forecast simulations and analyses, and are available as templates. These applications provide examples of convenient ways to control the input and output streams, the frequency and selection of diagnostic and prognostic fields for output, and the simulation start and end times. The application routine examples reside on the SGI workstation *hera.gsfc.nasa.gov*, in the directory */production/geos_das/geos1.1/applications*. Some of them are described here in detail:

gcmprod.f   -   A simple application routine designed to read and follow namelist-supplied directions to simulate a specific period and direct all "activated" diagnostics to an output stream. The application reads one namelist to establish the initial and final time and date of the simulation, the frequency of the output stream, and other run control parameters such as timestep and asselin filter strength. Another namelist is read in which logical flags determine the selection of diagnostics to be activated and directed to the output stream.

gcmprodn.f   -   An application routine which is designed to handle a somewhat more complex output stream for diagnostic and prognostic fields. The namelist controlled interface for the diagnostics involves the specification of an HHMMSS format variable for each activated diagnostic separately. Diagnostics may be averaged for any time period up to the length of the simulation, and the averaging period may be centered about the current time or may extend from the previous time to the present. The application determines how many different averaging periods and types are present, and directs the output to the appropriate number of separate output streams. Separate output routines are called to properly direct the diagnostic output. Control over the begin and end times of the simulation are also governed by namelist parameters.

amip.f   -   An experiment-specific application routine that was designed to handle the control of an extended multi-year simulation with complex diagnostic output requirements. The application was written to direct diagnostic output to several output data streams each with a pre-specified set of diagnostics. Separate output routines are called for each data stream, providing them with the required list of diagnostic quantities.

In addition to flexible application routines, the GEOS GCM system also incorporates user defined output routines that can be called by the application. The output routines developed at the DAO write a combination of prognostic and/or diagnostic quantities, on model sigma levels or interpolated to pressure levels, in the Phoenix Output Format (see Section 11.2).

Just like the application routines, several output routines have been developed by the DAO and are available as examples. Some of them are described here:

diagprs.f - An output routine which accepts as arguments a specific list of diagnostic quantities and interpolates them to an argument specified list of pressure levels. The routine uses the model provided GETDIAG subprogram to obtain the proper time-averaged quantities. The code is written to distinguish between different quantities and attempts to use an appropriate interpolation algorithm. Output is written in Phoenix Format.

diagsig.f - Designed to accept an argument-specified list of diagnostics, and direct output in Phoenix Format to one output stream. The GETDIAG routine is used to retrieve diagnostic quantities in the proper units from the model.

glaoutc.f - When this output routine is called, all prognostic quantities and all activated diagnostic quantities are interpolated to an argument-list specified set of pressure levels. All output is directed to a Phoenix Format data stream.

sigoutc.f - All model prognostic and activated diagnostic quantities are directed to a single sigma-level Phoenix Output Format data set.

progprs.f - Designed to direct model prognostic quantities to a single output stream. Quantities are interpolated to a list of pressure levels.

progsig.f - Model prognostic quantities are simply directed to a single sigma-level Phoenix format data set.

11.1 Production Namelists

Two general namelists have been designed to setup and control the Production runs of the GEOS GCM. The namelists include information about the beginning date and time of the forecast, the ending date and time of the forecast, the duration of each job segment, and output characteristics.

The first namelist is called INPUT, and contains the parameters to control the beginning and ending times of each experiment, as well as some output information. The following INPUT namelist and subsequent description can be used as is or as a template for Users to build upon within their own Applications:

```
&INPUT
  JOB     = '    1234',
  XLAB    = 'E1234  GEOS-GCM    CLIMATE SIMULATION EXPE',
            'RIMENT                                    ',
  NYMDB   =  850101 ,
  NHMSB   =  000000 ,
  NYMDE   =  860101 ,
  NHMSE   =  000000 ,
  NDT     =  225    ,
  LEAP    = .TRUE.  ,
  MATS    = .FALSE. ,
  QQINIT  = .FALSE. ,
  ALPHA   =  0.05   ,
  NDSEG   = 2400000 ,
  NDOUT   =  060000 ,
  PLEVS   =     1000.0,  950.0 , 900.0,  850.0,  800.0,
                700.0,  600.0 , 500.0,  400.0,  300.0,  250.0,
                200.0,  150.0 , 100.0,   70.0,   50.0,   30.0, 20.0
&END
```

PARAMETER	TYPE	DESCRIPTION
JOB	Character*8	Experiment Identifier (Usually a name or experiment number)
XLAB	Character*80	User Assigned Description of Current Experiment
NYMDB	Integer	Beginning Date of Experiment in YYMMDD format
NHMSB	Integer	Beginning Time of Experiment in HHMMSS format
NYMDE	Integer	Ending Date of Experiment in YYMMDD format
NHMSE	Integer	Ending Time of Experiment in HHMMSS format
NDT	Integer	Time step (in seconds) of the hydrodynamics
LEAP	Logical	Logical Flag to use the Leapfrog Time Scheme
MATS	Logical	Logical Flag to use the Matsuno Time Scheme
QQINIT	Logical	QQINIT is a Logical flag parameter used by the Turbulence parameterization scheme. QQINIT should only be set to TRUE if the GEOS GCM is starting from an initial condition which does not contain Turbulent Kinetic Energy as a prognostic state variable. After one successful call to GCMDRV, QQINIT should be set to FALSE.
ALPHA	Real	Asselin Filter Coefficient, α, to be used with the Leapfrog Time Scheme, where $q_n^{Filt} = q_n(1 - \alpha) + \alpha \left(\frac{q_{n+1} + q_{n-1}}{2} \right)$.
NDSEG	Integer	Current job segment time interval in HHMMSS format. The total time of a GEOS simulation is given as (NYMDE,NHMSE) - (NYMDB,NHMSB). This total time is divided into a number of smaller job segments, which run in succession on the computer. The job segment size is determined by the User, depending on the desired size of the Output stream and/or the CPU time restrictions within the computer QUEUE. Note, HH may be any number of hours, and not limited to a 24 hour day (ie., 5 day job segments would be defined as NDSEG = 1200000).
NDOUT	Integer	Output frequency for Prognostic fields in HHMMSS format.
PLEVS	Real	Levels used for Sigma to Pressure Interpolation to create Pressure Level Output. (Maximum number of levels = 50)

When the GEOS GCM is run during for a particular experiment, no diagnostic quantities will be produced or saved unless the User has explicitly enabled the desired diagnostics from the Applications program. Using the DAO supplied applications directly or as templates, a convenient NAMELIST method has been adopted for diagnostic control. Diagnostic quantities which are of interest to the User may be enabled by the application by including

74

the Diagnostic Name from the Diagnostic Menu (Section 7) in the namelist INDIAG. For those Users employing the *gcmprod.f* application described in Section 11, simply preface the Diagnostic Name with the letter **L**. This variable will then be treated as a logical parameter. Those parameters set to TRUE will be enabled for the GEOS GCM simulation. An example of the INDIAG namelist using the Logical variable syntax is shown below:

```
&INDIAG
  LUFLUX  = .TRUE.,
  LVFLUX  = .TRUE.,
  LHFLUX  = .TRUE.,
  LMOISTT = .TRUE.,
  LMOISTQ = .TRUE.,
  LRADLW  = .TRUE.,
  LRADSW  = .TRUE.,
  LPREACC = .TRUE.,
  LPRECON = .TRUE.,
  LOLR    = .FALSE.,
  LEVAP   = .FALSE.,
  LU2M    = .FALSE.,
  LV2M    = .FALSE.,
  LT2M    = .FALSE.,
  LQ2M    = .FALSE.,
&END
```

In this example, the diagnostic quantities **UFLUX, VFLUX, HFLUX, MOISTT, MOISTQ, RADLW, RADSW, PREACC,** and **PRECON** will all be enabled during the simulation. The remaining diagnostics **OLR, EVAP, U2M, V2M, T2M,** and **Q2m** will be disabled during the run. It should be noted that explicitly defining the logical diagnostic parameters to FALSE in the INDIAG namelist is not necessary since this is the default. Using this method in conjunction with the application *gcmprod.f* will produce diagnostic quantities whose output frequency is governed by the INPUT namelist parameter NDOUT.

For those Users interested in a more sophisticated diagnostic output frequency algorithm, each diagnostic may be written out at its own unique frequency by using the DAO application *gcmprodn.f.* In this case, a particular diagnostic is turned on, or enabled, by specifying a non-zero diagnostic frequency, in HHMMSS format, for that diagnostic. The diagnostic frequency name is the same as the diagnostic name (from the Diagnostic Menu, Section 7) preceded by the letter **N** (eg, NUFLUX = 030000). In this example, the diagnostic UFLUX will be accumulated and written out every 3 hours. Every diagnostics has its own frequency, thus certain diagnostics may be written out more frequently than others. A separate file is defined for each unique diagnostic frequency. Thus, if the user turns on a total of 24 diagnostics, 12 with a 6 hour frequency, 10 with a 3 hour frequency, and 2 with a half-hour frequency, a total of 3 diagnostic datasets will be created. Finally, diagnostics are accumulated and written out with the time-stamp at the end of the accumulation period.

A time-stamp which occurs at the middle of the accumlating period may be obtained by making the diagnostic frequency negative. An example of the INDIAG namelist using the frequency variable syntax is shown below:

```
&INDIAG
 NUFLUX  = 030000,
 NVFLUX  = 030000,
 NHFLUX  = 030000,
 NMOISTT =-060000,
 NMOISTQ =-060000,
 NRADLW  =-060000,
 NRADSW  =-060000,
 NPREACC = 060000,
 NPRECON = 060000,
 NOLR    = 060000,
 NEVAP   = 060000,
 NU2M    = 010000,
 NV2M    = 010000,
 NT2M    = 010000,
 NQ2M    = 010000,
&END
```

In this example, four output data streams will be produced. Diagnostics **U2M**, **V2M**, **T2M**, and **Q2M** will be averaged over a one-hour frequency and written out with a time-stamp at the end of each hour. Diagnostics **UFLUX**, **VFLUX**, and **HFLUX** will be averaged over a three-hour time-period. Diagnostics **PREACC**, **PRECON**, **OLR**, and **EVAP** will be averaged over a six-hour period and written out with a time-stamp at the end of the averaging period. Diagnostics **MOISTT**, **MOISTQ**, **RADLW**, and **RADSW** will also be averaged over a six-hour period but will be written out with a time-stamp associated with the middle of the averaging period. All other diagnostics are disabled.

11.2 Phoenix Format

The Phoenix Format used in the archiving of the GEOS AMIP and the GEOS-DAS 5-Year Re-analysis employs a self-documenting output stream which describes each field and its attributes for each time period on the output dataset. At each output time period, Header information is given which describes the horizontal and vertical dimensions of the output, the time period of the output, and variable descriptions of the data type. The number and type of fields are User Defined.

The Phoenix format allows for writing data in three different ways (or configurations). The first, configuration #1, is simply a sequence of distinct 2-dimensional fields (such as sea-level pressure, topography, or selected individual levels of specific quantities such as wind or moisture). The second method, configuration #2, is 3-dimensional data which are ordered by quantity for each level. It is assumed that all quantities written in this manner are defined for all levels. The third, configuration #3, is 3-dimensional data which are ordered by level for each quantity. Here, the number of levels associated which each quantity may vary. The specific configurations used within any dataset are determined by the User. The following sample code may be used to read any Phoenix Format Output stream:

```
C ********************************************************************
C ****               GODDARD LABORATORY FOR ATMOSPHERES         ****
C ********************************************************************

      PARAMETER  ( IDIM = 144 )    ! IDIM=144 for 2.5 degree Longitude
      PARAMETER  ( JDIM = 091 )    ! JDIM=091 for 2.0 degree Latitude
      DIMENSION Q( IDIM,JDIM  )

      CHARACTER*8  XLABEL(10) , JOB,  NAME
      DIMENSION    SIGE (50) , NDLEV(100), ZLEV(50)
      DIMENSION     IDUM(100), RDUM(100)
      CHARACTER*8  NAMES(100), NAMEU(100), NAMED(100), CDUM(100)
      CHARACTER*40 DESCS(100), DESCU(100), DESCD(100), DDUM(100)


C ********************************************************************
C ****                      READ HEADER                         ****
C ********************************************************************

      DATA KU  /10/
      READ(KU,END=500) JOB, NYMD, NHMS, NYMDO, NHMSO,
     .                 XLABEL, IM, JM,
     .                 NSFLD, NUFLD, NDFLD,
     .                 PTOP, NULEV, (ZLEV(K),K=1,NULEV),
     .                 NLAY, (SIGE(K),K=1,NLAY+1),
     .                 NDUM, (DDUM(N),IDUM(N),RDUM(N),CDUM(N),N=1,NDUM)

      READ(KU) ( NAMES(N), DESCS(N),            N=1,NSFLD ),
```

```
    .          ( NAMEU(N), DESCU(N),            N=1,NUFLD ),
    .          ( NAMED(N), DESCD(N), NDLEV(N), N=1,NDFLD )

C ************************************************************************
C ****                   READ 2-DIMENSIONAL FIELDS                    ****
C ************************************************************************

      DO N=1,NSFLD
      READ(KU) ZLEVID,NAME,Q
      ENDDO


C ************************************************************************
C ****   READ 3-DIMENSIONAL FIELDS (ORDERED ALL FIELDS FOR EACH LEVEL)   ****
C ************************************************************************

      DO L=1,NULEV
      DO N=1,NUFLD
      READ(KU) ZLEVID,NAME,Q
      ENDDO
      ENDDO


C ************************************************************************
C ****   READ 3-DIMENSIONAL FIELDS (ORDERED ALL LEVELS FOR EACH FIELD)   ****
C ************************************************************************

      DO N=1,NDFLD
      DO L=1,NDLEV(N)
      READ(KU) ZLEVID,NAME,Q
      ENDDO
      ENDDO

  500 CONTINUE
      STOP
      END
```

PARAMETER	TYPE	DESCRIPTION
JOB	Character*8	Experiment Identifier (Usually a name or experiment number)
XLAB	Character*80	User Assigned Description of Current Experiment
NYMD	Integer	Current Date of Experiment in YYMMDD format
NHMS	Integer	Current Time of Experiment in HHMMSS format
NYMD0	Integer	Beginning Date of Experiment in YYMMDD format
NHMS0	Integer	Beginning Time of Experiment in HHMMSS format
IM	Integer	Longitudinal dimension of data
JM	Integer	Latitudinal dimension of data
NLAY	Integer	Number of GCM vertical levels used in Experiment
SIGE	Real	GCM Sigma-Edge values
PTOP	Real	Model Top Pressure used in Experiment
ZLEV	Real	Upper-Air Level Values archived on data (Pressure or Sigma Level)
NSFLD	Integer	Number of 2-Dimensional Fields written in Config. #1
NUFLD	Integer	Number of 3-Dimensional Fields ordered by Level written in Config. #2
NDFLD	Integer	Number of 3-Dimensional Fields ordered by Quantity written in Config. #3
NAMES	Character*8	Names of 2-Dimensional Fields defined by NSFLD
DESCS	Character*40	Description of 2-Dimensional Fields defined by NSFLD
NAMEU	Character*8	Names of 3-Dimensional Fields ordered by Level defined by NUFLD
DESCU	Character*40	Description of 3-Dimensional Fields ordered by Level defined by NUFLD
NULEV	Integer	Number of Upper-Air Levels associated with all fields in Config. #2
NAMED	Character*8	Names of 3-Dimensional Fields ordered by Quantity defined by NDFLD
DESCD	Character*40	Description of 3-Dimensional Fields ordered by Quantity defined by NDFLD
NDLEV	Integer	Number of Upper-Air Levels associated with each field in Config. #3
NDUM	Integer	Number of User-Defined Header variables. NDUM, DDUM, IDUM, RDUM, and CDUM may be used by Users to add REAL, INTEGER, or CHARACTER information in the Header concerning the User's experiment.
DDUM	Character*40	User-Defined Description of Header variables
IDUM	Integer	User-Defined Integer Header variables
RDUM	Real	User-Defined Real Header variables
CDUM	Character*8	User-Defined Character Header variables
PLEVS	Real	Levels used for Sigma to Pressure Interpolation to create Pressure Level Output. (Maximum number of levels = 50)
ZLEVID	Real	Level Indentifier (Pressure or Sigma Level) of Quantity being read
NAME	Character*8	Character Name of Quantity being read
Q	Real	Two-Dimensional Quantity being read

It should be noted that the Datasets produced for the GEOS-1 DAS 5-year re-analysis and the GEOS-1 GCM AMIP simulation have the following characteristics and User-Defined Header information:

- The horizontal resolution for all data is constant for all time periods.

- All horizontal data, $q(i, j)$, is written with $i = 1$ corresponding to *Longitude* $= -180$ (International Dateline), and $j = 1$ corresponding to *Latitude* $= -90$ (South Pole).

- The data written in Configuration # 1 are generally surface data (such as Sea-Level Pressure, Surface Topography, Land/Water Masks, etc.).

- The data written in Configuration # 2 are generally Upper-Air prognostic quantities (such as wind, temperature, moisture, etc.).

- The data written in Configuration # 3 are generally GCM Model Diagnostic quantities (such as Diabatic Heating). Some Diagnostics are only defined at one level (such as Precipitation, Outgoing Longwave Radiation, etc.).

The User-Defined Header information has been defined as:

NDUM	=	2
DDUM(1)	=	'OUTPUT RECORD TYPE (INTEGER)'
IDUM(1)	=	-1 FIRST GUESS
		0 AFTER ANALYSIS (or STRAIGHT FORECAST)
		1 INITIALIZED ANALYSIS
RDUM(1)	=	0.100000E+16
CDUM(1)	=	'LOG8R'
DDUM(2)	=	'UNDEFINED FILL VALUE (REAL)'
IDUM(2)	=	0
RDUM(2)	=	0.100000E+16
CDUM(2)	=	'UNDEF'

11.3 Geopotential Heights on Sigma Surfaces

In the GEOS-1 GCM, the pressure gradient computed on sigma surfaces is derived by removing the large-scale component due to a mean potential temperature and surface pressure. Therefore, the *perturbation* geopotential heights have been archived on the GEOS-1 GCM sigma level datasets.

The pressure gradient on a constant pressure surface is related to the gradient on a constant sigma surface by

$$\nabla_p \Phi = \nabla_\sigma \Phi + c_p \theta \nabla_\sigma p^\kappa \,, \tag{25}$$

while the hydrostatic equation is given as

$$\frac{\partial \Phi}{\partial p^\kappa} = -c_p \theta \,. \tag{26}$$

Defining $\Phi = \overline{\Phi} + \Phi'$ and $\theta = \overline{\theta} + \theta'$, we may write

$$\frac{\partial \left(\overline{\Phi} + \Phi' \right)}{\partial p^\kappa} = -c_p \left(\overline{\theta} + \theta' \right) \tag{27}$$

or

$$\frac{\partial \overline{\Phi}}{\partial p^\kappa} = -c_p \overline{\theta} \qquad \Longrightarrow \qquad \overline{\Phi} = -c_p \overline{\theta} \left(p^\kappa - p_0^\kappa \right) \tag{28}$$

$$\frac{\partial \Phi'}{\partial p^\kappa} = -c_p \theta' \,. \tag{29}$$

Thus, we may express the pressure gradient on sigma surfaces as

$$
\begin{aligned}
\nabla_\sigma \Phi + c_p \theta \nabla_\sigma p^\kappa &= \nabla \left(\overline{\Phi} + \Phi' \right) + c_p \left(\overline{\theta} + \theta' \right) \nabla p^\kappa \\
&= \nabla \overline{\Phi} + \nabla \Phi' + c_p \overline{\theta} \nabla p^\kappa + c_p \theta' \nabla p^\kappa \\
&= -c_p \overline{\theta} \nabla p^\kappa + \nabla \Phi' + c_p \overline{\theta} \nabla p^\kappa + c p \theta' \nabla p^\kappa \\
&= \nabla \Phi' + c_p \theta' \nabla p^\kappa
\end{aligned}
\tag{30}
$$

where

$$\begin{aligned}
\Phi'_\ell = \Phi_\ell - \overline{\Phi}_\ell &= \Phi_\ell - c_p \overline{\theta}\,(p_0^\kappa - p_\ell^\kappa) \\
\theta'_\ell = \theta_\ell - \overline{\theta} \quad &; \quad \overline{\theta} = 280/1000^\kappa \\
&\quad\; p_0 = 1000 \,.
\end{aligned} \tag{31}$$

11.4 Interpolation from Sigma to Pressure Surfaces

While the GEOS GCM uses the sigma coordinate in the vertical for the discritization of the primitive equations, the current analysis system requires "first guess" fields to be on prescribed pressure surfaces. In addition, it is often desirable to process model output on pressure surfaces for scientific studies and comparisons to observations. The method used for the sigma coordinate to pressure coordinate interpolation is consistant with the form of the hydrostatic equation used in the GEOS GCM.

The vertical grid and index notation for sigma levels used in the GEOS GCM is given by

$$\Phi \quad P^\kappa \quad \theta \quad q \qquad \qquad \ell - 1$$
$$q_*$$
$$\ell e$$
$$\Phi \quad P^\kappa \quad \theta \quad q \qquad \qquad \ell$$
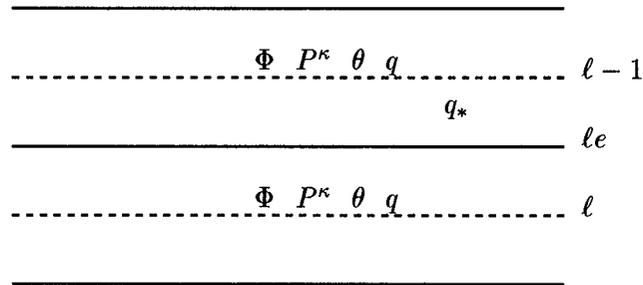
Figure 6: Vertical placement and index notation for sigma levels in the GEOS GCM

The form of the hydrostatic equation used in the GEOS GCM is given by

$$\frac{\partial \Phi}{\partial P^\kappa} = -c_p \theta \tag{32}$$

where Φ is the geopotential height, and $\theta = T/P^\kappa$. Similarly, for an arbitrary quantity, q, we may define

$$\frac{\partial q}{\partial P^\kappa} = c \tag{33}$$

where c is a constant. Thus, we may write

$$\frac{\partial q}{\partial P^\kappa} = c \qquad \Longrightarrow \qquad \frac{q_{\ell-1} - q_\ell}{P^\kappa_{\ell-1} - P^\kappa_\ell} = \frac{q_{\ell-1} - q_*}{P^\kappa_{\ell-1} - P^\kappa_*} \tag{34}$$

or

$$q_* = q_{\ell-1} \left[1 - \frac{P^{\kappa}_{\ell-1} - P^{\kappa}_*}{P^{\kappa}_{\ell-1} - P^{\kappa}_{\ell}} \right] + q_{\ell} \left[\frac{P^{\kappa}_{\ell-1} - P^{\kappa}_*}{P^{\kappa}_{\ell-1} - P^{\kappa}_{\ell}} \right] \tag{35}$$

This method is used for the winds, temperature, and relative humidity. Specific humidity at pressure levels is obtained from the previously interpolated temperature and relative humidity. For target pressures above the first model level, a linear extrapolation in P^{κ} from levels 1 and 2 is used. For target pressures between the surface pressure and the lowest model level, the quantity is assumed constant and is equal to its value in the lowest model level. For target pressures greater than the surface pressure (below topography), the quantity is undefined. It should also be noted that all GEOS GCM diagnostic quantities on pressure surfaces have been similarly linearly interpolated in P^{κ}.

The method used in the interpolation of geopotential heights, in particular, must be intimately linked to the finite-differencing scheme used in the background model in order to minimize computational error and prevent spurious height gradients (or geostrophic imbalances). The technique described here, formulated at UCLA by Arakawa and Suarez (personal communication), uses two separate interpolation algorithms depending on whether you are above or below the nearest sigma-level interface, ℓe, and has the following properties:
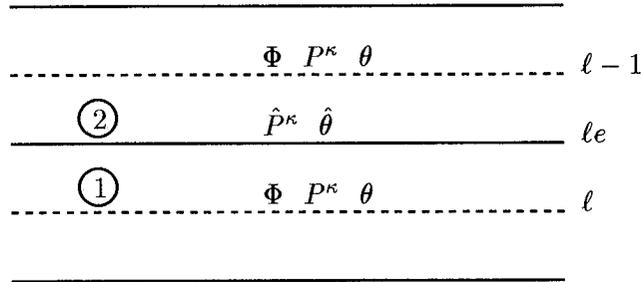

Figure 7: Index notation for vertical interpolation of Geopotential Heights

$$
\begin{array}{llll}
1) & \Phi_{P_1} = \Phi_{\ell} & & \text{for } P_1 = P_{\ell} \\
2) & \Phi_{P_2} = \Phi_{\ell-1} & & \text{for } P_2 = P_{\ell-1} \\
3) & \Phi_{P_1} = \Phi_{P_2} & & \text{for } P_1 = P_2 = \hat{P}_{\ell e} \\
4) & \nabla_p \Phi_{P_1} = \nabla_\sigma \Phi_{\ell} + c_p \theta_{\ell} \nabla_\sigma P^{\kappa}_{\ell} & & \text{for } P_1 = P_{\ell} \\
5) & \nabla_p \Phi_{P_2} = \nabla_\sigma \Phi_{\ell-1} + c_p \theta_{\ell-1} \nabla_\sigma P^{\kappa}_{\ell-1} & & \text{for } P_2 = P_{\ell-1}
\end{array}
$$

Thus, the interpolation not only preserves the heights on sigma surfaces whose target pressure coincides with the sigma level pressure, but also the horizontal gradient of the height on pressure surfaces is defined accurately as the horizontal gradient of the sigma level height plus the term corresponding to the horizontal gradient of the surface pressure.

We begin by writing the hydrostatic equation in the form

$$\frac{\partial \Phi}{\partial P^\kappa} = -c_p \theta \ . \tag{36}$$

Following Arakawa and Suarez (1983), we may write

$$\Phi_{\ell-1} = \Phi_\ell + c_p \hat{\theta}_{\ell e}(P_\ell^\kappa - P_{\ell-1}^\kappa), \tag{37}$$

$$\hat{\theta}_{\ell e} = \frac{(\hat{P}_{\ell e}^\kappa - P_{\ell-1}^\kappa)\theta_{\ell-1} + (P_\ell^\kappa - \hat{P}_{\ell e}^\kappa)\theta_\ell}{(P_\ell^\kappa - P_{\ell-1}^\kappa)} . \tag{38}$$

Thus, for the two regions in Figure 7, we have:

1) For $P_\ell \geq P_1 \geq \hat{P}_{\ell e}$

$$\Phi_{P_1} = \Phi_\ell + c_p \int_{P_1}^{P_\ell} \Theta_1 dP^\kappa \tag{39}$$

2) For $\hat{P}_{\ell e} \geq P_2 \geq P_{\ell-1}$

$$\Phi_{P_2} = \Phi_{\ell-1} + c_p \int_{P_{\ell-1}}^{P_2} \Theta_2 dP^\kappa \tag{40}$$

where

$$\Theta_1(P^\kappa) = \frac{(P_\ell^\kappa - P^\kappa)\hat{\theta}_{\ell e} + (P^\kappa - \hat{P}_{\ell e}^\kappa)\theta_\ell}{(P_\ell^\kappa - \hat{P}_{\ell e}^\kappa)} \tag{41}$$

$$\Theta_2(P^\kappa) = \frac{(\hat{P}_{\ell e}^\kappa - P^\kappa)\theta_{\ell-1} + (P^\kappa - P_{\ell-1}^\kappa)\hat{\theta}_{\ell e}}{(\hat{P}_{\ell e}^\kappa - P_{\ell-1}^\kappa)} \tag{42}$$

Here $\Theta_1(P^\kappa)$ and $\Theta_2(P^\kappa)$ are the interpolated θ values from levels ℓ and $\ell-1$ to the pressure P. Using (42) in (39), we may define

$$I_1 = \int_{P_1}^{P_\ell} \Theta_1 dP^\kappa$$

$$= \int_{P_1}^{P_\ell} \frac{(P_\ell^\kappa - P^\kappa)\,\hat{\theta}_{\ell e} + (P^\kappa - \hat{P}_{\ell e}^\kappa)\,\theta_\ell}{(P_\ell^\kappa - \hat{P}_{\ell e}^\kappa)} dP^\kappa \tag{43}$$

or

$$I_1 = \frac{1}{(P_\ell^\kappa - \hat{P}_{\ell e}^\kappa)} \left[\hat{\theta}_{\ell e}\left(P_\ell^\kappa[P_\ell^\kappa - P_1^\kappa] - \frac{1}{2}[P_\ell^{\kappa\,2} - P_1^{\kappa\,2}]\right) \right.$$
$$\left. + \theta_\ell \left(\frac{1}{2}[P_\ell^{\kappa\,2} - P_1^{\kappa\,2}] - \hat{P}_{\ell e}^\kappa[P_\ell^\kappa - P_1^\kappa]\right) \right] \tag{44}$$

$$= \left(\frac{P_\ell^\kappa - P_1^\kappa}{P_\ell^\kappa - \hat{P}_{\ell e}^\kappa} \right) \left[\hat{\theta}_{\ell e}\left(P_\ell^\kappa - \frac{1}{2}[P_\ell^\kappa + P_1^\kappa]\right) \right.$$
$$\left. + \theta_\ell \left(\frac{1}{2}[P_\ell^\kappa + P_1^\kappa] - \hat{P}_{\ell e}^\kappa\right) \right] \tag{45}$$

$$= \frac{1}{2}\left(\frac{P_\ell^\kappa - P_1^\kappa}{P_\ell^\kappa - \hat{P}_{\ell e}^\kappa} \right) \left[\hat{\theta}_{\ell e}\left(P_\ell^\kappa - P_1^\kappa\right) - \theta_\ell \left(2\hat{P}_{\ell e}^\kappa - P_\ell^\kappa - P_1^\kappa\right) \right]\ . \tag{46}$$

Similary, we may define

$$I_2 = \int_{P_{\ell-1}}^{P_2} \Theta_2 dP^\kappa$$

$$= \int_{P_{\ell-1}}^{P_2} \frac{(\hat{P}_{\ell e}^\kappa - P^\kappa)\,\theta_{\ell-1} + (P^\kappa - P_{\ell-1}^\kappa)\,\hat{\theta}_{\ell e}}{(\hat{P}_{\ell e}^\kappa - P_{\ell-1}^\kappa)} dP^\kappa \tag{47}$$

or

$$I_2 = \frac{1}{(\hat{P}_{\ell e}^\kappa - P_{\ell-1}^\kappa)} \left[\theta_{\ell-1}\left(\hat{P}_{\ell e}^\kappa[P_2^\kappa - P_{\ell-1}^\kappa] - \frac{1}{2}[P_2^{\kappa\,2} - P_{\ell-1}^{\kappa\,2}]\right) \right.$$
$$\left. + \hat{\theta}_{\ell e}\left(\frac{1}{2}[P_2^{\kappa\,2} - P_{\ell-1}^{\kappa\,2}] - P_{\ell-1}^\kappa[P_2^\kappa - P_{\ell-1}^\kappa]\right) \right] \tag{48}$$

$$= \left(\frac{P_2^\kappa - P_{\ell-1}^\kappa}{\hat{P}_{\ell e}^\kappa - P_{\ell-1}^\kappa}\right) \left[\theta_{\ell-1}\left(\hat{P}_{\ell e}^\kappa - \frac{1}{2}[P_2^\kappa + P_{\ell-1}^\kappa]\right)\right.$$
$$\left. + \hat{\theta}_{\ell e}\left(\frac{1}{2}[P_2^\kappa + P_{\ell-1}^\kappa] - P_{\ell-1}^\kappa\right)\right] \tag{49}$$

$$= \frac{1}{2}\left(\frac{P_2^\kappa - P_{\ell-1}^\kappa}{\hat{P}_{\ell e}^\kappa - P_{\ell-1}^\kappa}\right) \left[\theta_{\ell-1}\left(2\hat{P}_{\ell e}^\kappa - P_2^\kappa - P_{\ell-1}^\kappa\right) + \hat{\theta}_{\ell e}\left(P_2^\kappa - P_{\ell-1}^\kappa\right)\right] . \tag{50}$$

Therefore, for the interpolation of heights within regions (1) and (2) from Figure 7, we may write:

1) For $P_\ell \geq P_1 \geq \hat{P}_{\ell e}$

$$\Phi_{P_1} = \Phi_\ell + \frac{c_p}{2}\left(\frac{P_\ell^\kappa - P_1^\kappa}{P_\ell^\kappa - \hat{P}_{\ell e}^\kappa}\right) \left[\hat{\theta}_{\ell e}\left(P_\ell^\kappa - P_1^\kappa\right) - \theta_\ell\left(2\hat{P}_{\ell e}^\kappa - P_\ell^\kappa - P_1^\kappa\right)\right] \tag{51}$$

2) For $\hat{P}_{\ell e} \geq P_2 \geq P_{\ell-1}$

$$\Phi_{P_2} = \Phi_{\ell-1} + \frac{c_p}{2}\left(\frac{P_2^\kappa - P_{\ell-1}^\kappa}{\hat{P}_{\ell e}^\kappa - P_{\ell-1}^\kappa}\right) \left[\theta_{\ell-1}\left(2\hat{P}_{\ell e}^\kappa - P_2^\kappa - P_{\ell-1}^\kappa\right) + \hat{\theta}_{\ell e}\left(P_2^\kappa - P_{\ell-1}^\kappa\right)\right] \tag{52}$$

11.5 Sea-Level Pressure

In addition to the archiving of surface pressure, which is a prognostic variable in the GEOS-1 GCM, on all GEOS Production output streams, the sea-level pressure is also computed and archived. Also, during the GEOS data assimilation cycle, sea-level pressure rather than surface pressure is analyzed. The method used to compute sea-level pressure from surface pressure involves integrating the hydrostatic equation from sea-level to the surface, and an extrapolation of the temperature profile below topography.

The hydrostatic equation may be written as:

$$\frac{\partial p}{\partial z} = -\rho g = -\frac{pg}{RT} \ . \tag{53}$$

Integrating (53) from sea-level, sl, to the surface, s, we may write

$$\int_{sl}^{s} \frac{dp}{p} = -\int_{sl}^{s} \frac{d\Phi}{RT} \tag{54}$$

where we have used $d\Phi = g\,dz$. Assuming a mean temperature, $\overline{T}$, between the sea-level and surface, (54) may be written as

$$\ln\left(\frac{p_s}{p_{sl}}\right) = -\frac{\Phi_s}{R\overline{T}} \tag{55}$$

or

$$p_{sl} = p_s e^{\Phi_s/R\overline{T}} \ . \tag{56}$$

The mean temperature $\overline{T}$ is defined as the average of the surface and sea-level temperatures:

$$\overline{T} = \frac{1}{2}\left(T_s + T_{sl}\right) \tag{57}$$

where T_{sl} is obtained by assuming the temperature follows the moist adiabatic lapse rate

$$\frac{dT}{dz} = -\beta \qquad \Longrightarrow \qquad T_{sl} = T_s + \frac{\beta \Phi_s}{g} \tag{58}$$

where $\beta = 6.5^\circ \frac{K}{km}$. The surface temperature used for the sea-level pressure calculation is obtained by averaging the potential temperature, θ, in the lowest 100 mb of the model.

This allows variable resolution changes in the PBL while maintaining consistent sea-level pressure values between resolutions. We have

$$T_s \equiv \overline{\theta} p_s^\kappa \qquad ; \qquad \theta = T/p^\kappa \tag{59}$$

where

$$\overline{\theta} = \frac{\sum_\ell \theta_\ell \Delta \sigma_\ell}{\sum_\ell \Delta \sigma_\ell} \tag{60}$$

such that

$$\sum_\ell \Delta \sigma_\ell = \frac{\sum_\ell \Delta p_\ell}{\pi} \approx \frac{100 \ mb}{\pi} \ . \tag{61}$$

Here $\pi = p_s - p_{top}$.

12 GEOS Unix Script

The GEOS GCM is currently being run on NASA/GSFC's Cray C-90 computer system under the Cray UNICOS environment. There are five essential components to the basic script which are needed in order to perform experiments with the GEOS GCM:

- Create GEOS GCM NAMELIST for model parameters and diagnostics
- Create DIAGSIZE Subroutine for enabled diagnostics
- Remote copy frozen GEOS Libray, Application and Output Routines from *geos_das@dao*
- Compile User Application and Output Routines
- Load and Run GEOS simulation

Each of these elements are briefly discussed in the following subsections.

12.1 Creating the GEOS GCM Namelist

The following example shows the creation of a typical GCM namelist to be used during a GEOS simulation:

```
###################################################################
######
######                   Setup GCM Namelist
#####
###################################################################

/bin/rm gcmrun.namelist
cat > gcmrun.namelist <<'EOF'
 &INPUT
  JOB      = '    1234',
  XLAB     = 'E1234  GEOS-GCM   CLIMATE SIMULATION EXPE',
           'RIMENT                                    ',
  NYMDB    =  850101 ,
  NHMSB    =  000000 ,
  NYMDE    =  860101 ,
  NHMSE    =  000000 ,
  NDT      =  225     ,
  LEAP     = .TRUE.   ,
  MATS     = .FALSE.  ,
```

90

C-2

```
ALPHA    =  0.05   ,
NDSEG    =  2400000 ,
NDOUT    =  060000 ,
PLEVS    =      1000.0,  950.0 , 900.0,  850.0,  800.0,
                700.0,  600.0 , 500.0,  400.0,  300.0,  250.0,
                200.0,  150.0 , 100.0,   70.0,   50.0,   30.0, 20.0
&END
&INDIAG
 NUFLUX  = 030000,
 NVFLUX  = 030000,
 NHFLUX  = 030000,
 NMOISTT =-060000,
 NMOISTQ =-060000,
 NRADLW  =-060000,
 NRADSW  =-060000,
 NPREACC = 060000,
 NPRECON = 060000,
 NOLR    = 060000,
 NEVAP   = 060000,
 NU2M    = 010000,
 NV2M    = 010000,
 NT2M    = 010000,
 NQ2M    = 010000,
 &END
'EOF'
```

For a complete description of GCM Namelist parameters, see Section 11.1.

12.2 Creating the DIAGSIZE Subroutine

Using the DIAGSIZE subroutine is a convenient method to allocate just enough permanent memory during a run to be used for diagnostic storage. All GEOS GCM diagnostic quantities are stored in the single diagnostic array QDIAG which is located in the DIAG COMMON. In order to minimize the maximum memory requirement used by the model, the GEOS GCM libraries are compiled with room for only one horizontal diagnostic array. All production DAO applications contain a call to subroutine DIAGSIZE, which expands the size of the DIAG COMMON to include the total number of surface and upper-air diagnostics the User has enabled. For the diagnostics enabled in the preceeding section, the appropriate DIAGSIZE subroutine should be defined as:

```
######################################################################
######
######    Create DIAGSIZE Routine to control Total Diagnostics
```

```
######
################################################################

/bin/rm diagsize.f
cat > diagsize.f <<'EOF'
      subroutine diagsize
      parameter (    imr = 144 )
      parameter (    jmr =  90 )
      parameter ( nlayr =  20 )
      parameter ( ndiags =  11 )
      parameter ( ndiagu =   4 )
      common /diag/ ndiagmx,qdiag(imr,jmr+1,ndiags+ndiagu*nlayr)
      ndiagmx = ndiags + ndiagu*nlayr
      return
      end
'EOF'
```

We see that the User needs to simply assign the appropriate values for the number of surface diagnostics (NDIAGS) and the number of upper-air diagnostics (NDIAGU) which are enabled in the User's namelist.

12.3   Remote copy frozen GEOS Library

In order to gain access to the GEOS GCM, the User must remote copy the frozen production system from the DAO production workstation, *geos_das@dao*. In addition to the GEOS GCM library, the User may also remote copy production application programs and output routines. The COMMON files associated with these programs must also be copied to the User's local directory. Finally, the GEOS GCM boundary conditions and other GEOS input datasets must be obtained from the production workstation. An example of the syntax necessary for these remote copies is as follows:

```
#############################################################
######
######    Get Frozen GCM, Applications, and Output Routines
######
#############################################################


rcp geos_das@dao:/production/geos_das/geos1.1/gcm/vc5.2b20.macro vc5.2b20

rcp geos_das@dao:/production/geos_das/geos1.1/applications/gcmprodn.f .
rcp geos_das@dao:/production/geos_das/geos1.1/applications/progprs.f .
rcp geos_das@dao:/production/geos_das/geos1.1/applications/progsig.f .
```

```
rcp geos_das@dao:/production/geos_das/geos1.1/applications/diagprs.f .

rcp geos_das@dao:/production/geos_das/geos1.1/applications/vrslvb20.com vrslv.com
rcp geos_das@dao:/production/geos_das/geos1.1/applications/vstate.com .
rcp geos_das@dao:/production/geos_das/geos1.1/applications/vreal.com .
rcp geos_das@dao:/production/geos_das/geos1.1/applications/vphyscom.com .
rcp geos_das@dao:/production/geos_das/geos1.1/applications/vmetric.com .
rcp geos_das@dao:/production/geos_das/geos1.1/applications/metricc.com .
rcp geos_das@dao:/production/geos_das/geos1.1/applications/vbudget.com .
rcp geos_das@dao:/production/geos_das/geos1.1/applications/pblparm.com .
rcp geos_das@dao:/production/geos_das/geos1.1/applications/iau.com .

rcp geos_das@dao:/production/geos_das/geos1.2/data/bc144091.y1985 gcmbcs
rcp geos_das@dao:/production/geos_das/geos1.2/data/gcmo3.data .
rcp geos_das@dao:/production/geos_das/geos1.2/data/zonalT.data .
```

12.4   Compile User Application and Output Routines

Since the GEOS GCM library only contains subroutines from GCMDRV and below, the User must provide compiled Main Programs, or Applications, to perform specific experiments. For complete consistancy with the GEOS library, the Application and Output routines should be compiled in the same manner as the background model. An inline *compile* routine to accomplish this is shown below:

```
###################################################################
######
######    Create COMPILE Routine and Compile Userappl & Output
######
###################################################################

/bin/rm compile
cat > compile <<'EOF'
/lib/cpp -P -I . $1.f $1.cpp
fpp -dec $1.cpp > $1.fpp
cft77 -i 64 -a static -V -exm $1.fpp
mv $1.fpp.o $1.o
'EOF'
chmod +x compile

./compile gcmprodn
./compile progprs
./compile progsig
./compile diagprs
./compile diagsize
```

Here we have compiled those routines which were remote copied in Section 12.3.

12.5   Load and Run GEOS Simulation

Following successful compilations, the User must load the Application and Output routines together with the GEOS GCM library, creating an executable *a.out*. Then, assuming that an appropriate GEOS GCM Restart has been brought to the current local directory as *gcmrst*, the GEOS simulation may be performed:

```
#################################################################
######
######   Load GCM, Applications and Output Routines, and Run
######
#################################################################


segldr -M,s -l ./vc5.2b20 -- gcmprodn.o progsig.o progprs.o diagprs.o diagsize.o


assign -a gcmrun.namelist          fort.11
assign -a gcmrst                   fort.12

assign -a prog.sig    -N ieee -F f77 fort.34
assign -a prog.prs    -N ieee -F f77 fort.35
assign -a diag.prs.a  -N ieee -F f77 fort.41
assign -a diag.prs.b  -N ieee -F f77 fort.42
assign -a diag.prs.c  -N ieee -F f77 fort.43

assign -a gcmbcs      -N ibm  -F COS fort.16
assign -a gcmo3.data               fort.20
assign -a zonalT.data              fort.52

setenv NCPUS 4
a.out
```

Note that **NCPUS** has been set as an environmental variable equal to 4 in order to take advantage of the macro-tasking properties of the GEOS GCM. In this example, file units 34, 35, 41, 42, 43 are associated with Output data streams, and file units 16, 20, 52 are input datasets and boundary conditions for the GEOS GCM. Once the GEOS GCM simulation has been completed, the resulting output data streams should be moved to permanent storage.

Acknowledgements

References

Arakawa, A. and V.R. Lamb, 1981: A potential enstrophy and energy conserving scheme for the shallow water equations. *Mon. Wea. Rev.*, **109**, 18-36.

Arakawa, A. and M.J. Suarez, 1983: Vertical differencing of the primitive equations in sigma coordinates. *Mon. Wea. Rev.*, **111**, 34-45.

Asselin, R., 1972: Frequency filter for time integrations. *Mon. Wea. Rev.*, **100**, 487-490.

Blackadar, A.K.,1977: High Resolution Models of the Planetary Boundary Layer. *Advances in Environmental Science and Engineering, Vol 1* Editors Pfafflin and Zeigler, Gordon and Breach, Scientific Publishers.

Bloom, S.C., L.L. Takacs, and E. Brin, 1991: A scheme to incorporate analysis increments gradually in the GLA assimilation system. *Ninth Conf. on Numerical Weather Prediction*, Denver, CO, Amer. Meteor. Soc., 110-112.

Burridge, D.M. and J. Haseler, 1977: A model for medium range weather forecasting—adiabatic formulation, *Tech. Report. No. 4, European Center for Medium Range Weather Forecasts*, Brachnell, Berkshire, UK.

Chou, M.-D., 1984: Broadband water vapor transmission functions for atmospheric IR flux computation. *J. Atmos. Sci.*, **41**, 1775-1778.

Chou, M. -D., and L. Peng, 1983: A parameterization of the absorption in 15-micron CO_2 spectral region with application to climate sensitivity studies. *J. Atmos. Sci.*, **40**, 2183-2192.

Clarke, R. H., 1970: Observational studies in the atmospheric boundary layer. *Quart. J. Roy. Meteor. Soc.*, **96**, 91-114.

Davies, R., 1982: Documentation of the solar radiation parameterization in the GLAS climate model. NASA Tech. Memo. 83961, 57 pp. [Available from the U.S. Department of Commerce, National Technical Information Service, 5285 Port Royal Road, Springfield, VA 22161]

Dorman, J. L., and P. J. Sellers, 1989: A global climatology of albedo, roughness length and stomatal resistance for atmospheric general circulation models as represented by the Simple Biosphere model (SiB). *J. Appl. Meteor.*, **28**, 833-855.

Fox-Rabinovitz, M., H. M. Helfand, A. Hou, L. L. Takacs, and A. Molod, 1991: Numerical experiments on forecasting, climate simulation and data assimilation with the new 17 layer GLA GCM. Ninth Conference on Numerical Weather Prediction. 21-25

October 1991, Denver, CO, 506-509.

Gates, W. Lawrence, 1992: AMIP: The Atmospheric Model Intercomparison Project. *Bull. Am Met. Soc.*, **73**, 1962-1970

Harshvardhan, R. Davies, D. A. Randall, and T. G. Corsetti, 1987: A fast radiation parameterization for atmospheric circulation models. *J. Geophys. Res.*, **92**, 1009-1016.

Helfand, H. M., and J. C. Labraga, 1988: Design of a non-singular level 2.5 second-order closure model for the prediction of atmospheric turbulence. *J. Atmos. Sci.*, **45**, 113-132.

Helfand, H. M., M. Fox-Rabinovitz, L. Takacs, and A. Molod, 1991: Simulation of the planetary boundary layer and turbulence in the GLA GCM. Proceedings of the AMS Ninth Conference on Numerical Weather Predicition, 21-25 October 1991, Denver, CO, 514-517.

Helfand, H. M., M. and S. D. Schubert, 1994: Climatology of the simulated Great Plains low-level jet and its contribution to the continental moisture budget of the United States. *J. Climate*, **submitted**.

Higgins, R. W., and S. D. Schubert, 1993: Low-frequency synoptic-eddy activity in the Pacific storm track. *J. Atmos. Sci.*, **50**, 1672-1690.

Kalnay, E., M. Kanamitsu, J. Pfaendtner, J. Sela, M. Suarez, J. Stackpole, J. Tuccillo, L. Umscheid, and D. Williamson, 1989: Rules for the interchange of physical parameterizations, *Bull. Am Met. Soc.*, **70**, 620-622.

Kondo, J., 1975: Air-sea bulk transfer coefficients in diabatic conditions. *Boundary Layer Meteor.*, **9**, 91-112.

Lacis, A. A., and J. E. Hansen, 1974: A parameterization for the absorption of solar radiation in the Earth's atmosphere. *J. Atmos. Sci.*, **31**, 118-133.

Lanczos, C., 1966: *Discourse on Fourier Series*. Hafner Publishing, 255 pp.

Large, W. G., and S. Pond, 1981: Open ocean momentum flux measurements in moderate to strong winds. *J. Phys. Oceanogr.*, **11**, 324-336.

Meador, W. E., and W. R. Weaver, 1980: Two-stream approximations to radiative transfer in planetary atmospheres: A unified Descriptoin of existing methods and a new improvement. *J. Atmos. Sci.*, **37**, 630.643.

Mintz, Y. and Y. Serafini, 1984: Global fields of monthly normal soil moisture as derived from observed precipitation and an estimated potential evapotranspiration. Final

scientific report under NASA grant NAS 5-26, Part V, Dept. of Meteorology, University of Maryland, College Park, MD

Moorthi, S., and M. J. Suarez, 1992: Relaxed Arakawa Schubert: A parameterization of moist convection for general circulation models. *Mon. Wea. Rev.*, **120**, 978-1002.

Panofsky, H. A., 1973: Tower Micrometeorology. In Workshop on Micrometeorology, D. A. Haugen (ed.), American Meteorological Society, Bosston, 392 pp.

Phillips, N. A., 1957: A coordintate system having some special advantages for numerical forecasting. *J. Meteor.*, **14**, 184-185.

Platt, H. R., and Harshvardahn, 1988: Temperature Dependance of Cirrus Extinction: Implications for Climate Feedback. *J. Geoph. Res.*, **93**, 11051-11058.

Posey, J. W., and P. F. Clapp, 1964: Global distribution of normal surface albedo. *Geofis. Int.*, **4**, 33-48.

Reynolds, R. W., 1988: A real time global sea surface temperature analysis. *J. Climate*, **1**, 75-86.

Rodgers, C. D., 1968: Some extension and applications of the new random model for molecular band transmission. *Quart. J. Roy. Meteor. Soc.*, **94**, 99-102.

Rosenfield, J. E., M. R. Schoeberl, and M. A. Geller, 1987: A computation of the stratospheric diabatic circulation using an accurate radiative transfer model. *J. Atmos. Sci.*, **44**, 859-876.

Sadourney, R., 1975: The dynamics of finite difference models of the shallow water equations, *J. Atmos. Sci.*, **32**, 680-689.

Schemm, J., S. Schubert, J. Terry, and S. Bloom, 1992: Estimates of monthly mean soil moisture for 1979-1989. NASA Tech. Memo. No. 104571, Goddard Space Flight Center, Greenbelt, MD 20771.

Schubert, S. D., J. Pfaendtner and R. Rood, 1993: An assimilated data set for Earth Science applications, *Bull. Am Met. Soc.*, **74**, 2331-2342

Schubert, S., M. Suarez, C. K. Park, and S. Moorthi, 1993: GCM Simulations of intraseasonal variability in the Pacific/North American region. *J. Atmos. Sci.*, **50**, 1991-2007.

Shapiro, R., 1970: Smoothing, filtering and boundary effects. *Rev. Geophys. Space Phys.*, **8**, 359-387.

Suarez, M. J., and L. L. Takacs, 1994: Documentation of the Aries/GEOS Dynamical Core Version 2, NASA Tech. Memorandum 104606-Vol(in press), NASA, Goddard Space Flight Center, Greenbelt, MD.

Sud, Y. C., and A. Molod, 1988: The roles of dry convection, cloud-radiation feedback processes and the influence of recent improvements in the parameterization of convection in the GLA GCM. *Mon. Wea. Rev.*, **116**, 2366-2387.

Sud, Y. C., P. J. Sellers, Y. Mintz, M. D. Chou, G. K. Walker, and W. E. Smith, 1990: Influence of the Biosphere on the Global Circulation and Hydrological Cycle - A GCM Simulation Experiment. *Agric. and Forest Meteo.*, **52**, 113-180.

Yaglom, A. M., and B. A. Kader, 1974: Heat and mass transfer between a rough wall and turbulent fluid flow at high Reynolds and Peclet numbers. *J. Fluid Mech.*, **62**, 601-623.

REPORT DOCUMENTATION PAGE

1. AGENCY USE ONLY (Leave blank)	2. REPORT DATE September 1994	3. REPORT TYPE AND DATES COVERED Technical Memorandum

4. TITLE AND SUBTITLE
Technical Report Series on Global Modeling and Data Assimilation
Volume 1 - Documentation of the Goddard Earth Observing System
(GEOS) General Circulation Model - Version 1

6. AUTHOR(S)
Lawrence L. Takacs, Andrea Molod, and Tina Wang
Max J. Suarez, Editor

5. FUNDING NUMBERS
C - NAS5-32332
Code 910

7. PERFORMING ORGANIZATION NAME(S) AND ADDRESS (ES)
Laboratory for Atmospheres
Data Assimilation Office
Goddard Space Flight Center
Greenbelt, Maryland 20771

8. PEFORMING ORGANIZATION REPORT NUMBER
94B00128

9. SPONSORING / MONITORING ADGENCY NAME(S) AND ADDRESS (ES)
National Aeronautics and Space Administration
Washington, DC 20546-0001

10. SPONSORING / MONITORING ADGENCY REPORT NUMBER
TM-104606, Vol. 1

12a. DISTRIBUTION / AVAILABILITY STATMENT
Unclassified - Unlimited
Subject Category 46
This publication is available from the NASA Center for AeroSpace
Information, 800 Elkridge Landing Road, Linthicum Heights, MD
21090-2934, (301)621-0390.

12b. DISTRIBUTION CODE

13. ABSTRACT (Maximum 200 words)

This technical report documents Version 1 of the Goddard Earth Observing System (GEOS) General Circulation Model (GCM). The GEOS-1 GCM is being used by NASA's Data Assimilation Office (DAO) to produce multiyear data sets for climate research. This report provides a documentation of the model components used in the GEOS-1 GCM, a complete description of model diagnostics available and a User's Guide to facilitate GEOS-1 GCM experiments.

14. SUBJECT TERMS
GEOS, EOS, GCM, Documentation, Diagnostics, User's Guide, DAO

15. NUMBER OF PAGES
114

16. PRICE CODE

17. SECURITY CLASSIFICATION OF REPORT	18. SECURITY CLASSIFICATION OF THIS PAGE	19. SECURITY CLASSIFICATION OF ABSTRACT	20. LIMITATION OF ABSTRACT
Unclassified	Unclassified	Unclassified	UL